



UiT The Arctic University of Norway

Faculty of Science and Technology
Department of Physics and Technology

Assessment of Solar Photovoltaics and Wind Energy for Increased Electrification and Grid Independent Farming

Moritz Rürger

EOM-3901 Master's thesis in energy, climate and environment 30 SP

June 2022

Abstract

A solution towards increased electrification and reduced greenhouse gas emissions in the agriculture is local renewable energy production. Not only is it a sustainable and environmentally positive project, but with remarkably increasing electricity prices renewable energy projects can also be economically favorable for farmers, by reducing grid dependence and hence high electricity costs. In this thesis, solar and wind conditions at a farm in Southwestern Norway are mapped with the goal of estimating potential energy production. An isolated building with a suitable consumption profile is chosen to investigate, size and design a complete on-grid PV system. Comparing energy production estimates from the proposed PV system and wind turbine with consumption data from the farm allows analyzing the economics to map the profitability of the two systems alone and as a combined Hybrid Power System, in addition to proposing ways of utilizing potential surplus energy for increased electrification of the farm's machine park.

Calculations show that a PV system on the Southwest facing rooftop of the chosen building can give an average annual energy production above 70 MWh, with maximum monthly production in the range of 12-13 MWh. Based on the estimated energy production, the building sees an energy surplus of up to 8 MWh between April and September. When looking at the total consumption of the entire farm, the PV system can cover up to 80% in the months with maximum production. Different variants of using PV energy to supply a charging station for an electric tractor are proposed, and opportunities, challenges, and outlook regarding the introduction of electric tractors discussed. Wind energy production estimates show annual production around 7 MWh, and a significantly lower specific production yield compared to the PV system. The economic analysis reveals a critical spot price of 0.13 NOK/kWh for the PV system to be a profitable project, and it shows short payback periods of 4-5 years and annual electricity savings up to 100 000 NOK with recently observed spot prices in the NO2 area. The analysis also indicates that the wind turbine is an unprofitable investment, but a combined Hybrid Power System seems profitable but highly dependent on spot prices, investment costs and energy production, with a critical spot price of 0.88 NOK/kWh.

The thesis proposes progressive investments in local renewable energy at a farm and shows that this can support electrification and sustainable farming, while at the same time lead to significant long-term economic profits for the farmer.

Table of Contents

Abstract

List of Tables

List of Figures

Acknowledgements

Abbreviations

Nomenclature

- 1 Introduction 1**
 - 1.1 Background..... 1
 - 1.2 Idea and Aim of Thesis..... 2
 - 1.2.1 Electric Tractor..... 3
 - 1.3 Significance 4
 - 1.4 Study Area 4
 - 1.5 Structure of the Thesis..... 6
- 2 Background Theory 9**
 - 2.1 Transmittance 9
 - 2.2 Solar Radiation Components 9
 - 2.3 Photovoltaic Effect 10
 - 2.4 PV Technologies and Structures..... 11
 - 2.4.1 Prices and Outlook 12
 - 2.5 PV Cell Efficiency..... 13
 - 2.6 Installation Considerations 14
 - 2.6.1 On-Grid 14
 - 2.6.2 Off-Grid..... 15
 - 2.6.3 On-Grid with Energy Storage Backup 15
 - 2.7 Components..... 16

2.7.1	Inverter	16
2.7.2	Cables	17
2.7.3	Protective Devices.....	19
2.7.4	Battery Energy Storage	20
2.8	I-V Characteristics	21
2.9	Performance Ratio	22
2.10	Temperature Effect	23
2.11	Energy Production	24
2.12	Wind Energy	24
3	Data and Methodology	27
3.1	Solar Radiation Analysis in ArcGIS.....	27
3.2	Temperature and Wind Data.....	27
3.3	Simulation in PVsyst	29
3.4	Consumption Data	30
3.5	PV System Sizing	30
3.5.1	PV Module	31
3.5.2	Inverter	31
3.5.3	Cables.....	33
3.6	AutoCAD.....	34
3.7	Hybrid Power System.....	35
3.8	Economic Analysis	36
4	Results and Discussion	39
4.1	Solar Potential.....	39
4.1.1	Solar Radiation Analysis in ArcGIS	39
4.1.2	Calculated Energy Production Estimates	42
4.1.3	Simulation in PVsyst.....	45
4.2	Energy Production and Consumption.....	48

4.2.1	Consumption of the Cow Shed.....	48
4.2.2	Consumption of the entire farm	49
4.3	PV System Sizing	51
4.3.1	PV Module	51
4.3.2	Inverter	53
4.3.3	DC Cables	56
4.3.4	AC Cables	57
4.4	PV System Design	59
4.5	Electric Tractor	62
4.5.1	Charging System	62
4.5.2	Economic Aspects and Profitability	67
4.5.3	Outlook.....	69
4.6	Wind Energy Production	70
4.7	Performance Comparison	73
4.8	Economic Analysis	75
4.8.1	Case: PV System	78
4.8.2	Case: Wind Turbine	80
4.8.3	Case: Hybrid Power System.....	81
4.8.4	Summary/Comparison.....	82
4.9	Uncertainties and Limitations.....	83
4.9.1	Area Solar Radiation in ArcGIS.....	83
4.9.2	PV Energy Estimates and Energy Consumption.....	84
4.9.3	PVsyst Simulation	86
4.9.4	PV System Sizing and Design.....	87
4.9.5	Electric Tractor Charging.....	87
4.9.6	Wind Data and Wind Energy Estimates.....	88
4.9.7	Economic Analysis.....	89

5	Summary and Conclusion	93
5.1	Summary.....	93
5.2	Conclusion.....	93
5.3	Further Work	94
	Appendix	97
A	Solar Maps.....	97
B	Array/Inverter Configuration	98
C	Cable Sizing	100
D	Installation Methods.....	103
E	Energy Output Wind Turbine.....	104
F	Python Code for Wind Energy Estimates	105
G	Excel Model for Economic Analysis	106
H	Spot Prices.....	109
	Bibliography	111

List of Tables

Table 1 - Average solar irradiation on the Cow Shed for all months of 2021. Given in (Wh/m ²).....	42
Table 2 - Monthly energy production values, and total annual production for the PV system in (kWh)	44
Table 3 - Electrical and mechanical characteristics for the NE275-30P PV module [64]	52
Table 4 - Data for the S5-GC33K inverter [65].....	54
Table 5 - Summary of the PV system with the chosen components	56
Table 6 - Data for the 2.5 mm ² XLPE Cable [68]	56
Table 7 - Data for the PFSP 3x25/16 Cable [69].....	57
Table 8 - Data for the E-20 HAWT Wind Turbine [73].....	70
Table 9 - Spot price scenarios and corresponding NPV of the PV system	78
Table 10 - Minimum annual energy production and maximum degradation rate required for NPV = 0 for the spot price scenarios.....	79
Table 11 - Spot price scenarios and corresponding NPV of the wind turbine	80
Table 12 - Spot price scenarios and corresponding NPV of the HPS	81
Table 13 - Critical values for energy production and investment costs for each spot price scenario.....	82
Table 14 - Data for the module, inverter and ambient temperature used in the calculations ..	98
Table 15 - Data for the module, inverter and cables used for cable sizing	100
Table 16 - Current Carrying Capacities in Amps for methods of installation - PVC insulation, three loaded conductors (Cu or Al) [32]	103
Table 17 - Annual average wind speed and the corresponding estimated energy output from the E-20 SWT [73]	104
Table 18 - Monthly spot prices for NO2 from January 2019 to March 2022 in NOK/kWh. Collected from Nord Pool [58].....	109

List of Figures

Figure 1 - Map showing the farm's location in Southwestern Norway. Created in Google Maps	5
Figure 2 - Map showing the entire area of the farm and the location of the Cow Shed relative to the other main buildings. Created in ArcGIS. Spatial Reference: UTM Zone 33N. Server Layer Credits: Kartverket, Geovekst, kommuner – Geodata AS	6
Figure 3 - Representation of the solar radiation components [9]	10
Figure 4 - Multijunction GaInP/Ga(In)As/Ge solar cell and Heterojunction CdTe solar cell [15] [16].....	11
Figure 5 - Shape and appearance of a Monocrystalline and a Polycrystalline solar module and partitions of a single cell [18].....	12
Figure 6 - Simple Three-Phase Inverter Circuit [79]	17
Figure 7 - Cross section of a XLPE insulated Solar PV cable [80].....	18
Figure 8 - I-V curve and power output curve for an operating PV cell [81].....	22
Figure 9 - Locations of the weather station and the farm. The distance between them is 4.25 km. Created in Google Earth.....	28
Figure 10 - Monthly energy consumption of the Cow Shed for 2019-2021	39
Figure 11 - The part of the rooftop of the Cow Shed (dotted lines) used to obtain average irradiation values. Created in ArcGIS. Spatial Reference: UTM Zone 33N. Server Layer Credits: Kartverket, Geovekst, kommuner og OSM – Geodata AS.....	40
Figure 12 - The result of Area Solar Radiation, run in ArcGIS for each month. The highest and lowest irradiation values for each month are shown on the bars in (Wh/ m ²). Spatial Reference: UTM Zone 33N. Server Layer Credits: Kartverket, Geovekst, kommuner og OSM – Geodata AS	41
Figure 13 - Monthly average temperatures for the timeseries of the dataset (°C), and calculated total efficiencies of the PV modules (%)	43
Figure 14 - PVsyst monthly PV production and calculated monthly PV production	45
Figure 15 - PVsyst monthly irradiation and ArcGIS monthly irradiation. Given in (kWh/ m ²)	46
Figure 16 - Average monthly consumption of the Cow Shed and estimated PV energy production.....	48
Figure 17 - Difference between PV production and average consumption. Hence, the amount of energy surplus or deficit looking at PV production and consumption exclusively	49
Figure 18 - Average monthly consumption of the entire farm and estimated PV production	50
Figure 19 - Percentage ratio of the consumption of the entire farm covered by PV production	51
Figure 20 – Single-line diagram showing the PV system design. The informative tables present data for each component. Created in AutoCAD	60
Figure 21 - More detailed single-line diagram of the PV system. The figure shows a partition of the system, looking at one of the inverters exclusively. Created in AutoCAD	61
Figure 22 - Single-line diagram of the AC supplied charging station. Created in AutoCAD.....	63

Figure 23 - Position of the charging station at the barn, and the cable connecting it to the PV system. Created in ArcGIS. Spatial Reference: UTM Zone 33N. Server Layer Credits: Kartverket, Geovekst, kommuner – Geodata AS	64
Figure 24 - Four alternatives for connecting the charging station to the DC side of the PV system. (a): Charging station supplied only from PV system; (b): Charging station supplied from PV system and ESU; (c): Charging station supplied from PV system and grid; (d): Charging station supplied from PV system, ESU and grid. Created in AutoCAD	66
Figure 25 - Power curve for the E-20 HAWT Wind Turbine, including cut-in, cut-out and rated wind speeds	71
Figure 26 - Variations in measured wind speed for 2021 and 48-hour moving average	71
Figure 27 - Variations in hourly energy production from the wind turbine and 48-hour moving average	72
Figure 28 - Monthly specific production yield in (kWh/kW) for the PV system and the wind turbine.....	73
Figure 29 - PV and wind energy production combined and compared to consumption of the Cow Shed	74
Figure 30 - PV and wind energy production compared to consumption of the entire farm....	75
Figure 31 - NPVs for the three cases for the different spot price scenarios.....	83
Figure 32 - Average monthly wind speeds for 2016-2021	89
Figure 33 - Solar maps for each month of 2021 for the entire rooftop of the Cow Shed. Created in ArcGIS. Spatial Reference: UTM Zone 33N. Server Layer Credits: Kartverket, Geovekst, kommuner og OSM – Geodata AS	97

Acknowledgements

I would like to thank Professor Matteo Chiesa for excellent supervision through the entire process of the Project Paper and this final Master's thesis. His commitment and creativity have guided me into the right directions and made it possible to find topics of my own interest at each stage of the process. I am also thankful to all the other professors and lecturers at the faculty, and especially those at UiT in Narvik for making it possible for me to take courses from there on several occasions while living in Tromsø.

As this thesis uses a specific farm for a case study, the cooperation with the owners of the farm has been essential for the shaping of this thesis. I would therefore like to express my gratitude towards Mikal and Kristine Hetland for providing me with all information about the farm that I desired.

I would also like to thank family and friends, and especially my girlfriend, for all the support. Finally, I would like to thank my classmates for the five last years, from every sleepy lecture to every late and lively Saturday night at Prelaten. I would never have made it through this study without you. We have worked hard, but also been able to let loose together, and in that way created memories and friendships that will last for a long time.

Moritz Rüger

Tromsø, June 2022

Abbreviations

AC	Alternating Current
Ah	Ampere Hour
Al	Aluminum
BES	Battery Exchange System
BIPV	Building-Integrated Photovoltaics
CAD	Computer-Aided Design
CCC	Current Carrying Capacity
CSA	Cross-Sectional Area
Cu	Copper
DC	Direct Current
DNV	Det Norske Veritas
DoD	Depth of Discharge
DSM	Digital Surface Model
ESU	Energy Storage Unit
GIS	Geographic Information System
GW	Gigawatt
HAWT	Horizontal Axis Wind Turbine
HPS	Hybrid Power System
IGBT	Insulated-Gate Bipolar Transistor
IT	Insulated Terra
kW	Kilowatt
kWh	Kilowatt-hour
MET	Norwegian Meteorological Institute
MPPT	Maximum Power Point Tracking

MW	Megawatt
MWh	Megawatt-hour
NEK	Norwegian Electrotechnical Committee
NOCT	Nominal Operating Cell Temperature
NOK	Norwegian Krone
NPV	Net Present Value
NVE	Norwegian Water Resources and Energy Directorate
Pa	Pascal
PCC	Point of Common Coupling
PLR	Partial Load Ratio
PR	Performance Ratio
PV	Photovoltaic
SPD	Surge Protective Device
STC	Standard Test Conditions
SWT	Small Wind Turbine
TEK17	Norwegian Building Code
TIF	Tagged Image Format
TN	Terra Neutral
USD	US Dollar
UTM	Universal Transverse Mercator
V2V	Vehicle-to-Vehicle
VAWT	Vertical Axis Wind Turbine
WACC	Weighted Average Cost of Capital
Wh	Watt-hour
Wp	Watt-peak

Nomenclature

Symbol	Description	SI Unit
S	Solar radiation	$W \cdot m^{-2}$
G	Solar irradiation	$W \cdot h \cdot m^{-2}$
V	Voltage	$kg \cdot m^2 \cdot s^{-3} \cdot A^{-1}$
I	Current	A
P	Power	$kg \cdot m^2 \cdot s^{-3}$
η	Efficiency	
μ	Temperature Coefficient	$^{\circ}C^{-1}$
T	Temperature	$^{\circ}C$
A	Area	m^2
ρ	Electrical Resistivity	$kg \cdot m^3 \cdot s^{-3} \cdot A^{-2}$
L	Length	m

1 Introduction

1.1 Background

Increasing energy efficiency, decreasing emissions, the development of green energy sources, and generally the seek after sustainability, is asked for in more and more parts of the society. The agriculture is a sector that humans are totally dependent on, but it is also a sector where energy consumption and greenhouse gas emission is significant. With the increasing requirements on energy efficiency and sustainable energy, in combination with the high expectations on service and production in the agriculture, measures and practices must be implemented to fulfill both [1]. In 2018 the total greenhouse gas emissions from tractors and other machines in Norwegian agriculture were estimated to be 290 000 tons CO₂ equivalents (CO₂e), which equals the emissions of about 180 000 private cars over a year. An electrification of agriculture machines could help reduce the greenhouse gas emissions and contribute to more sustainable farming [2]. This electrification, however, does not come without challenges. It would obviously lead to a larger electricity demand on the farms. Many of Norway's rural farms already depend upon fragile and old electricity grids, which often need to transport the electricity over long distances to reach the farms. Increasing the stress on these grids to meet the increasing demands an electrification leads to, could result in frequent grid blackouts, or require expensive and time-consuming grid upgrade. This would, among other things, include an upgrade of distribution lines and surge protections, in addition to the construction of new transformers and substations. A solution towards fulfilling the complex expectations of electrification and service and production quality, while avoiding the electricity demand to overtake the available supply from the electricity grid, is local renewable energy development at the farms.

Solar Photovoltaics (PV) was long seen as an unsuitable technology for the Norwegian climate. Recent development regarding efficiency and thermodynamics of PV has, however, increased the interest, as both low temperatures and high albedo effect due to snow and ice are favorable conditions for PV energy production. By the end of 2021 there was a total of about 205 MW installed PV in Norway, thereof more than 90% grid connected [3]. The remarkable rise in electricity spot prices in Norway during the last year has acted as a springboard for the expansion of residential PV, and the growth is expected to continue in the years to come. Favorable subsidies, such as investment support and grid export deals, also contribute to the growth.

Attention to how PV can be deployed with low competition with other land uses is increasing, and there is no doubt that the agriculture is a field with huge potential for PV, due to large available areas on both buildings and acres. Research has been performed on how transparent concentrator PV systems can work in dual-use with cropland, showing that they can provide comparable energy production to a traditional system [4]. PV can also work as a solution to the increased demands due to electrification in farming in the future and compensate for fragile grids in rural districts. In addition, increasing electricity prices and decreasing PV prices enable both remarkable reduction in electricity costs for farmers due to reduced grid dependence, and fast payback for well-sized and financed PV projects.

Wind energy is another renewable energy technology with potential in the agriculture. Large available areas enable further development in the small wind turbine market. Turbines for industrial and agricultural use are relatively untested in Norway, but their ability to produce energy both day and night and both summer and winter, makes it an interesting technology to combine with PV. This thesis looks at opportunities regarding energy production at a farm in Southwestern Norway. Performances of a PV system and a wind turbine are investigated to assess their abilities of leading towards self-supply on parts of the farm, supporting electrification and sustainable agricultural operation.

1.2 Idea and Aim of Thesis

Recently, the requirements on sustainability in farming have been given more attention, and regulations and programs have been developed with the goal of increasing energy efficiency and decreasing greenhouse gas emissions in Norwegian agriculture. This thesis is based on the idea of investigating renewable energy production and its effect on future farming. The farm investigated in this thesis is located in Southwestern Norway, and there is no present energy production at the farm. The building used to assess solar potential and PV performance is chosen based on its location, usage, and energy consumption. These factors are further discussed in Section 1.4. The renewable energy installations introduced in this thesis are meant as a first initiative towards self-supply at the farm. The goal is hence not to cover the entire energy consumption at the farm from own produced renewable energy, but to introduce a way of starting progressive investments in different technologies.

The solar radiation conditions at the building are analyzed using the software ArcGIS. The results of the solar radiation analysis are based on the results of the Project Paper, which identified the most suitable rooftop for PV installation. Potential energy production from a PV

system on the specified rooftop is estimated by using an analytical method and through simulation in PVsyst, and results are compared, and deviations discussed. Energy production estimates are also compared to consumption data from the farm. Further, PV system components are sized and chosen, resulting in a complete proposed system design. Wind conditions are explored and potential wind energy production from a proposed wind turbine at the farm is estimated with the help of a Python code taking wind speeds and the turbine's power curve as input. The performance is compared to the PV system. Finally, an economic analysis looks at the PV system and the wind turbine alone, in addition to a combined Hybrid Power System, with the goal of assessing the profitability of these projects.

In short, the main aim is to investigate the possibilities of renewable energy production at the farm, to reduce grid dependence and hence electricity costs, in addition to illuminating measures to enhance electrification and reduce greenhouse gas emissions. Along the way, the goal is to propose ways of combining these.

1.2.1 Electric Tractor

A way of using potential surplus produced energy from the PV system is by distributing it for charging of an electric tractor. Replacing the established combustion engine tractor with an electric tractor running on batteries, and hence electrifying the farm's machine park, would be a huge step towards reducing greenhouse gas emissions and contributing to sustainable farming. Other positive effects on health would be the reduced noise and the reduced inlet of toxic gases emitted from combustion engines. This thesis looks at the opportunities of charging the electric tractor with energy produced by the PV system. The PV system supplies the charging station during times with sufficient production, while energy is imported from the grid during times where the PV system does not produce enough. Electric tractors are still in early stages, and there are few commercially available electric tractors on the market. They are hence relatively untested, and their capabilities and challenges are unmapped at larger scales. The challenges consider battery capacity, working time and investment costs, and the development of battery energy density and battery costs will be decisive for the development of electric tractors in the future. In addition, due to a tractor's standard lifetime of about 15 years, the electrification of the machine park will possibly take time. Yet this is not necessarily a disadvantage as it gives developers time to present better and competitive electric tractors with the ability to phase out diesel tractors. Electric tractors will possibly play a large role in the future electrification of the agriculture sector, and large producers like John

Deere, CNH, H2Trac BV, and AGCO have started the production of electric tractors. There are still several challenges regarding the introduction of electric tractors in everyday farming, but it is undoubtedly an interesting future project for increased electrification and sustainability in the agriculture.

The goal of this part of the thesis is to present opportunities and challenges regarding the introduction of electric tractors in the agriculture. Suggestions on implementing a charging system for the electric tractor in combination with a PV system are included, and variants, problems and solutions are discussed. Finally, this work can lead to a business plan for PV system providers or other energy companies and consulting firms, which is based on including charging systems for electric tractors or other machines in their products and services. The business plan would be specialized to energy solutions in the agriculture, looking at the projection of the system, performing economic analyses and completing the final installation. As electric tractors are still in early stages, this part is more of a hypothetical approach for future boost of electrification in the agriculture.

1.3 Significance

Not only does energy production on farms reduce the stress on the power grid and help reduce the costs of grid upgrade, but it can also be directly economically favorable for the farmers. With electricity prices expected to stay high in the future, increased independence from energy suppliers can reduce electricity costs of high-consuming farms significantly. Several renewable energy sources have large unused potential in the agriculture. The development of these technologies at farms is not only economically favorable for the farmers, but it also helps meeting the increased energy demands due to electrification, and establishes greener and more sustainable farming communities, which everyone will profit from. Additionally, it can pave way for inspiring agriculture sectors in other countries where renewable energy is not as developed as in Norway. There are several positive outcomes from renewable energy development and smart energy utilization in the agriculture, and it is undoubtedly an important field of research in the years to come.

1.4 Study Area

This thesis is based on using a farm as a case study for renewable energy production. The farm is located at 59.16°N, 6.11°E, in the Southwestern part of Norway, in the Ryfylke area in Rogaland.

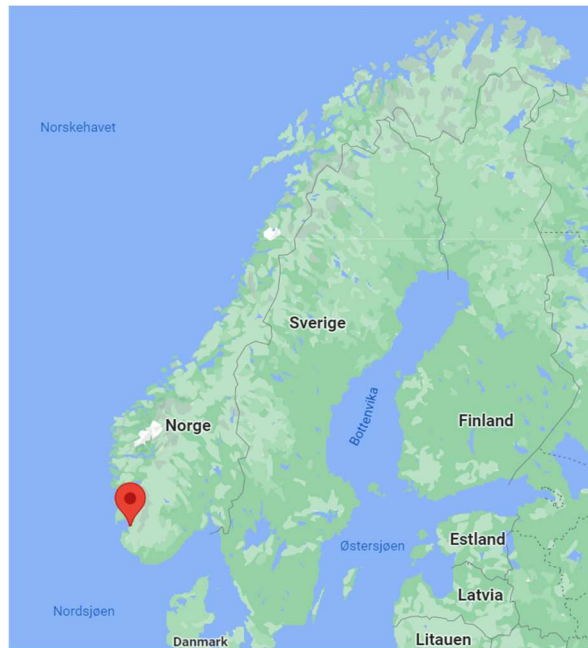


Figure 1 - Map showing the farm's location in Southwestern Norway. Created in Google Maps

The farm consists of several buildings, including the main house and buildings holding pigs, sheep, and cows. In this thesis, one of the buildings is used for analysis of solar radiation and potential PV energy production. The building holds 50 cows in the summer and 160 in the winter and is from here on called the Cow Shed. The Cow Shed has an annual energy consumption of about 60 000 kWh, which is almost four times the consumption of an average Norwegian household [5]. The main energy consumption in the Cow Shed is for lightning and electrical automatized processes like a milking robot and feeding systems, in addition to temperature regulation and circulation in the large milk tank. A control room also provides uninterrupted overview of the milking habits of each cow and a monitoring system. The Cow Shed lies at almost 600 meters away from the other large buildings at the farm. Both the isolated location and an amount of energy consumption which is thinkable to cover with own produced energy makes the Cow Shed an interesting project. Additionally, the energy consumption of the Cow Shed can be read directly from the electric meter, while the other buildings located closer to each other share meters. Developing sufficient own energy production to supply the Cow Shed could possibly enable complete grid independence. This would again allow the introduction of a microgrid where the Cow Shed could function as an autonomously operating island. The map below shows the entire area of the farm inside the black borderline, and the location of the Cow Shed and the other main buildings at the farm.



Figure 2 - Map showing the entire area of the farm and the location of the Cow Shed relative to the other main buildings. Created in ArcGIS. Spatial Reference: UTM Zone 33N. Server Layer Credits: Kartverket, Geovekst, kommuner – Geodata AS

1.5 Structure of the Thesis

Chapter 2 presents the background theory necessary to understand the methodology and results presented in the thesis. The chapter introduces the solar radiation components, theoretical knowledge on principles and technologies of PV cells, a more practical approach on installation methods and components of a PV system, and a section of wind energy.

Chapter 3 presents the methodology used to obtain the results of the research. It also introduces the collected datasets applied on calculations and analyses. It presents tools such as ArcGIS, PVsyst and AutoCAD, and describes the process of PV system sizing and assessing the economics of the project.

Chapter 4 provides the results, discussion, and uncertainties of the thesis. This chapter presents the solar potential and estimated PV energy production and compares it to energy consumption at the farm. It shows the components sized and chosen for the PV system design and further introduces variants of implementing a PV-supplied charging station. Wind

resources and wind energy production estimates are presented and compared to the PV system performance. The economics are presented, with focus on Net Present Values for the different cases. Finally, uncertainties and limitations for all parts of the results are discussed.

Chapter 5 summarizes the methods and concludes the results of the thesis. In addition, it suggests improvements and further work.

8 Appendices are added for further understanding of calculations performed and data and information applied in this thesis. The Appendices show how results, and discussions around these, are obtained.

It must be noticed that parts of this thesis are directly transferred from the Project Paper.

2 Background Theory

2.1 Transmittance

A proportion of the solar radiation that enters the Earth's atmosphere is reflected or absorbed, and never reaches the surface. This can happen due to e.g., the presence of air molecules, water vapor, clouds, dust, pollutants, forest fires or volcanoes. The transmittance is a property that refers to the ratio of the energy that reaches Earth's surface to that which reaches the upper limit of the atmosphere. In other words, the proportion of solar radiation that is transmitted through the atmosphere. Transmittance values range from 0 to 1, where 0 means that no radiation is transmitted and 1 means that all radiation reaching the atmosphere also reaches the surface [6].

2.2 Solar Radiation Components

The solar radiation that reaches the Earth's surface is divided into two components, direct and diffuse radiation. Direct solar radiation is the solar radiation that has not been affected of scattering in the atmosphere and is hence the most intensive radiation component reaching the surface. A proportion of the sunlight that passes through the atmosphere and reaches Earth's surface is scattered and reflected on its way. In this way, the affected radiation reaches the surface with lower intensity. This proportion is called diffuse solar radiation, and it reduces the direct radiation with a factor depending upon the atmospheric conditions [7]. This means that the diffuse proportion is a value between 0 and 1, where a low value usually refers to a clear sky and a higher value refers to a more overcast sky. The sum of direct radiation (S_{dr}) and diffuse radiation (S_{df}) is called the global solar radiation (S_g) [8].

$$S_g = S_{dr} + S_{df} \quad (1)$$

The global radiation received per unit area at the surface is the solar irradiation (G_g) and is usually measured in [Wh/m^2]. Figure 3 shows the different radiation components. The extraterrestrial radiation which is the radiation that reaches the top of the Earth's atmosphere, the diffuse radiation due to scattering in the atmosphere or in clouds, and the direct radiation (beam radiation on the figure) which reaches the surface without any influence. The figure also visualizes the radiation which is scattered or absorbed in the atmosphere. The radiation

reflected due to the effect of albedo is also included. Albedo describes the fraction of the solar radiation that is reflected by the surface [9].

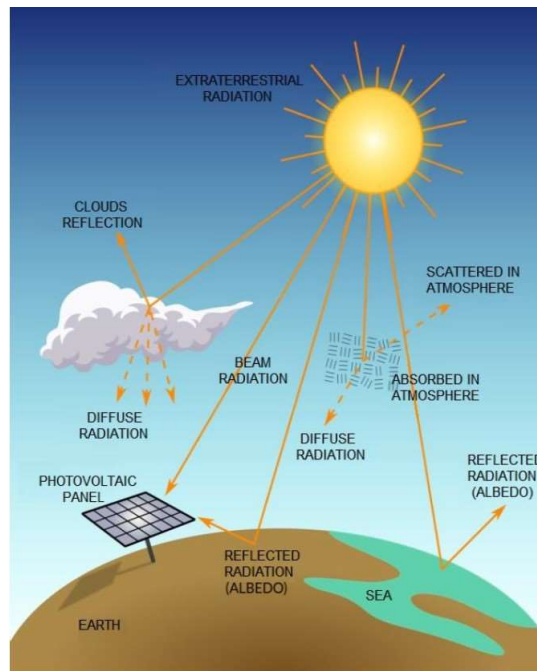


Figure 3 - Representation of the solar radiation components [9]

2.3 Photovoltaic Effect

The solar irradiation received at the surface can be seen as energy in the form of photons. When a Photovoltaic cell is hit by photons, the photon energy of the irradiation is absorbed and transferred to the electrons in the atoms of the cell. By combining two semiconductor materials in a positive-negative (p-n) junction, an electric potential between the n- and p-type semiconductor layers enables electrons to move across the junction to the p-type semiconductor, leaving a static positive charge behind. At the same time, the remaining holes move across the junction and leave a static negative charge behind. These static charges set up an electric field across the depletion region. The built-in electric field creates the force necessary to drive the current into an external circuit. When the photon energy from the solar radiation is greater than the bandgap energy, the energy gap between the conduction and valence band of the semiconductors, electrons move and create an electric flow. This gives rise to the electric current through the external circuit, which is connected to the terminals of the PV cell [10] [11].

2.4 PV Technologies and Structures

There are several types of PV cells, with different structures and materials. This section briefly discusses buildup, pros and cons, and economics for a few of the main types.

Multijunction solar cells are built up of several individual semiconductor junctions [12], which means that they consist of several p-n junctions. The different semiconductor materials absorb different wavelengths of radiation, leading to a better utilization of the solar spectrum, and hence leading to higher efficiencies. But this technology has high production costs and low availability, which makes it unsuitable for private use [13].

Heterojunction solar cells are built up of a p-n junction that consists of two different materials with different charges. This favors the electron and hole dissociation. An example of a heterojunction solar cell is the CdTe solar cell, where CdS is used as n-type and CdTe as p-type. Another example is the CIGS solar cell, which uses CdS as n-type and CIGS as p-type. These combinations give high absorption properties and thin layers. CdTe and CIGS cells are also called thin film cells due to their manufacturing process. In Homojunction solar cells, on the other side, both the n-type and p-type are of the same semiconductor material. An example is the Silicon solar cell, with n-type Si and p-type Si. The junction is usually doped by impurities like Phosphorus and Boron, which donate extra electrons and extra holes respectively, leading to the wanted charge separation [14].

The figure below shows the structure of a Multijunction GaInP/Ga(In)As/Ge solar cell to the left, and a Heterojunction CdTe solar cell to the right.

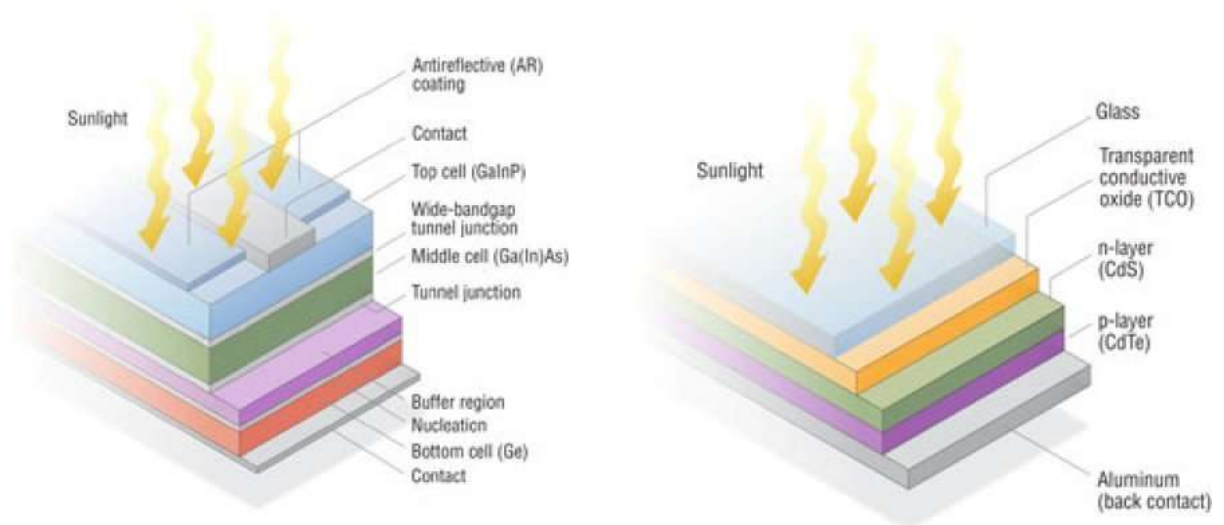


Figure 4 - Multijunction GaInP/Ga(In)As/Ge solar cell and Heterojunction CdTe solar cell [15] [16]

The most used solar cells are Monocrystalline and Polycrystalline Silicon (Si) solar cells. In Monocrystalline Si solar cells, the entire cell has a single continuous crystal lattice structure. Monocrystalline cells have a high efficiency, but require a complicated manufacturing process, which leads to higher costs compared to Polycrystalline cells. Polycrystalline cells have several grains of monocrystalline silicon which are melted and assembled into complete cells. They have a slightly lower efficiency, but they are cheaper due to the easier manufacturing process [17] [14]. Silicon cells usually outmatch thin film cells in residential installations due to their efficiency. At the same time, thin film cells are more suitable for installation on curved surfaces on buildings or vehicles.

Figure 5 shows the visual difference between a Monocrystalline module and cell and a Polycrystalline module and cell.

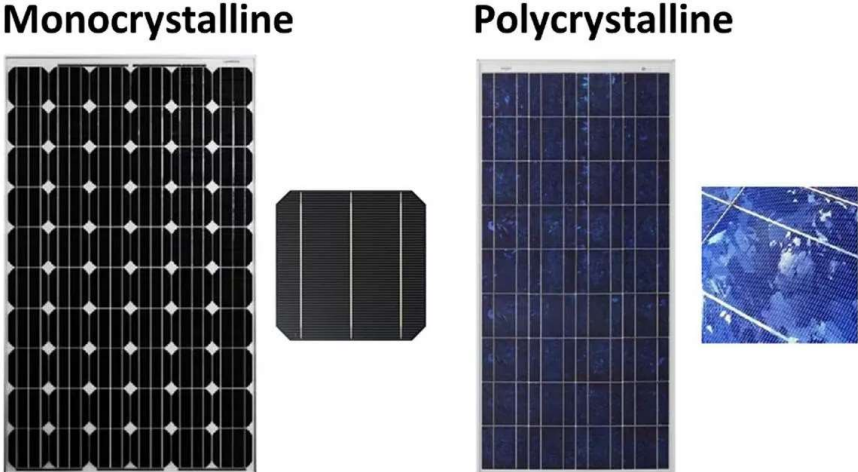


Figure 5 - Shape and appearance of a Monocrystalline and a Polycrystalline solar module and partitions of a single cell [18]

2.4.1 Prices and Outlook

PV was an expensive and low efficient technology in early years, but recent efficiency increase and price reduction has made PV one of the largest growing renewable energy resources. The global installed capacity increased with 275% from 2013 to 2020, while PV costs were reduced by 50% on global average during the same period [19]. Main factors that contributed to the lowering prices were favorable cost of capital, hardware costs and suitable profit margins, among others [20]. PV is expected to catch up with hydropower by 2030, providing almost 15% of the total electricity generation. At the same time, it will count as the cheapest renewable energy source. Silicon PV dominates the market with 95% of the share and is expected to continue to dominate due to major improvements in cost and efficiency. As

Silicon PV efficiencies continue to increase, it will be difficult for rival technologies, like thin film, to extend their market share without seeing substantial changes in prices and manufacturing costs [21]. Generally, prices for the different PV technologies depend on the complexity of the manufacturing process, which makes Polycrystalline Si the cheapest alternative, followed by Monocrystalline Si and thin film. Contrary to the decreasing prices that have been seen over many years, however, 2021 saw a price rise for PV projects. A remarkable commodity price increase for materials like polysilicon, copper and aluminum led to a near 50% manufacturing cost increase for PV modules [22]. Increased shipping costs and shipping delays due to the COVID-19 pandemic also contributed to the price hike. This brings a new challenge to the PV market and can force developers and buyers to delay projects or increase purchase prices. The prices are expected to remain high through 2022, but despite this more than 200 GW of new PV installations globally are expected during this same year [23].

2.5 PV Cell Efficiency

As mentioned, efficiency is an important parameter for comparing both costs and performance for PV technologies. The efficiency of a PV cell is defined as the ratio of the cell's energy output to the energy input from the incoming radiation. Factors like the wavelength of the light, the temperature of the PV cell and the reflection properties of the material affect the efficiency. Different types of PV cells are therefore tested at Standard Test Conditions (STC) to determine efficiencies achieved in the laboratory. At STC, the total irradiation is 1000 W/m^2 , the PV cell device temperature is 25°C and the air mass is 1.5 [24]. Multijunction cells have achieved efficiencies close to 40% under STC [25]. The nominal power output of a PV cell is also based on the cell's performance at STC. It is a measurement on the maximum possible power output at STC and is usually given in watt-peak [Wp]. The nominal power output is stated by the manufacturer and is an important factor for choosing the type of PV cells.

Once installed outside factors like radiation, shading, orientation, temperature, time of year and dust affect the PV cell's efficiency. Considering commercial PV cells, as of 2021, Monocrystalline N-type cells with Interdigitated back contact (IBC) are the most efficient (20-22.6%), followed by Monocrystalline N-type heterojunction (HJT) cells (19-21.7%) [26].

2.6 Installation Considerations

An important consideration when it comes to the utilization and the investment of a PV system is whether to install it as an on-grid or an off-grid system. In Norway, many energy suppliers offer deals that make the export of own produced energy to the grid an economically favorable initiative for customers. In that way, well-sized and financed PV investments can pay for themselves by selling surplus energy to the grid. On-grid systems also require lower investment costs compared to off-grid systems that include expensive energy storage systems. Pros and cons for three different ways of installing a PV system are discussed in the following sections.

2.6.1 On-Grid

At times with higher energy production than consumption, the surplus energy can be sent to the electricity grid, and in that way lead to an economic income from the energy supplier. Several energy suppliers offer deals that involve buying surplus energy from customers. The energy supplier then controls the energy meter and sends power to the grid if more is produced than consumed, and the customer usually gets paid the same amount as the current spot price, or a fixed amount, for each kWh sent to the grid. This enables an exchange in energy, where the PV system exports energy to the grid when the production is sufficient, and the grid supplies the consuming loads with energy when the production is lower. This utilization requires an on-grid system, which means that the system is connected to the electricity grid. A benefit with the on-grid system is that there is no need for expensive batteries for energy storage, as all produced energy is distributed instantly, either to the loads or to the grid. An on-grid system, however, requires components for controlling and converting voltage and frequency out from the PV system in order to fulfill the requirements of the grid. To ensure power quality there are regulations that must be followed and met at the Point of Common Coupling (PCC), which is a common interconnection point for systems connected to the same grid [27]. In Norway these regulations are given in the document “Forskrift om leveringskvalitet i kraftsystemet” (FoL), and they cover situations like over voltages, under voltages, voltage drops and asymmetric voltages. The regulations concern the grid company and makes sure they operate with a satisfying supply quality in the transmission system. Issues regarding power quality in the grid are reactive power control and unbalanced production. In Norway the large range of IT grids makes uneven production distribution between phases an issue, as this can create asymmetrical voltages [28]. Grid connection can also lead to breaks in the PV production during blackouts in the electricity grid, as the export

to a damaged grid affects the safety of possible service workers. During a grid blackout the PV system is hence disconnected from the grid.

In a grid connected system the generated electricity is converted from DC to AC in the inverter, and in the distribution board it is either sent to AC consuming loads or to the grid, depending on the amount of energy available.

2.6.2 Off-Grid

Off-grid means that the PV system has no direct connection to the electricity grid. The energy exchange with the grid can hence not take place, and systems for energy storage should be installed to efficiently utilize the PV system in the case of surplus energy production. This energy can be stored, and then used at times with lower or no production, like at night or on cloudy and rainy days. The problem regarding breaks in production during grid blackouts is removed. Off-grid systems are very suitable for the electrification of remote or offshore places, where the grid is either weak or not present.

In an off-grid system with a battery bank, the generated DC power is converted in the charge controller to fit the DC input requirements of the battery bank. Additionally, DC loads can be supplied. The inverter then converts the rest of DC power to AC.

2.6.3 On-Grid with Energy Storage Backup

By combining a grid connected system with an energy storage system, like a battery bank, the utilization of produced and stored energy from batteries during a grid blackout is enabled. This system could work as an on-grid system during normal grid operation, while also donating some power for the charge of the battery bank. In the case of a blackout in the electricity grid, it could then work as an off-grid system, and loads can be supplied by the stored energy from the battery bank. In this way the loss of energy production from an on-grid system during a grid blackout is removed, and at the same time the economic gains from grid export during normal operation are maintained.

On-grid systems with battery backup are suitable in areas with unstable grid supply. Like in an off-grid system, the produced DC power is converted in the charge controller and sent either to the battery bank, DC loads or to the inverter. The inverter then converts to AC power, and like in an on-grid system, the distribution board sends this power to AC loads or to the grid.

2.7 Components

2.7.1 Inverter

To be able to send surplus energy to the electricity grid, certain regulations regarding power quality must be met, as discussed in Section 2.6.1. The inverter plays a decisive role in converting the DC power produced by the PV modules to useful AC power qualified for potential grid export. Thus, the inverter both converts DC voltage and current from the PV modules to AC voltage and current, and controls the quality of the output power. A PV inverter consists of four main parts, that together perform these tasks. The maximum power point tracker (MPPT) is a circuit inside the inverter that seeks to maximize the power output from the inverter at any time. MPPT can follow different strategies and algorithms to combine the input voltage and current into the inverter in such a way that the power output is always optimized. Maximum power point tracking is a crucial process in order to maximize efficient usage of the PV system. Bulk capacitors are the second main part, and they are used to restrain ripple currents from reaching back to the PV modules. In addition, they protect the Insulated-Gate Bipolar Transistor (IGBT). The DC/AC inverter is the third main part and is where the DC power is converted into AC power with the desired output voltage and frequency. The inverter circuit consists of multiple IGBTs with a diode connected in anti-parallel to each transistor. The diodes protect the transistors from reverse over voltages. The configuration can be seen in Figure 6, which shows the input DC voltage, the three half bridges composed by the transistors and diodes and the connections between each half bridge and one of the three phases. By controlling the turn on and turnoff of the transistors the output voltage will follow a square wave. Using the Pulse Width Modulation (PWM) technique the waveform is made as sinusoidal as possible. The last part of the inverter is a line filter, usually a LC filter. The filter controls the quality of the output power and assures low harmonic distortion of the sinusoidal voltages [29].

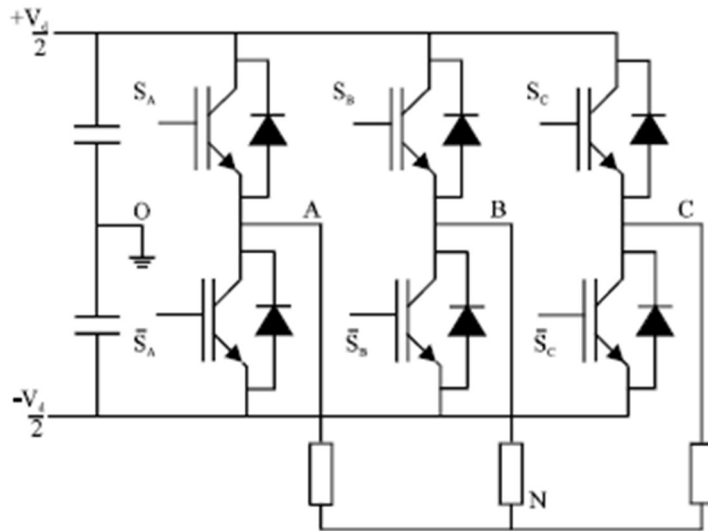


Figure 6 - Simple Three-Phase Inverter Circuit [79]

There are three main types of inverters based on the way the inverter is connected to the PV system.

Using a central inverter there is only one inverter for the entire system. This configuration requires a DC combiner box, which gathers all parallel connected PV strings, and connects them to the inverter. The set-up with a central inverter is cheap and easy to manage, but it also makes the system sensitive to production loss in single modules and downtime of the inverter [29].

When using string inverters each string of PV modules is connected to an inverter. This set-up has low maintenance loss, wide input voltage range and several MPPT inputs. However, it is more expensive than the central inverter, and the problem regarding failure of one single module is not erased, as the entire string would still suffer [30].

Microinverters are connected to one or a few PV modules, which means that DC power produced from each module is converted to the desired AC power right at the module. Microinverters enable independent MPPT for each module, leading to optimized performance and reduced loss in case of single failures. On the other side, this set-up requires higher initial costs and complex management due to the high number of components [29] [30].

2.7.2 Cables

There are two main types of cables in a PV system, DC cables and AC cables. The DC cables are the connections between the PV modules, and the modules and the inverter. On the other

side of the inverter, the rest of the electrical equipment is connected through AC cables. In the DC section of a PV system the cables need to be able to withstand several challenging conditions. Unlike typical PVC insulated DC cables, PV cables have an XLPE insulation with a high resistance to sunlight, heat, freezing and regular contact with rainwater [29] [31]. XLPE PV cables are constructed with copper or aluminum conductors, flame retardant cross-linked polyethylene insulation and a flame retardant cross-linked outer sheath, as shown on the figure below.

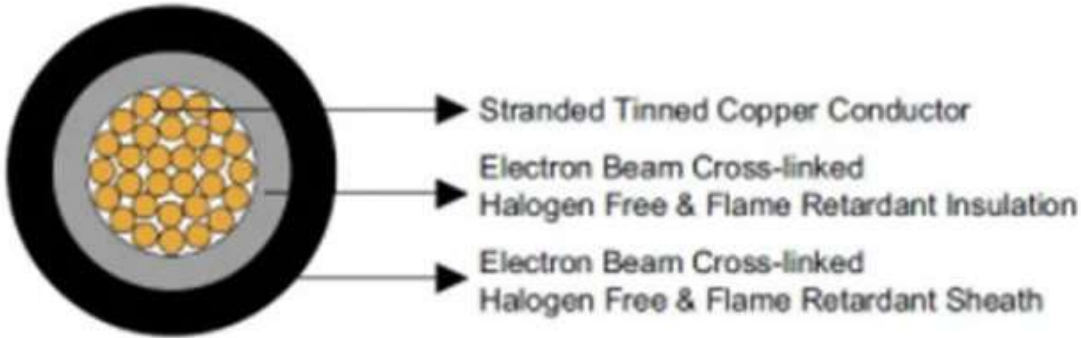


Figure 7 - Cross section of a XLPE insulated Solar PV cable [80]

When it comes to selecting and mounting cables in a PV system, several requirements are established. The cables must be dimensioned to support the maximum output voltage from the modules. Exceeding the voltage rating of the cable can lead to break down of the insulation between cable cores, or between a cable core and earth, which can cause short-circuit or fire. Cables must also be able to withstand the maximum short circuit current of the system, for protection against overload [29]. Cables should not be mounted directly to the surface of the rooftop/building, they should have support to prevent stress fractions due to wind and snow loads, and they should be protected against sharp edges. The cables should also be dimensioned to keep the voltage drop at a minimum. Out of the output voltage from the PV modules, a portion is lost on its way to the loads that consume the generated electricity. The length and cross section of the cable, the power factor and the resistivity and reactance of the conducting material all affect the voltage drop through a cable. The voltage drop in a PV

system can possibly be high, due to low output voltage and high output current. However, the voltage drop should not exceed 3% of the modules' voltage at maximum power [32].

Several cable manufacturers offer many different variants of cables based on technical data, like temperature range, nominal voltage and current and bending radius, cable structure, installation methods and other properties.

2.7.3 Protective Devices

Every section of a PV system needs a sufficient protective system to protect components and surroundings against fault situations. These situations can occur due to failures in the different components, like the PV modules, cables, inverters, or batteries, or due to external impacts like lightning. Several devices, both on the DC and AC side of the system, form the protection system. They are also necessary to be able to perform service on the system or isolate specific parts.

Switch disconnectors are installed on the DC and AC side of the inverter and close to the PV modules and enable service and maintenance. The inverter needs to be able to switch off in case of a blackout of the grid, if the system is grid connected. Fuses or circuit-breakers are installed to protect cables from over-current. Over-currents can occur due to short-circuit currents or ground faults, and protective devices are therefore sized based on the maximum possible circuit currents [33]. These devices also protect the modules against reverse currents, which can occur due to certain modules being shaded or covered, leading to faults or temporary unbalances in the system [34]. The advantage of a circuit-breaker, in addition to providing isolation, is the automatic switch off in case of a fault, and the manual reset afterwards. Fuses are single use devices, as they usually blow out or melt during the fault. They are, however, cheaper, and smaller than the costlier and larger circuit-breakers [35]. Surge Protective Devices (SPD) are installed to protect against over voltages. SPD must be chosen based on operating voltage values and are primarily meant to protect modules, cables, and inverters. Although inverters generally have internal protection against over voltage, SPD at the inverter's terminals can prevent surges from reaching the inverter and hence restrain the need of service and maintenance [34].

All exposed conductive parts of all the equipment in a PV system must be grounded to protect against indirect contacts [34]. The equipment is connected to a grounding conductor which

transports potential ground fault currents to earth. The two types of grounding in PV systems are equipment grounding and system grounding.

2.7.4 Battery Energy Storage

Adding batteries to a PV system is especially useful if there are times where the energy output from the system is higher than the consumption. A PV system generally produces the most during daytime when the spot prices are low. At the afternoon and evening the spot prices usually rise, while the energy production decreases or cuts out at the same time. By storing potential surplus produced energy at times with highest production in batteries, this energy can be used later at the day during the low production hours. This can result in a cost-effective utilization of the PV system, as decreasing the dependence on the grid in afternoon and evening hours can reduce electricity costs due to higher spot prices at those times.

A large number of manufacturers offer several battery types on small and large scale and with different technologies. When choosing batteries for the PV system, there are some certain specifications that should be considered for the many options. Obviously, the capacity of the battery, the total amount of energy that can be stored in the battery in [kWh] or [Ah], needs to be dimensioned based on the available output from the PV modules. Meanwhile the power rating is the amount of power the battery can supply at a given time in [kW]. The depth of discharge (DoD) is another important factor to notice. Due to the chemical composition of a battery, it always needs to retain some charge. Discharging a battery 100% will shorten its lifetime, hence DoD refers to the maximum portion of the battery's capacity that should be used. The round-trip efficiency refers to ratio between the energy needed to charge the battery and its useful energy output. A higher round-trip efficiency is important for an efficient use, and for making the battery cost-effective [36]. The battery life cycle describes the lifetime of a battery, as it refers to the number of complete charge-discharge cycles the battery can perform before the nominal capacity drops to less than 80% of the initial capacity [37].

In a PV system, the battery is supplied with DC power from the PV modules. It can be connected between the modules and the inverter in a DC coupled configuration, or after the inverter in an AC coupled configuration, in which case it will require an own inverter converting from AC to DC. Additionally, the DC-DC converter of the charge controller converts the DC power to the desired input level [38]. A charge controller ensures the optimal working conditions for the battery by preventing it from overcharging and limiting excessive

discharge. Modern charge controllers also include MPPT, to maximize charging of the battery [39].

A battery is not only functional for energy storage and autonomy in a PV system. It can also work as a voltage stabilizer by suppressing voltage variations and protect loads from damage. Another area of use is to supply electrical loads like motors or other inductive loads with the sufficiently high starting currents needed [37].

2.8 I-V Characteristics

The final set up of modules in a PV system, the PV array, can consist of modules connected both in series and parallel. Modules connected in series create a string, and the number of modules in a string depends on the inverter input voltage. The voltage output of a string of PV modules is added up for each module in the string, which means that the open-circuit voltage V_{OC} of each module times the number of modules gives the maximum total voltage output of the string. The string output voltage must fit the inverter voltage range and should hence deliver a voltage higher than the minimum inverter voltage and lower than the maximum inverter voltage [40]. Modules connected in parallel determine the current output of a PV array. Like the voltages add up in a series connection, the current adds up for each module connected in parallel. The maximum total output current is then given by the short-circuit current I_{SC} of each module times the number of modules in parallel. At the same time, the voltage remains constant. The correct configuration of series and parallel connected modules in PV system is important to get the desired output values for voltage and current, and for fitting those to the inverter and battery input ranges.

Open-circuit voltage V_{OC} is the maximum voltage that a PV cell can deliver and occurs when the current is 0. V_{OC} depends on the ambient temperature and the temperature coefficient of the cell and increases with decreasing temperature [41]. The short-circuit current I_{SC} occurs when the cell is short circuited and the voltage is 0, and it is the maximum current output from a cell. I_{SC} also depends upon factors like temperature, cell area and absorption and reflection properties of the material.

The maximum power output of a PV cell is obtained at a certain voltage V_{MPP} and current I_{MPP} . This value is called the maximum power point P_{MPP} . The I-V curve in Figure 8 shows the varying current output with voltage for an operating PV cell. It also shows the power

output curve in green, reaching its maximum in P_{MPP} . The maximum power point is given by Equation 2.

$$P_{MPP} = I_{MPP}V_{MPP} \quad (2)$$

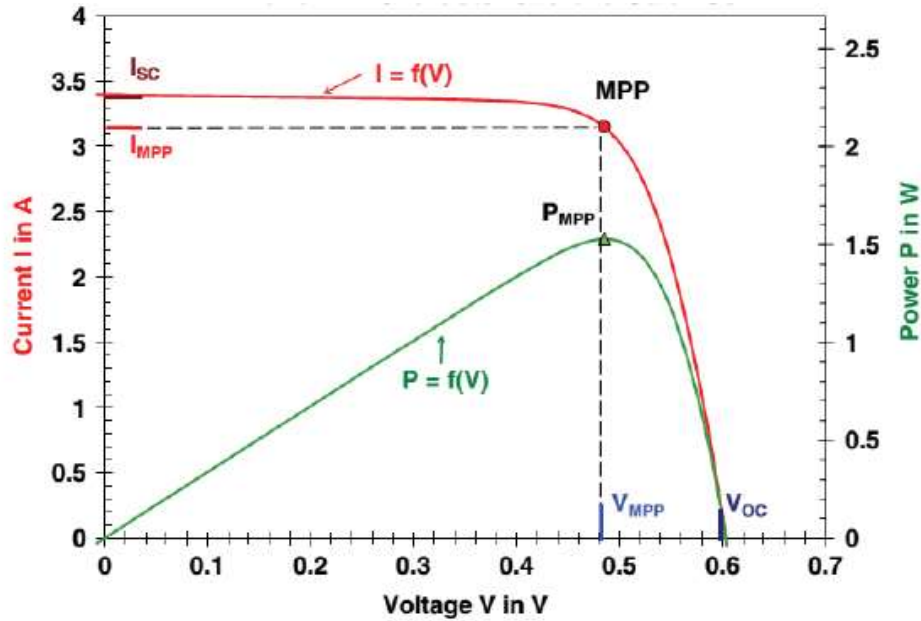


Figure 8 - I-V curve and power output curve for an operating PV cell [81]

2.9 Performance Ratio

The performance ratio (PR) is the ratio of the actual energy output of a PV system to the theoretical output. It describes the proportion of energy that is available after the impacts of energy reducing mechanisms in the installation. PR can hence be calculated by the following simplified Equation 3 [42].

$$PR = \frac{\text{Actual PV output in kWh p.a.}}{\text{Nominal PV output in kWh p.a.}} \quad (3)$$

The actual output is read from a solar generation meter, while the nominal output is given by the incoming solar irradiation at the PV modules times the efficiency of the modules. High-performance PV systems can reach a PR of up to 80% [42]. A factor that affects PR is

conduction loss in the cables of the system. Out of the output voltage from the PV system, a portion is lost on its way to the loads that consume the generated electricity. The length and cross section of the cable, the power factor and the resistivity and reactance of the conducting material all affect the voltage drop through a cable. The voltage drop in a PV system can possibly be high, due to low output voltage and high output current. However, the voltage drop should be kept at a minimum to maintain a high PR. At maximum load, the voltage drop from the PV module to the consumer circuit should not exceed 3% of the module's voltage at maximum power [32]. Another important factor that affects PR is loss in the inverter. The inverter converts from direct current (DC) to alternate current (AC), and up to 7% of the total production can be lost in the inverter [43]. The efficiency of the inverter depends on the conditions, and in particular the ratio between the total capacity of the inverter and the actual power generated. This ratio is called the partial load ratio (PLR). A low PLR leads to low conversion efficiency in the inverter, which means that the conversion efficiency is at its lowest, and power loss at its greatest, when there is minimal production [43]. This is why the inverter in a PV system should have a proper capacity, and not be over dimensioned.

2.10 Temperature Effect

A solar cell's performance is affected by the temperature, as both efficiency and performance ratio depend linearly on the operating temperature. Lower temperatures lead to higher performances, which is why cold and clear weather is considered as the best condition for PV production [44]. This is also an interesting ability for PV projects in Norway, as low temperatures in the country can possibly equalize the disadvantage of lower irradiation compared to warmer southern countries. A solar cell's temperature coefficient describes the variation in power output from a PV module when temperature varies from STC. Different types of solar cell technologies have different temperature coefficients. Some average temperature coefficients are 0.446%/°C for Mono c-Si cells, 0.387%/°C for Multi c-Si, 0.234%/°C for a-Si, and 0.172%/°C for CdTe cells [45]. The effect of temperature coefficient on the total efficiency of a PV module can be expressed with the following equation (4).

$$\eta_{PV} = \eta_{ref} - \mu(T - T_{ref}) \quad (4)$$

η_{PV} is the total efficiency of the module, η_{ref} is the reference efficiency at 25°C, μ is the temperature coefficient, T is the actual operating temperature of the module and T_{ref} is the reference temperature (25°C). Temperature coefficients can be useful when determining which PV technology to install in different climates. Low temperature coefficients are suitable for warm areas, where temperatures are higher than STC temperature, in order to minimize the efficiency loss. At the same time, high temperature coefficients are preferable in colder areas, to make use of the enhanced efficiency. Another value that can be used to analyze a PV module's performance during different temperatures is the nominal operating cell temperature (NOCT). NOCT is stated by the manufacturer and gives the module temperature at irradiance of 800 W/m² and ambient temperature of 20°C [46].

2.11 Energy Production

Based on the incoming solar irradiation, the temperature effect on the efficiency and the performance ratio, the total energy production of a PV system can be estimated with the following equation (5).

$$P_{PV} = G_g \cdot \eta_{PV} \cdot PR \cdot A \quad (5)$$

In Equation 5, P_{PV} is the total energy output of the PV system, that is the available energy on the AC side of the inverter. The production will give values in [Wh] or [kWh] based on the unit of the average global irradiation value, G_g . η_{PV} is the efficiency of the PV cells which is related to the operating temperature through Equation 4. PR is the performance ratio, and A is the total area covered by PV modules.

2.12 Wind Energy

Trying to meet the energy demands at a farm only with PV is difficult due to the large seasonal variations in energy production. Wind energy can provide a more stable source of energy, when looking at seasonal variations, and contribute to meeting the demands in the periods with lower PV production. The wind industry in Norway has grown steadily since the early 1990s, and the total installed capacity was slightly below 4 GW at the end of 2020. Wind energy has hence become an important contributor to the renewable energy supply, and accounts for 10% of the production capacity in Norway [47]. Wind turbines convert the

kinetic energy of the wind into electrical power through the rotation of turbine blades and conversion in the generator. Hence the amount of energy produced by a wind turbine depends on the wind speed at the specific location. Many areas along the Norwegian west coast experience favorable wind conditions, proximity to the grid, and large areas with relatively low population density, which makes these advantageous for wind energy projects [48]. Investment in wind energy projects has increased notably in recent years, but most projects are connected to utility-scale wind farms. Using wind energy as a renewable energy source at residential or industrial level is still relatively untested in Norway.

Like PV systems, small wind turbines (SWTs) can be installed at residential level and connected to the electricity grid as an on-grid system. In that way, surplus energy can be sent to the grid and result in economic income. They can also be installed as off-grid systems with energy storage. Off-grid SWTs have traditionally been suitable for rural electrification and hybrid systems in combination with PV. The rotor, the generator/alternator and the tower are the main components of a SWT. Most small turbines also use a tail to hold the turbine faced against the wind and to enable folding at high rotational speeds. The tower is commonly latticed, guyed or tubular, and the rotor blades can be produced by several materials like plastic, wood, or aluminum, depending on the design. When it comes to the generator, the most common technology is the direct drive permanent magnet. Another technology is the induction generator, which requires a gearbox to drive the generator at higher speeds. The output of the generator is usually three-phase AC which must then be conditioned through an inverter before it can be fed to the grid. The inverters synchronize with the grid voltage and frequency with only small conversion losses [49].

There are two different main designs of SWTs, horizontal axis wind turbines (HAWT) and vertical axis wind turbines (VAWT). The HAWT is a proven technology, presents higher performances and efficiencies than VAWT and hence dominates the SWT market. The prices are also higher for VAWT compared to HAWT. VAWT, however, requires less space and emits lower noise levels. Additionally, it does not need to be installed into the wind direction [49].

The nominal power, or rated power, of a wind turbine is obtained at a certain nominal wind speed. The International Electrotechnical Commission (IEC) defines small wind turbines as turbines with a nominal power output less than 50 kW [49]. The relation between power output and wind speed for a wind turbine is presented through a power curve, which is an

important tool for estimating energy production. Two other important parameters are the cut-in and cut-out wind speeds for the turbine. The cut-in wind speed is the minimum wind speed required for the blades to start rotating and the turbine to generate power. If the wind speed reaches the cut-out wind speed, the braking system of the turbine stops the rotation of the rotor blades to avoid risk of damage.

Economics and environmental and social considerations are the largest challenges for residential wind energy installation. Prices for SWTs are unavailable and varying, and the limited access to manufacturers and installers in Norway makes it challenging to forecast costs of purchase, installation, and maintenance for a wind turbine. Social concerns like noise, vibrations, shadowing and aesthetic impacts, and environmental concerns like the impacts on birds, recreation and landscape are also challenges, both on utility and residential level. These considerations can cause delays, downscaling, increased costs, and cancellation of wind energy projects.

3 Data and Methodology

3.1 Solar Radiation Analysis in ArcGIS

To map the solar potential on the buildings on the farm the software ArcGIS Pro is used. ArcGIS Pro is a professional desktop GIS application from Esri, which makes it possible to visualize and analyze data and maps. It allows creating tables, layouts, charts, reports, and other presentations of data [50]. ArcGIS Pro includes a tool called Area Solar Radiation which derives incoming solar radiation from a raster surface. The tool considers parameters such as latitude, for calculations such as solar declination and solar position, as well as the sky size, diffuse proportion, transmittivity and surrounding landscape, vegetation, and infrastructure. It allows the determination of the period for the analysis, and the interval for the calculations [6]. To obtain a map suitable for solar radiation analysis in ArcGIS, a Digital Surface Model (DSM) is downloaded from the website hoydedata.no. The model, which is downloaded as a TIF-file, is then uploaded to ArcGIS. In the next step, the ArcGIS Pro account must be connected to a server at Geodata, which is market leading in Norway when it comes to Geographical Information Systems and associated technologies [51]. An account in Geodata is created, and a layer that contains all building footprints in Norway is saved for usage in ArcGIS. The layer with building footprints is then uploaded to ArcGIS. This is necessary in order to be able to perform the solar radiation analysis only on rooftops of buildings, which is much less time consuming than an analysis of the rooftops and all the surrounding terrain. A smaller polygonal area around the specific building is extracted from the DSM using the Extract by Mask tool to reduce computing times, and Area Solar Radiation is performed on the extracted area with the layer containing building footprints as mask. In this thesis, only the parts of the rooftops that are found suitable for PV installation based on the solar radiation analysis are taken into further research. The Extract by Mask tool is then again used to isolate the desired rooftop on the specified building (see Figure 11), and Area Solar Radiation is run. After each run, values for diffuse, direct, and global irradiation on the desired area can be obtained. The mean values for global solar irradiation are collected, and this results in Table 1. The values resulting from the Area Solar Radiation tool are given in $\left[\frac{Wh}{m^2}\right]$.

3.2 Temperature and Wind Data

Temperature data is used in this thesis to investigate the PV system's dependence on temperature. The dataset contains average monthly temperature values from the weather

station Fister – Sigmundstad (station nr. SN45870), from January 2019 to September 2021. The weather station lies 4.25 km away from the farm in overhead line, and at roughly the same height (station at 30 meters above sea level [52]). Measurements from the weather station should hence give an adequate indication on the climate at the farm. An uncertainty could be the weather station’s location straight by the sea, which can affect the temperatures, and hence make them differ from the ones at the farm which is located a bit further inland. However, for the purposes of this thesis, rather looking at temperature variations than exact values, it should be acceptable to neglect this, as variations in temperature can be assumed to be similar. The temperature dataset is downloaded from the website seklima.met.no, owned by the Norwegian Meteorological Institute (MET), which allows free collection of climatological data and statistics from weather stations all over Norway. The same weather station and website is also used to obtain temperature measurements necessary in the process of sizing the PV system. Additionally, wind data is collected for estimating potential wind energy production. The dataset contains hourly average wind speeds for 2021. There are probably irregularities between the wind speeds at the weather station and the farm. The surrounding terrain can affect the wind speeds differently, but for the purpose of this thesis the wind speed data should give reasonable indications. Uncertainties regarding the wind speed dataset are also discussed in Sections 4.6 and 4.9.6.



Figure 9 - Locations of the weather station and the farm. The distance between them is 4.25 km. Created in Google Earth

3.3 Simulation in PVsyst

PVsyst is a photovoltaic software for sizing and simulating PV systems. The software is able to import geographical and meteorological data from several sources and presents a full report of the performance of a PV system at the given location. The report includes specific graphs and tables for total energy production [MWh/y], performance ratio [%], specific energy [kWh/kWp] and the different types of losses, among many other things. The configuration of the simulated PV system can be set up manually by choosing factors like available area, tilt, types of PV cells and inverter, and the number of strings and modules in series. It is therefore a good tool for analyzing a system's behavior and find potential improvements. Simulations can be performed for both on-grid and off-grid systems, and with different field types, like fixed tilted plane, seasonal tilt adjustments and several variants of tracking planes. PVsyst embeds a warning and errors messaging system which describes the present problem, in case of for example a mismatch, wrong sizing or unfulfilled requirements [53].

In this thesis PVsyst is used as a tool for comparing and validating the calculated energy production estimates of the PV system. Although there are several significant differences in the ways the results from the calculations and the simulation in PVsyst are obtained, it can give an indication on how realistic the calculated values are. In PVsyst, the Project design tool is used to simulate a system corresponding to the one the calculations are based on. The Cow Shed's coordinates (59.16°N, 6.11°E) are specified, and a meteorological data file from the area is imported. The data contains global and diffuse horizontal irradiation, ambient temperature, and wind velocity. PVsyst imports the meteorological data from a database called Meteonorm. The database creates synthetic data for any site by interpolation between the 3 nearest weather stations. If there are no stations close enough the synthetic data is generated with satellite data. For creating irradiation data in remote areas, satellite data is used if there is no radiation measurement station nearer than 50 km from the desired location. If the closest station is more than 10 km away, a mixture of station and satellite data is used. PVsyst also includes a tool for importing other meteorological data sources like Solargis, Reuniwatt and Vortex Solar, however, these are paid services and are not explored in this analysis [54]. Further, the orientation of the rooftop and the available area is specified and PVsyst then suggests a configuration with the type of PV modules and a corresponding inverter. These components can also be chosen from the internal database, which includes products from a large number of manufacturers. The simulation is run, resulting in a report including graphs

and tables describing the performance of the simulated PV system. These results are compared to the production estimates which are calculated based on the analysis in ArcGIS.

3.4 Consumption Data

Energy consumption data for the farm is used to compare energy production and consumption. The consumption data is collected from the website of the grid company Lyse Elnett, where consumption measurements for the whole farm can be viewed down to hourly resolution. The website also provides information on grid rent costs and other specifications regarding the farm's energy consumption. Every building does not have its own electric meter, which means that some meters measure the total consumption of several buildings. The building of interest in this thesis, however, has its own meter, and consumption can therefore be read directly from the meter. Monthly energy consumption in [kWh] is downloaded for all months from January 2019 to December 2021, for the Cow Shed only and for the entire farm. The monthly consumption values are given in whole numbers, but since the size of the values is in thousands of kilowatt-hours, this should not give any problems for the purpose of comparing them with estimated production values. The consumption data is also used in the economic analysis, for calculating costs connected to energy consumption. In this way, it enables calculating savings due to own energy production.

3.5 PV System Sizing

For a PV system to perform as efficiently as possible, it is important to choose the different components that build up the system carefully. There are many PV system sets available on the market, with all the needed components included, but in this case the components are chosen individually to get a deeper understanding behind the capabilities and challenges of each component. Components like the PV modules, inverters and cables are all dependent upon several characteristics unique for their performance. These characteristics must be matched in the best possible way to avoid losses due to for example mismatch in cells, undersized or oversized inverters, or incorrectly dimensioned cables.

Mostly, when sizing a PV system, the energy consumption of the specific building is the deciding factor for the size of the system. In this case, however, it has been shown that a PV system on the rooftop of the Cow Shed is able to produce significantly higher amounts of energy than the consumption during some months of the year. This enables the possibility to utilize this surplus energy in a smart way, and hence the process of sizing this system is based on maximizing the size of the system based on the available rooftop area rather than limiting

it to the energy consumption. It is sized as an on-grid system, where the maximum power output available on the rooftop is desired.

3.5.1 PV Module

PV modules are mainly categorized by the stated nominal power output at STC, but several electrical characteristics like maximum power point voltage and current, open-circuit voltage, short-circuit current and efficiencies determine the performance of a PV module. Temperature coefficients, nominal operating cell temperature (NOCT) and mechanical characteristics like the module's dimensions must also be considered in the sizing process. The goal in this thesis is to choose a commercially available module type suitable for installation on the rooftop of the Cow Shed.

3.5.2 Inverter

When choosing a suitable inverter for the PV system, it is important to coordinate the inverter's properties with the ones of the PV array. In this thesis the method used for choosing the inverter is based on proposing a specific inverter and performing calculations to test the suitability of the inverter in combination with the PV modules. When proposing an inverter, it must be considered whether it should be a central inverter, microinverter or string inverter. In this case a string inverter is chosen in order to avoid the high costs of installing microinverters and at the same time have MPPT inputs enough to optimize the production and take losses in single modules into account. As the voltage delivered by the PV modules depends on the number of modules connected in a string, the string size must be determined in order to match it with the input voltage of the inverter. The minimum string size should not deliver a voltage lower than the low end of the MPPT range of the inverter, or else the inverter is unable to optimize the possible output. The minimum and maximum string sizes are based on the maximum power point voltage V_{MPP} and open-circuit voltage V_{OC} of the PV modules, in addition to the minimum MPPT range and maximum DC input voltage of the proposed inverter. These properties are found on the datasheet of the inverter. The following equations (6-7) show the procedure of finding the minimum and maximum string sizes.

$$N_{S\ MIN} = \frac{\text{Minimum MPPT Range}}{V_{MPP}} \quad (6)$$

$$N_{S\ MAX} = \frac{\text{Maximum Input Voltage}}{V_{OC}} \quad (7)$$

Afterwards, the calculated maximum string size is checked up against the top end of the MPPT range. The voltage output of the string should stay within the MPPT range of the inverter. The inverter input voltage must also be matched to tolerate the PV output voltage in the case of extreme air temperatures, as V_{OC} increases with decreasing temperature. On the website seklima.met.no the coldest measured temperature in the period from 2007 to 2022 at the weather station Fister – Sigmundstad is collected [55]. With the PV module's NOCT and temperature coefficient the true output voltage of the modules in the case of a minimum temperature day is calculated and compared to the inverter's maximum input voltage. This is done by first finding the voltage change per °C:

$$\text{Voltage change per } ^\circ\text{C} = V_{OC} \cdot \text{Temperature Coefficient of } V_{OC} \quad (8)$$

Then calculating the voltage increase on a minimum temperature day:

$$\text{Voltage increase} = \text{Voltage change per } ^\circ\text{C} \cdot (\text{NOCT} - \text{Minimum Temperature}) \quad (9)$$

Before calculating the true module voltage on a minimum temperature day by adding the voltage increase to the open-circuit voltage:

$$\text{True module voltage} = V_{OC} + \text{Voltage increase} \quad (10)$$

The true module voltage will give a new output voltage of the maximum string size which must be within the maximum input voltage of the inverter. If the voltage output exceeds this

value with the string size calculated with Equation 7, this string size must be reduced until the output voltage is within the inverter input.

When the string size is determined the PV array configuration can be completed and matched to the available MPPT inputs. This gives rise to determining both the number of modules and inverters.

3.5.3 Cables

Connecting the different parts of a PV system with the proper cables is important for the performance, for minimizing losses and for protecting components against over-currents. In this case two separate cables are sized, a DC cable for the connection from the last PV module in a string to the inverter and an AC cable connecting the inverter to the distribution board. The standards of the Norwegian Electrotechnical Committee (NEK 400-7-712) on the installation of PV systems are followed during the sizing process. The AC cables connect each inverter to the distribution board, which means that the number of AC cables required is equal to the number of inverters. The DC cables connect the end of each string to the inverter input, which means that the number of DC cables required is equal to the number of strings. The DC cables must have a current carrying capacity (CCC) rating greater than or equal to the maximum short-circuit current, $I_{SC\ MAX}$, of the PV string. $I_{SC\ MAX}$ is calculated by adding a safety margin to the nominal short-circuit current, I_{SC} , of the PV modules. The CCC of the cable, called I_Z , is hence given in Equation 11.

$$I_Z \geq I_{SC\ MAX} \geq 1.25 \cdot I_{SC} \quad (11)$$

In addition, a maximum permissible voltage drop in percentage, ΔV_d , of 1.5% through the cable is used. The voltage drop, V_d , is calculated with the maximum power point voltage V_{MPP} of the modules in a string.

$$V_d = 1.5\% \cdot V_{MPP} \cdot N_S \quad (12)$$

In Equation 12, N_S is the number of modules per string. The cross-sectional area (CSA), A_{CABLE} , of the cable is then calculated with Equation 13.

$$A_{CABLE} = \frac{\rho \cdot 2 \cdot L \cdot I_B}{V_d} \quad (13)$$

Where:

- ρ = Resistivity of the conducting material (Cu or Al) in [$\Omega\text{mm}^2/\text{m}$]
- L = Length of the cable in meters (multiplied by 2 to consider the total circuit cable length)
- I_B = The load current that the cable must be able to conduct (in this case $I_{SC\ MAX}$)

Regarding the AC cable connecting the inverter to the distribution board, the same method is used, only with a separate cable length and I_B , which in this case is the maximum output current of the inverter. Again, the maximum permissible voltage drop is set to 1.5%, which means that the total voltage drop from the PV modules to the distribution board should not exceed 3%. It must be noticed that the length of the cables is assumed. To make use of the high output voltage of the PV strings, the assumptions are based on the inverters being located inside the building as close to the distribution board as possible, which leads to a significant distance between the modules and the inverters and a smaller distance between the inverters and the distribution board. The high DC voltage will then be transported longer than the lower AC voltage, which is done to minimize the voltage drops and be able to neglect phase compensation measures in the AC cables. From the calculated CSA, the closest standard CSA given by cable manufacturers is chosen, and the CCC and rated voltage for the cables are checked. The actual voltage drop through the chosen cable can then be calculated with Equation 13.

3.6 AutoCAD

The computer-aided design (CAD) software AutoCAD is used to make a design of the PV system sized with the steps presented above. AutoCAD is useful for the draft and design of 2D and 3D models for architecture, engineering, and construction [56]. The PV system design is made after the components are sized and chosen to give a complete overview of the system.

This is helpful for investigating the system and crucial for possible future installation. Other paid designing software like PVCAD, SOL CAD PV and PVcase are more specialized into designing PV systems, but AutoCAD is a software easy to use and includes several tools which make the design process precise and efficient. Its high degree of freedom also makes the design creative and independent. The Copy and Mirror tools enable quantifying of each component so that it only needs to be designed once, and the Table tool enables creating informative tables to support the drawings. In this thesis the design is presented in single-line diagrams, as a way to document the engineering process of the system. Single-line diagrams provide detailed overviews of the components' characteristics and their compatibility, and they show electrical connections and protective devices. Single-line diagrams are hence useful for ensuring that the components and circuits in the system fulfill the required codes and standards [57]. The PV system is designed as an on-grid system and shows the configuration and connection of each component from the PV modules to the grid. It includes the sized DC and AC cables and inverters, and protective devices as presented in Section 2.7.3. The connection to the grid through the Point of Common Coupling (PCC) is shown together with the energy supplier's controlling devices for energy export to the grid. AutoCAD is also used to design the charging systems for the electric tractor, and the resulting figures are found in Section 4.5.1.

3.7 Hybrid Power System

To investigate further decrease in the dependence on the electricity grid a Hybrid Power System (HPS) consisting of the presented PV system and wind power is explored. The goal is to investigate the performance of the HPS in relation to the PV system and the wind turbine alone and find correlations regarding energy production and compare those with energy consumption on the farm. In addition, the economics are investigated and compared. Wind power is often used in combination with PV to let the two technologies weigh up for each other, and hence increase the ability to meet the energy demands. A common phenomenon is lower wind speeds and higher solar irradiation in the summer, and higher wind speeds combined with lower irradiation in the winter. By estimating the production of a SWT at the farm, the mentioned coherences are analyzed. The average wind speed for each hour of 2021 is collected from the website seklima.met.no, owned by the Norwegian Meteorological Institute (MET). The weather station Fister – Sigmundstad is again used, as it was for collecting temperature data for the PV production estimates. The collected wind speed data will not give exact insights to the wind resources at the farm, due to the distance (4.25 km)

between the farm and the weather station. However, the data should be satisfying to give an indication on the wind power outlook at the farm. The power curve of the chosen turbine is found on the datasheet and gives power output values for each wind speed between the cut-in and cut-out values. Using a Python code, which takes the hourly wind speeds and the power curve as input, hourly energy production estimates in [kWh] are obtained. As the power curve dataset contains power values for each whole wind speed value, an interpolation function is used on the power curve dataset to assign values to decimal values of the wind speed dataset. By adding up hourly production estimates, both monthly and total annual production is calculated. The code is included in Appendix F.

A detailed design of the entire HPS is not provided in this thesis. Considerations regarding on-grid or off-grid installation of the wind turbine, including energy storage, in addition to possible combined hybrid controllers are not executed. The wind power system performance is investigated to map the potential of wind energy, and the ability of functioning as a component towards increased self-supply at the farm. The location of the turbine should be based on local wind speed measurements and wind directions but is not considered as there are no such statistics available for the specific site.

3.8 Economic Analysis

An economic analysis is performed in Excel to investigate the profitability of the PV system and the wind turbine. It investigates the economics of the PV system and the wind turbine individually and as a combined HPS and calculates profitability looking at the entire farm. Calculations for three separate cases are therefore performed. Looking at the entire farm enables the visualization of how own produced energy can reduce the total electricity costs of the farm and is therefore the most reasonable approach when assessing profitability.

To be able to perform the analysis several factors must be determined. The annual energy production from the PV system and the wind turbine are crucial factors when looking at the economic aspects. Energy consumption collected from Lyse Elnett is another important factor. For the PV system and the wind turbine, investment, installation, and maintenance costs are specified, in addition to supporting deals and degradation rates. The costs connected to energy consumption are divided into two sets of values. Costs regarding grid rent are collected from the grid company Lyse Elnett and include four different rates. The fixed link is a fixed annual cost, as is the fee to the energy fond Enova. The energy link and consumption fee are based on the consumption and are given in NOK/kWh. Costs regarding electricity are

collected from the energy supplier NorgesEnergi. These include a fixed annual subscription cost, a consumption-based tax to ensure that the consumed energy comes from renewable energy sources, and the electricity cost itself, based on consumption and spot price. Electricity spot prices vary from hour to hour during a day and can have large fluctuations through a year, based on several factors like energy production capacity, energy demand, transmission capacity and CO₂ prices. Determining a spot price for a 20-year period is hence difficult and brings along many uncertainties. The spot prices used in this analysis are based on historical market data gathered from Europe's leading power market Nord Pool, and a report from the Norwegian Water Resources and Energy Directorate (NVE) on the long-term power market. The farm is located inside the NO2 spot price area in Norway. From Nord Pool the prices for each month of the years 2019 to 2021, in addition to the three first months of 2022, are collected for NO2. This results in an average electricity price of 0.5 NOK/kWh [58]. However, a remarkable increase is observed from an average price of 0.1 NOK/kWh in 2020 to 0.76 NOK/kWh in 2021 and 1.49 NOK/kWh in the first quarter of 2022. Reasons for these variations are discussed in Section 4.9.7.2, and an overview of the monthly prices is provided in Appendix H. NVE has estimated the development of electricity prices from 2021 to 2040, which is a useful span for the economic analysis. The estimates are based on three scenarios for fuel and CO₂ prices, where the high scenario leads to electricity prices around 0.7 NOK/kWh, the basis scenario to around 0.55 NOK/kWh and the low scenario to around 0.4 NOK/kWh. Generally, NVE expects higher electricity prices in Norway in the future due to the increased transmission capacity to Europe [59]. Based on this, it seems reasonable to create scenarios covering a rather large range of spot prices, to analyze how they influence the profitability of the project. Once determined, the spot price is the same for each year of the analysis. This is obviously a rather rough assumption, but necessary for the model to work smoothly. The model is used to create spot price scenarios rather than change the spot price over the period of the analysis.

The above-mentioned data lay the basis for the economic analysis. The amount of energy needed from the grid after the own produced energy supply is taken into account is calculated. By comparing electricity costs with and without own energy production, annual savings due to reduced grid dependence are obtained. The costs are based on the consumption data and the available electricity prices. Cash flow analyses then enable measuring the profitability of the project. The cash flow shows all economic activities related to the energy system, such as investments, maintenance costs and savings due to own production, and it hence includes both

inflows and outflows. For all calculations, a period of 20 years is used. The cash flows then enable the calculation of the net present value (NPV), which is used to analyze the profitability of the project. NPV describes the present value of all future cash flows over the entire lifetime of an investment and is widely used in finance analyses on the value of a business, investment security and capital project [60]. A positive NPV indicates that the annual incomes and savings exceed the anticipated costs and indicates a profitable project over the given period. A negative NPV indicates an unprofitable project, which usually dictates that the project should not be considered from an economic view. Determining the Weighted Average Cost of Capital (WACC) of the project is necessary to calculate NPV. The WACC is a complex description of the minimum return that must be earned based on the investment costs. Renewable energy projects are generally characterized by higher up-front capital expenditures, but also lower operating expenses, compared to carbon technologies. Due to the high initial costs, the WACC is hence an important variable in renewable energy financing. Usually, investments with higher risks lead to higher WACCs [61]. The NPV is calculated with the financial function NPV in Excel. The first argument of the function is the WACC, and the second argument is the series of cash flows over the 20-year period. An advantage with calculating NPV in Excel is the further usage of the Goal Seek function. This function enables easy obtaining of critical values for several parameters in order to get a NPV equal to 0. The resulting values then describe the limit where the project becomes either profitable or unprofitable. These parameters can be energy production, investment costs or electricity prices. The payback period describes the time it takes to recover the initial investment costs, where the project reaches the break-even point. In this case this will describe the number of years with savings from increased grid independence necessary to payback the investment and installation costs.

4 Results and Discussion

4.1 Solar Potential

The solar potential on the Cow Shed is explored using ArcGIS and PVsyst. Solar maps and the following irradiation values obtained in ArcGIS, energy production estimates and comparisons to PVsyst results are presented in the sections below.

Figure 10 presents the monthly energy consumption of the Cow Shed in [kWh] for the years 2019-2021. The total annual consumption is around 60 000 kWh, and the bars indicate a pattern with higher consumption during the winter months, and lower consumption in the summer. This can be related to the usage of the Cow Shed, as it holds more cows in the winter leading to increased consumption for heating, feeding, milking, and monitoring, among other things.

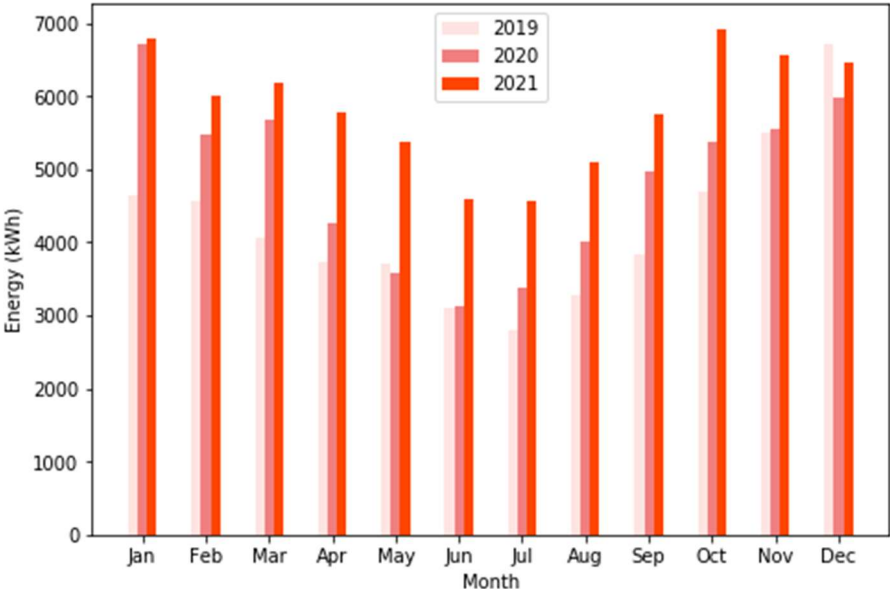


Figure 10 - Monthly energy consumption of the Cow Shed for 2019-2021

The isolated location and amount of energy consumption of the Cow Shed, as mentioned in Section 1.4, make it an interesting object for solar potential assessment and energy production estimation. The further sections investigate the possibility of covering the consumption with own produced energy from a PV system on the building’s rooftop.

4.1.1 Solar Radiation Analysis in ArcGIS

The solar analysis in ArcGIS is performed for every month of the year 2021, on the rooftop of the Cow Shed. The analysis clearly emphasizes the Southwest facing part of the rooftop marked with the dotted lines in Figure 11 as the most suitable for PV installation. It receives

significantly higher monthly irradiation compared to the rooftop on the other side of the building, facing Northeast. Thus the Southwest facing part is used for further analysis regarding solar irradiation and potential PV energy production.

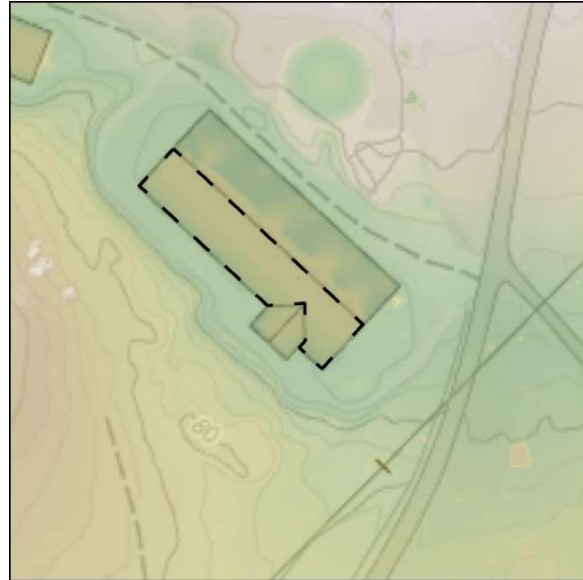


Figure 11 - The part of the rooftop of the Cow Shed (dotted lines) used to obtain average irradiation values. Created in ArcGIS. Spatial Reference: UTM Zone 33N. Server Layer Credits: Kartverket, Geovekst, kommuner og OSM – Geodata AS

By running the solar analysis in ArcGIS for every month of the year 2021, this time only on the mentioned part of the rooftop of the Cow Shed (marked with dotted lines), the solar maps in Figure 12 are obtained. The maps show how the incoming solar irradiation on the rooftop varies through the year. The dark red colors in the summer months describe the obvious fact that the rooftop receives the most amount of irradiation from May to August, compared to the lighter colors, and with that lower irradiation, in the rest of the year. The maximum and minimum irradiation values for each month are presented on the colored bars. The solar maps resulting from the analysis of both sides of the Cow Shed are presented in Appendix A. They show the monthly variations for both parts of the rooftop and confirm that the Southwest facing part receives higher irradiation compared to the Northeast facing part in every month of the year.

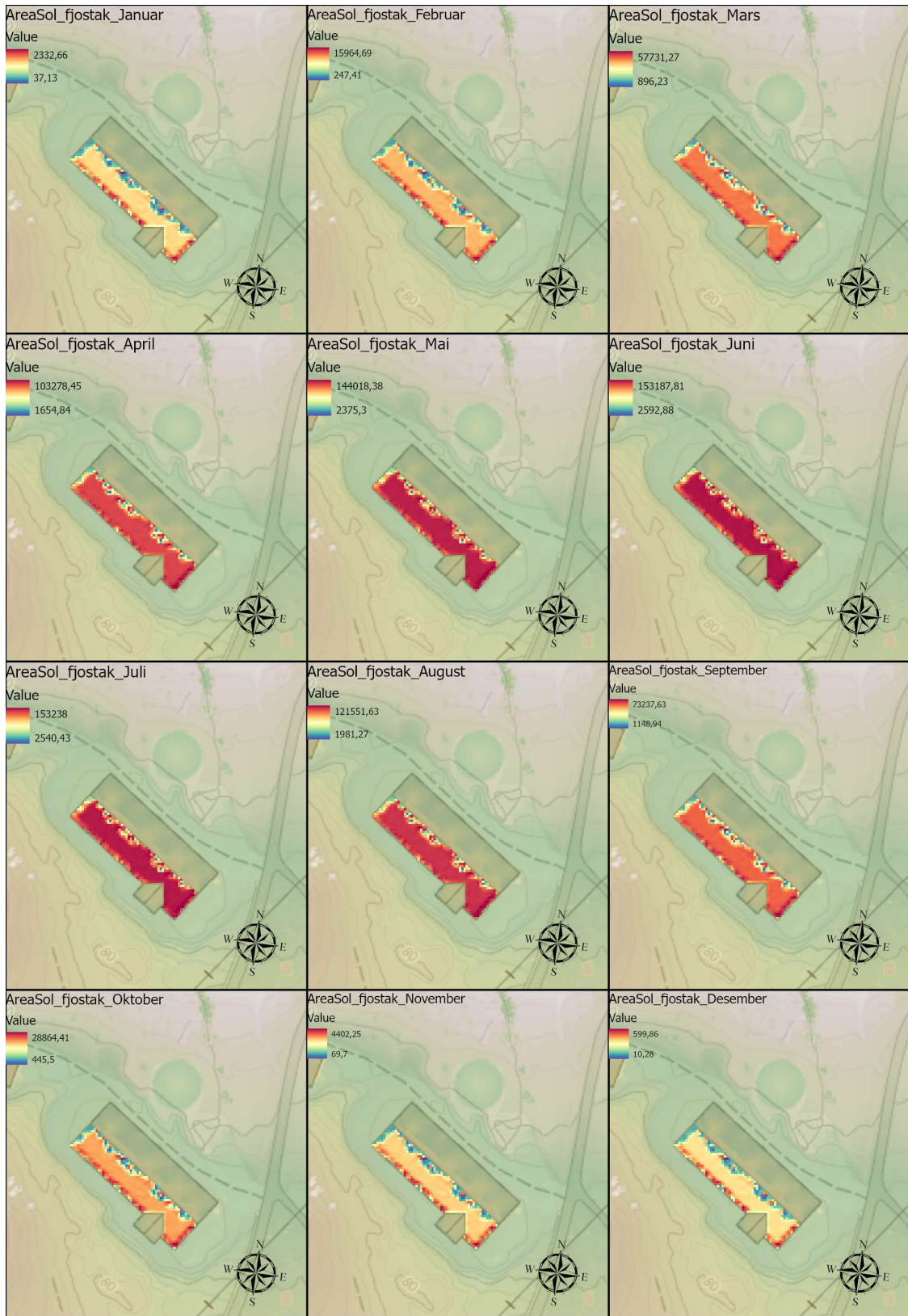


Figure 12 - The result of Area Solar Radiation, run in ArcGIS for each month. The highest and lowest irradiation values for each month are shown on the bars in (Wh/ m²). Spatial Reference: UTM Zone 33N. Server Layer Credits: Kartverket, Geovekst, kommuner og OSM – Geodata AS

By running the analysis for all months of 2021 only on the Southwestern part of the roof, the mean values of solar irradiation, corresponding with the solar maps in Figure 12, are obtained. They are given in [Wh/m²], and represent the average incoming solar irradiation through the entire month. These are the values that the estimated energy production values are based on through Equation 5.

Table 1 - Average solar irradiation on the Cow Shed for all months of 2021. Given in (Wh/m²)

Month	Average solar irradiation (Wh/m²)
Jan	1 308,54
Feb	9 909,92
Mar	40 966,92
Apr	83 459,16
May	125 744,64
Jun	137 066,07
Jul	135 710,56
Aug	102 217,10
Sep	54 748,59
Oct	18 723,64
Nov	2 535,02
Dec	328,08

4.1.2 Calculated Energy Production Estimates

Potential energy production from a PV system on the Southwest facing part of the rooftop of the Cow Shed is estimated in two different ways. The analytical method calculates monthly energy production based on the results from the solar radiation analysis in ArcGIS, the collected temperature dataset, and other parameters necessary to obtain results by using Equations 4 and 5.

The average solar irradiation values obtained from the analysis in ArcGIS can be used to estimate the monthly energy production in the case of PV installation on the rooftop. In this estimation, a specific type of solar cells is not chosen, which results in some necessary assumptions. Parameters like the solar cell’s efficiency, performance ratio and temperature coefficient, as well as the area filled with solar modules, are assumed to get an idea of the range of the potential energy production.

The area of the rooftop of the Cow Shed used for solar radiation analysis (See Figure 11) is 779 m², according to the analysis in ArcGIS. Some installation requirements must be fulfilled

when it comes to the setup of the PV modules. These requirements concern distances between modules and edges and ridges of the roof and can be found in the standards of the Norwegian Electrotechnical Committee (NEK 400-7-712). Furthermore, it is assumed that as much as possible of the roof is used for PV installation, which leads to an assumed area covered by PV modules of 700 m².

To take dust, pollution and other efficiency-reducing factors into account, the reference efficiency is set to 16%. The performance ratio is set to 70%, to take losses in cables and inverter into account. Higher percentages for efficiency and performance ratio are possible, but to avoid overestimation rather moderate values are chosen in this case. The temperature coefficient is set to 0.387%/°C. The operating temperature of the PV modules is based on the temperature data collected from the weather station. A factor is added to the measured air temperatures to take the self-generated heating of the modules into account. The monthly average temperature over the 3-year time series and total monthly average efficiency calculated from Equation 4 are shown in Figure 13, which describes the dependency of efficiency on temperature as discussed in Section 2.10. Efficiencies increase with decreasing temperatures, and since the average air temperature never exceeds 25°C the total efficiency is always higher than the reference efficiency. The annual average total efficiency is 21.3%, which is a high, but possible, efficiency given the low average temperatures through the year. Since PV modules can produce power with an efficiency higher than the nominal efficiency rating during cold and clear weather and the annual average temperature is 9.2°C, it is possibly favorable to choose PV modules with a high temperature coefficient for the system, to take advantage of the low temperatures.

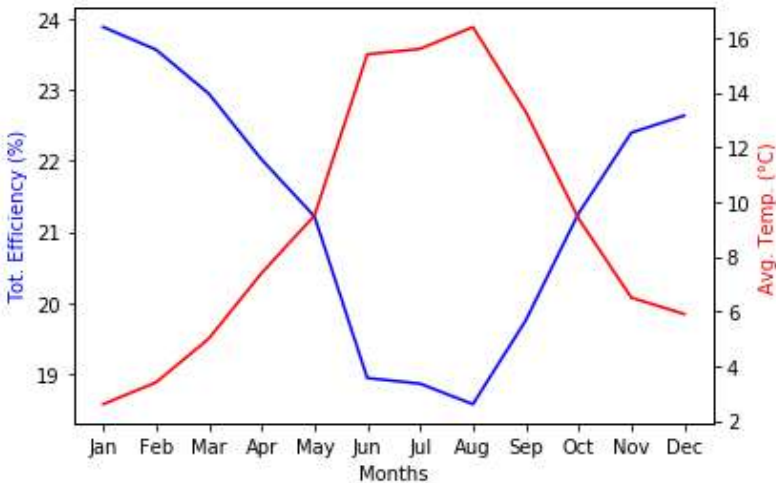


Figure 13 - Monthly average temperatures for the timeseries of the dataset (°C), and calculated total efficiencies of the PV modules (%)

Using Equations 4 and 5, the monthly average energy production from the PV system can be estimated. Monthly values and the annual total are shown in Table 2.

Table 2 - Monthly energy production values, and total annual production for the PV system in (kWh)

Month	Average Monthly Energy Production (kWh)
Jan	153,21
Feb	1 144,64
Mar	4 607,56
Apr	9 006,83
May	13 077,45
Jun	12 721,36
Jul	12 544,08
Aug	9 299,59
Sep	5 299,34
Oct	1 950,81
Nov	278,30
Dec	36,39
Total	70 119,57

The table shows clearly that the highest production is achieved in the summer months from April to August. In the three darkest months November, December and January the PV system only gives a small amount of energy output, while the production in February and March corresponds well with that in October and September, respectively. Comparing these values with the irradiation values in Table 1, a distinct coherence can be observed. However, in the summer months a shift is noticed. Although, from Table 1, the PV modules receive quite much less incoming irradiation in April than in August, the energy production is only slightly lower in April. The reason can be found by looking at the temperature graph in Figure 13. The significantly lower average temperature in April (7.4°C versus 16.4°C in August), leads to such a large increase in efficiency that it nearly equalizes the disadvantage of lower irradiation. The same can be observed in May and June, where the PV modules receive more irradiation in June, they actually produce more in May. Looking at Figure 13, this can also be correlated to the lower average temperature (9.5°C in May versus 15.4°C in June), and thus the higher total efficiency. However, looking at the variations in irradiation, efficiency, and production through the whole year, it is still clear that the irradiation plays the most important part in how the production varies.

4.1.3 Simulation in PVsyst

The monthly energy production is also estimated by simulating a PV system in the software PVsyst. The same available area is used as for the calculations leading to the results presented above, but other parameters vary due to the model of the simulation.

PVsyst gives higher monthly energy production, compared to the calculated values. The largest differences are found in the winter months. The simulation in PVsyst works with a notably higher Performance Ratio than the calculations. The average annual PR in the simulation is 83.6%, while the calculations are based on an assumed PR of 70%. Figure 14 compares the calculated estimates and the values obtained from PVsyst.

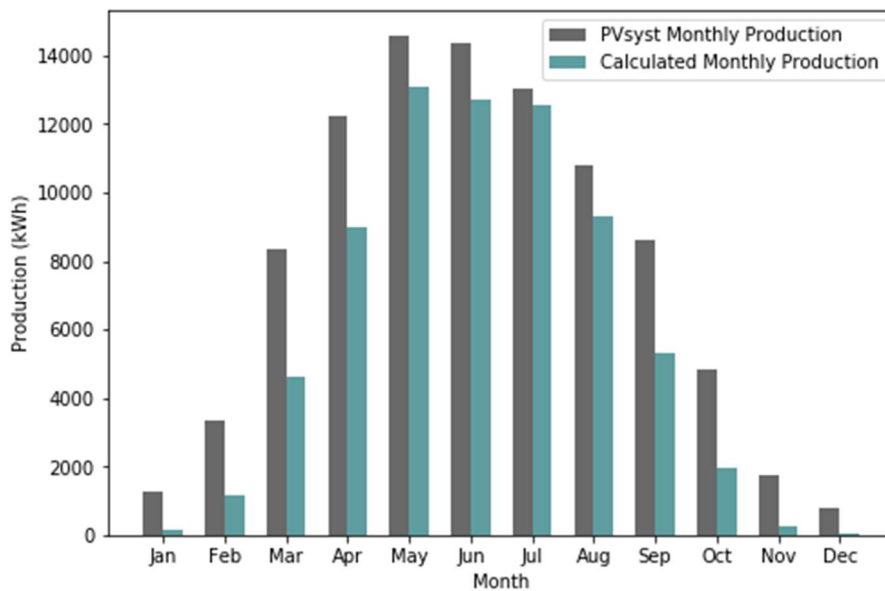


Figure 14 - PVsyst monthly PV production and calculated monthly PV production

PVsyst also uses higher monthly irradiation values than the average irradiation values obtained in ArcGIS. The largest differences are observed in the first half of the year, and the values are generally closer in the summer months. As the amount of incoming solar irradiation is important for energy production, this is a large factor to the higher production values in PVsyst. Figure 15 shows the monthly irradiation from the analysis in ArcGIS and the values used in the simulation in PVsyst.

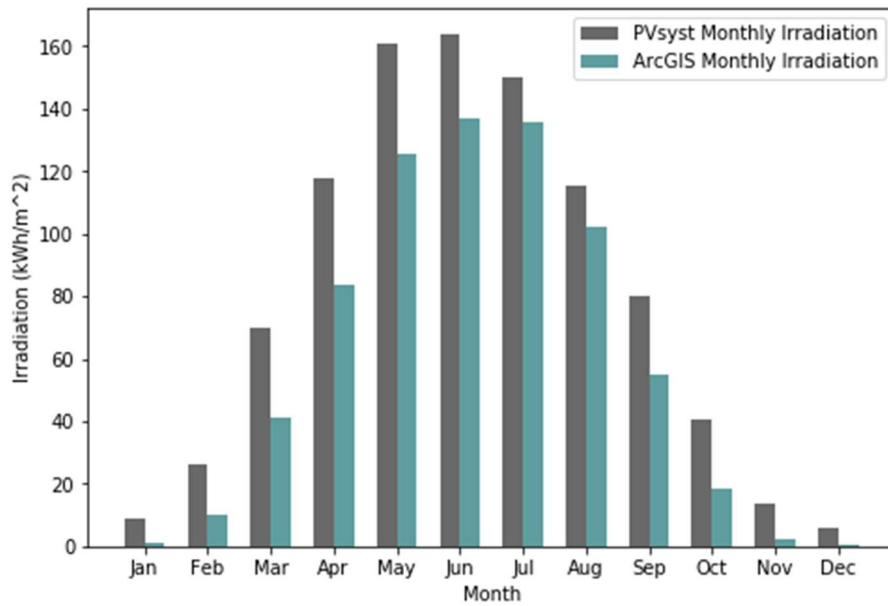


Figure 15 - PVsyst monthly irradiation and ArcGIS monthly irradiation. Given in (kWh/m²)

There are some reasons for the differences, based on the model of the simulation in PVsyst. A horizon profile is imported to the simulation from the Meteonorm web service. It creates a 360° horizon for the coordinates specified for the simulation. In that way shading from the surrounding terrain, like mountaintops and hillsides is included. Near shadings, however, like shading from edges of the roof is not included. It can be included by importing a 3D profile of the area into the project, but this is not executed in this simulation. This can be an explanation to the significantly larger differences in the winter months. Both the irradiation and production values from PVsyst differ quite heavily from the irradiation values from ArcGIS and the calculated production values in the winter. In the summer months the difference is remarkably smaller. The sun follows a much lower path during the winter months, which can make shading from the edge of the roof more significant. As the sun travels from East to West during the day, parts of the Southwest facing rooftop will be shaded from the edge. This can be seen in the solar maps from ArcGIS in Figure 12, where the uppermost part of the Southwestern rooftop receives less irradiation on average, compared to the rest.

The meteorological data used in the simulation in PVsyst is imported from Meteonorm, which collects data from stations nearby. This means that the irradiation values are not specifically from the rooftop of the Cow Shed, as the values from ArcGIS are. This can possibly lead to inaccuracies. Even though the horizon at the farm is included, it does not influence the global irradiation values used in PVsyst. These are only affected by the horizon and shadings at the

stations used to create the synthetic values. The remote location of the farm provides another uncertainty as it is highly possible that Meteonorm has had to use satellite data either partly or entirely in the process. The satellite data is possibly less accurate than measurements from ground stations [62]. During the simulation it is, unfortunately, not possible to find any information regarding which stations' and/or satellite's data is used to create the synthetic data in PVsyst. It may seem like PVsyst is a more reliable tool in or near larger cities, with available stations located more frequently, than at rural locations.

The temperature data obtained from the Meteonorm database shows slightly lower temperatures compared to the temperature dataset collected from MET. The data from Meteonorm gives an annual average temperature of 8.2°C, while the average temperature of the data collected from MET is 9.2°C. A reason for this can be that the Meteonorm file only contains data up to 2014. The recent warm period from 2018 – 2020 is then not included, as it is in the dataset from MET. At the same time, the Meteonorm file contains data from a longer time series than the dataset from MET.

Considering the uncertainties regarding the irradiation values used in the simulation in PVsyst, it is reasonable to say that the irradiation values obtained from the very specific analysis in ArcGIS possibly are equally reliable. PVsyst possibly overestimates the irradiation values especially in the first half of the year and in the winter months, and this has also been shown to be the case in previous studies comparing results from PVsyst and ArcGIS in Norway [63]. In addition, the simulation is working with an optimized system, and the calculations with rather conservative values (for PR especially). Despite the differences, similarities in the results can be noticed. PVsyst gives a good overview of the performance of an optimized system at the site and can clearly work as an indicator on the potential of a PV system. With the above-mentioned uncertainties in mind, however, it should not be trusted blindly, and the calculated production values can show themselves to be equally realistic. This can be supported by looking at the percent difference between irradiation values from PVsyst and ArcGIS, and production values from PVsyst and the calculations. The annual irradiation values from PVsyst are 33.73% higher than the values from ArcGIS. Accordingly, the resulting production values from PVsyst are 33.96% higher than the calculated values. This proves the method and assumptions made for the calculated energy production values to be highly accurate, as there are only the irradiation values that provide the differences between the two methods. This can also be seen by the similarity of the graphs in figures 14 and 15, which show that the variations in irradiation and energy production are strictly connected.

4.2 Energy Production and Consumption

An overview of the energy consumption at the farm is essential to get an understanding of the ability to decrease the dependence on the grid. Additionally, it is necessary to get an indication on how much of the consumption could be self-supplied by a PV system. This section presents comparisons on PV energy production and energy consumption both for the Cow Shed alone and the entire farm.

4.2.1 Consumption of the Cow Shed

Figure 16 shows the PV energy production estimates and the average monthly energy consumption of the Cow Shed for the years 2019-2021. It clearly shows the opposing variations in consumption and energy production over a year. Production is high in the summer, when the consumption is low, and lower in the winter, when the building consumes the most. It is also evident that a PV system, based on the estimated production values, can cover the entire consumption of the Cow Shed from April to August on a monthly scale. In January, February, October, November, and December only a smaller portion of the consumption is covered, while consumption and production are more or less equal in March and September.

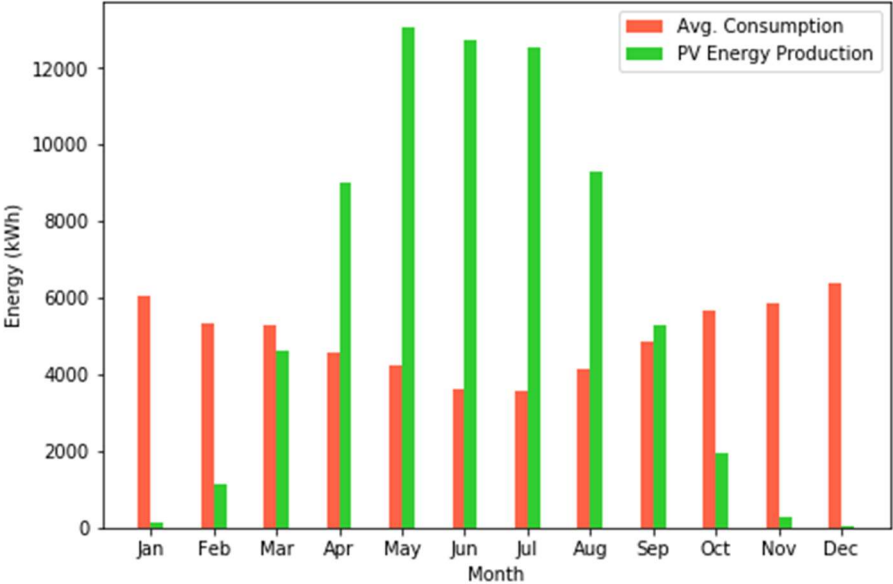


Figure 16 - Average monthly consumption of the Cow Shed and estimated PV energy production

The observations mentioned above are supported by Figure 17, which gives an overview of whether the Cow Shed experiences energy surplus or deficit, looking at average consumption and PV energy production exclusively. It shows the difference between production and consumption for each month, and thus shows in which months the production is higher than

the consumption, and by how much. The green bars represent months with higher production than consumption, leading to an energy surplus, and the red bars represent months with lower production than consumption, leading to energy deficit. The surplus energy reaches up to around 9000 kWh in the months with the highest production, while the months with the lowest production lead to energy deficits of up to 6000 kWh monthly. The large surplus in the summer and deficit in the winter indicates that an on-grid system is the most reasonable choice for installation. An off-grid system with energy storage would lead to high amounts of stored energy in the summer, which could lead to complete grid independence also at night or on cloudy days. However, seasonal storage, storing surplus energy from the summer for usage in the winter, is not an opportunity. An on-grid system enables income through grid export and saves the investment costs of energy storage, and hence seems more reasonable given the production and consumption profile.

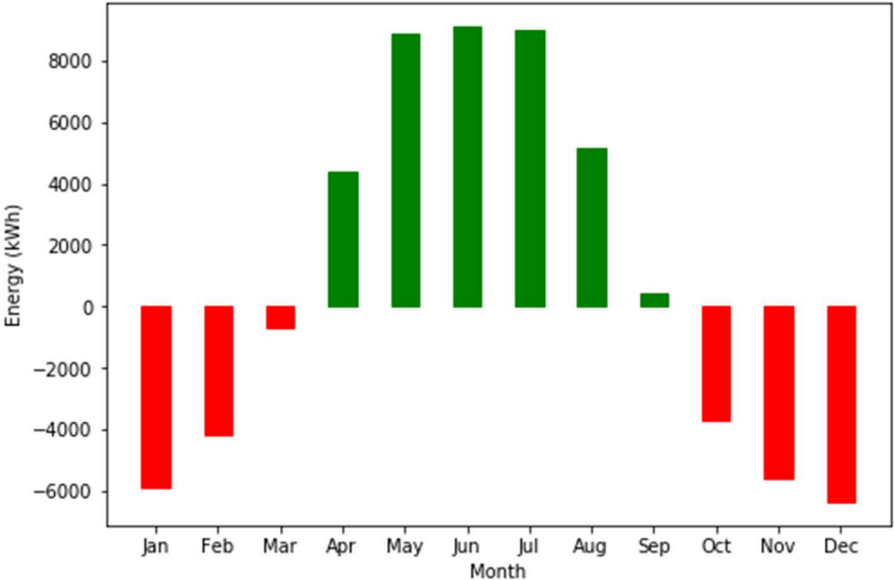


Figure 17 - Difference between PV production and average consumption. Hence, the amount of energy surplus or deficit looking at PV production and consumption exclusively

4.2.2 Consumption of the entire farm

As the analysis shows that the PV energy production is sufficient to cover the Cow Shed’s energy consumption in the summer months it is reasonable to compare the production values up against the total consumption of the entire farm. This consumption follows the same pattern as the consumption of the Cow Shed, with higher consumption in the winter and lower in the summer. The annual consumption lies at around 260 000 kWh, and in the winter the farm consumes almost twice the amount of energy monthly than an average Norwegian household over an entire year. In Figure 18 the PV production is plotted against the average

monthly consumption of the entire farm, showing that there is no month through the year where the production covers the entire consumption. In June and July, the production is close to the consumption, while it is only able to cover rather small portions in the rest of the year. The percentage of the consumption covered each month is shown in Figure 19. It supports the mentioned observations, showing that the covered percentage is very low from November to February (below 5%), but it also shows that the PV production can cover up to about 80% of the consumption in June and July, which is an impressive amount given the high consumption values of the entire farm. Given the same variables used for estimating the production values presented in Section 4.1.2, a PV system of the size of 1 038 m² would be sufficient to cover the consumption of the entire farm from May to July.

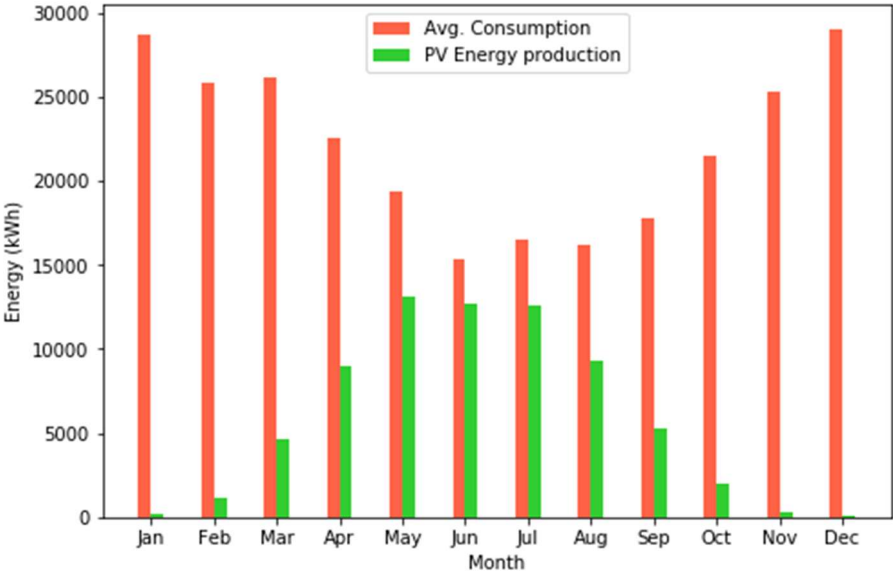


Figure 18 - Average monthly consumption of the entire farm and estimated PV production

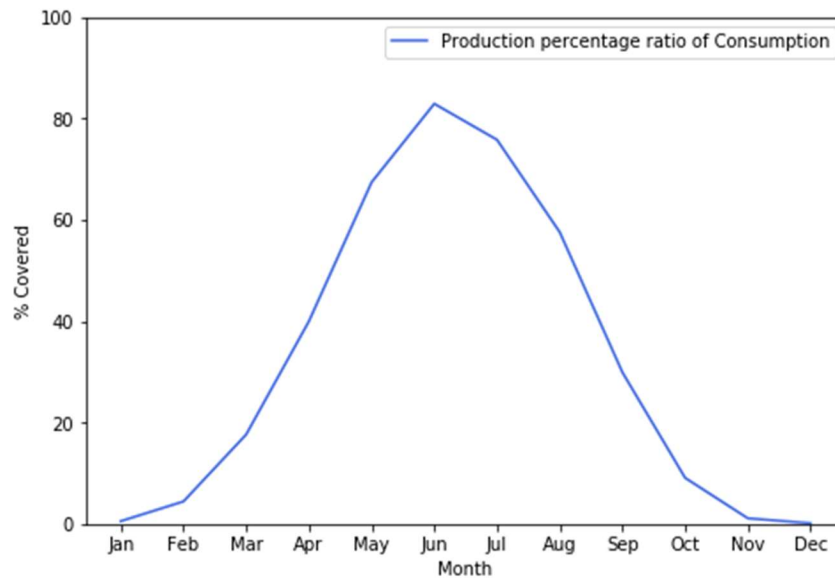


Figure 19 - Percentage ratio of the consumption of the entire farm covered by PV production

4.3 PV System Sizing

The main components of the PV system are sized and chosen to obtain a complete design of the system. The simulation in PVsyst revealed that the maximum possible number of 60-cell PV modules on the rooftop is 420, which means that the goal is to obtain a configuration with a PV array as close to this size as possible.

The chosen PV modules, inverters and cables are presented in the next sections.

4.3.1 PV Module

There are many varieties of PV modules from large amount of PV manufacturers available on the market. To make a realistic approach, a PV module from a Norwegian supplier is chosen. It is a polycrystalline module of the type NE275-30P from the manufacturer SunEnergy. It has a nominal power output of 275 Wp, and is also available in 250 Wp, 260 Wp and 270 Wp. There are several other modules with higher nominal power outputs and based on other technologies like monocrystalline cells, but in this case the simplicity of the purchase and the availability on the Norwegian market is prioritized when choosing the module type. The most important data for the module is shown in Table 3.

Table 3 - Electrical and mechanical characteristics for the NE275-30P PV module [64]

Model	SunEnergy NE275-30P
Nominal Power Output at STC (P_{MPP})	275 Wp
Maximum Power Point Voltage (V_{MPP})	31.74 V
Maximum Power Point Current (I_{MPP})	8.66 A
Open-Circuit Voltage (V_{oc})	37.70 V
Short-Circuit Current (I_{sc})	9.27 A
Solar Cell Efficiency	19.21 %
Solar Module Efficiency	16.90 %
Nominal Operating Cell Temp. (NOCT)	47°C±2°C
Temperature Coefficient of P_{MPP}	-0.45 %/°C
Temperature Coefficient of V_{oc}	-0.32 %/°C
Temperature Coefficient of I_{sc}	+0.05 %/°C
PV Cell	Poly156*156mm
No. of Cells	60
Dimensions	1640mm*992mm*35mm

The chosen module has a high durability against extreme environmental conditions, according to the datasheet. A high salt mist and ammonia resistance can be a favorable attribute, due to the coastal location of the farm. In addition, the datasheet states severe weather resilience, as the modules are able to withstand wind loads up to 2400 Pa and snow loads up to 5400 Pa. The snow load is not a decisive factor at the site, but the wind load resilience is of greater importance. The weight of 18.00 kg of each module would make the total array a significant extra load for the existing roof, and the structure and bearing capacity of the roof must hence be approved according to the Norwegian building code (TEK17) prior to the installation. The module has a warranty that guarantees a performance of minimum 95% of the nominal power over the first 5 years. It has a 10-year warranty on materials and workmanship and a 25-year linear performance warranty, guaranteeing minimum 80% performance in year 25.

A good warranty and low degradation rate are wanted when it comes to the economic aspects of a PV module. Different PV modules can also be compared by looking at the investment cost per installed watt-peak (NOK/Wp), or per kWh produced (NOK/kWh). The price for one module of the same type as chosen above is 1495 NOK, which gives a cost of 5.4 NOK/Wp.

Modules with higher nominal power give higher production but are also more expensive, while modules with lower nominal power produce less but are cheaper. The NOK/Wp is hence a good factor for the economic comparison of different modules. This is also the case when looking at different technologies. In this case a polycrystalline module is chosen, which operates with slightly lower efficiencies but is cheaper than for example monocrystalline modules. From the same supplier, a 320 Wp monocrystalline module is available for 2195 NOK. This gives a cost of 6.8 NOK/Wp but it also works with higher cell efficiencies of up to 21.79%. For the monocrystalline module to have the same NOK/Wp as the polycrystalline module, the price would have to be reduced to 1728 NOK, or the nominal power increased to 406 Wp. With the decreasing prices in the PV market in mind, it is not unthinkable that other technologies will be more widely used in private and small-scale PV systems in the future. In this case, the method used for sizing the PV system is based on maximizing the size of the system to the given area of the rooftop. This leads to a larger number of modules required compared to an off-grid system which is sized on the basis of the building's consumption. The higher investment costs can, however, be earned back through profits and smart utilization of the surplus energy.

4.3.2 Inverter

When it comes to available inverters on the market, also here several manufacturers offer different types of inverters with different attributes. Installation methods for central inverters, string inverters and microinverters are discussed in Section 2.7.1. In this case, a 33 kW three-phase string inverter is chosen. It is a Solis PV inverter from the large manufacturer Ginlong. Ginlong offers a large range of inverters for several system scales, both three-phase and single-phase. The S5-GC33K inverter features 3 MPPT inputs, where each MPPT can take 2 strings. This enables a flexible system design and makes it easier to find the optimal configuration for the PV array. The most important data for the chosen inverter is included in Table 4.

Table 4 - Data for the S5-GC33K inverter [65]

Model	Ginlong Solis S5-GC33K
INPUT DC	
Maximum PV Power	49.5 kW
Maximum Input Voltage	1100 V
MPPT Voltage Range	200-1000 V
Maximum Input Current	32 A
Maximum Short-Circuit Current	40 A
MPPT no./Maximum Input Strings no.	3/6
OUTPUT AC	
Rated Output Power	33 kW
Maximum Output Power	36.3 kW
Rated Grid Voltage	3/PE, 220 V(220/230 V)
Rated Grid Output Current	82.8 A
Maximum Output Current	82.8 A
Maximum Efficiency	98.6 %

To obtain an optimized configuration and performance 3 inverters need to be connected to the system. As each inverter has 3 MPPT inputs with 2 strings each, the 3 inverters can take a total of 18 input strings between them. Given the maximum input voltage each string can consist of 23 modules. This gives a PV array consisting of 414 modules, configured in 18 strings with 23 modules each, and covering an area of 672.2 m². As the maximum possible number of modules is 420, this is a satisfying result. The optimized array/inverter configuration is prioritized instead of installing 420 modules at any cost. The goal is to cover the largest possible area while at the same time the number of strings, number of modules per string, voltages, currents and power in modules and inverters cooperate. The calculations performed to obtain this configuration are shown in Appendix B.

In this case a configuration is chosen where each MPPT input takes 2 strings of modules. To fully optimize the production each string should have its own MPPT input, as this would reduce the effect production losses in single modules have on the total production. This leads to the question on the number of inverters and the size of the inverters that should be installed. As mentioned, a higher number of inverters leads to an optimization of the

production, and this could be done by installing microinverters at each module. This would also result in significantly higher investment costs, as inverters are one of the costliest components in a PV system. Fewer inverters are cheaper and easier to maintain, but at the same time it should not be compromised on the number of MPPT inputs. Choosing a larger inverter, which could be the case with a single central inverter, leads to a lower number of inverters required to obtain the desired output power, but the inverters must have enough MPPT inputs. In this system all PV modules are located close to each other at the same tilt and at the same rooftop. This mitigates the problem around shading of parts of the system, which would be more of a challenge if the system was covering several rooftops facing in different directions. A central inverter could hence be suitable, but due to the size of this PV system string inverters are chosen to make sure the production is more optimized than it would be with one central inverter. When choosing smaller inverters, the number of inverters required increases quickly. The three 33 kW inverters give a nominal AC power output of 99 kW. To obtain the same output with 10 kW inverters, 10 of those would be needed. This would probably increase the investment cost. To take both the performance and economic aspects into account it is reasonable to install the 3 string inverters, as they cover the MPPT demand well without leading to unnecessary high investment costs. The amount of installed nominal inverter power compared to the amount of installed nominal PV power, the DC-to-AC ratio, is an important factor on the performance of the system. Oversizing the inverter power means that it is able to operate during peaks in PV power production (maximum power point), which means that no power is clipped. However, at times where less irradiation or other factors contribute to lower production the inverter will work inefficiently if oversized. This is due to a low PLR which leads to low conversion efficiency in the inverter. By undersizing the inverter the peaks in PV production are clipped, which means that the inverter limits the available power within its capabilities. Under sizing leads to production loss during peak production hours, but, due to the higher PLR during “normal” production hours, the inverter can work more efficiently during larger parts of the day. As the weather conditions in Southwestern Norway are unstable, and peak production hours rather rare, a slightly under sized inverter is possibly a sensible choice at the site. The optimal DC-to-AC ratio for a PV system depends upon several factors like string size, inverter efficiency and proper maintenance and the inverter’s ability to cool. A series of studies done by ABB found an ideal DC-to-AC ratio, regardless of site conditions, slightly below 1.2, when sizing a system to maximize the output [66]. Table 5 visualizes a summary of the chosen system.

Table 5 - Summary of the PV system with the chosen components

Number of modules	414
Module area	672.2 m ²
Nominal PV power (DC)	113.85 kW
Number of inverters	3
Nominal inverter power (AC)	99.0 kW
DC-to-AC ratio	1.15

4.3.3 DC Cables

For the DC side a 2.5 mm² XLPE Solar Cable is chosen to connect the PV strings to the inverter inputs. It is a Multi Contact model from the manufacturer Stäubli, a Swiss global mechatronics solution provider and a leading manufacturer of connector systems [67]. There are several PV cable manufacturers on the market, but few Norwegian available suppliers offer them. The 2.5 mm² cable from Stäubli is available for purchase, and Table 6 shows the most important data for the cable.

Table 6 - Data for the 2.5 mm² XLPE Cable [68]

Model	FLEX-SOL-EVO-TX 2,5
Cross-Section Area (CSA)	2.5 mm ²
Rated Current	41 A
Rated Voltage	1500 V DC
Ambient Temperature	-40°C ...+90°C
Insulation	XLPE

From the table it is clear that the CCC of the cable is more than sufficient for conducting the maximum short-circuit current of each PV string. The same applies for the rated voltage and temperature capabilities. The cross-linked polyethylene insulation makes the cable resistant to effects like UV, ozone, heat, freezing and contact with water, and hence makes it suitable for outside mounting. Its resistance is also tested to acids, alkalis, and oil. A 1.5 mm² cable with CCC of around 15-30 A could also have been chosen. The voltage drop through the 2.5 mm² cable is 0.57%, while it would increase to 0.95% through a 1.5 mm² cable with the same length. Both are satisfying results, but 1.5 mm² PV cables are not very available on the market, which is why the 2.5 mm² is chosen despite possibly slightly higher prices. The

length of the DC cables is assumed to be 20 meters, following the idea of taking advantage of the high DC voltage and making the path of the DC cables as long as possible compared to the AC cable. This is not exactly an economically favorable measure, as 18 cables of 20 meters leads to a total required cable length of 360 meters. On the other side, the voltage drop is held at a minimum, which enhances the performance of the system. The voltage drop depends on the length, CSA, and load current, as expressed in Equation 13. Another reason for the possibility of using cables with low CSA is the voltage and current they are exposed to. As the PV array is made of strings with a high number of modules and no parallel connected strings, the output voltage is high, and the output current is low. This enables low CSA cables. Fewer modules per string would lead to a lower voltage over the cables, which again would lead to higher voltage drops in percentages. More parallel connections would result in higher currents for the cables to conduct, and this would affect the required CCC and hence the CSA. The 2.5 mm² cable has a good margin when it comes to CCC, and it could even be used for 3 parallel connected strings, based on the load current. This enables the opportunity to make changes in the PV configuration in the future, without necessarily having to change the cables.

4.3.4 AC Cables

For the AC side a PFSP 3x25/16 Cu cable is chosen to connect the AC side of the inverters to the main distribution board. The cable is made from the leading cable manufacturer Nexans, which is a widely outspread company with a high status in Norway. Regarding PFSP cables a large variety from several different manufacturers is available on the market, and these are certainly easier to look for than the DC solar cables. Both 2- and 3-wire cables can be found, and in this case a 3-wire cable is chosen. Table 7 shows the most important data for the cable.

Table 7 - Data for the PFSP 3x25/16 Cable [69]

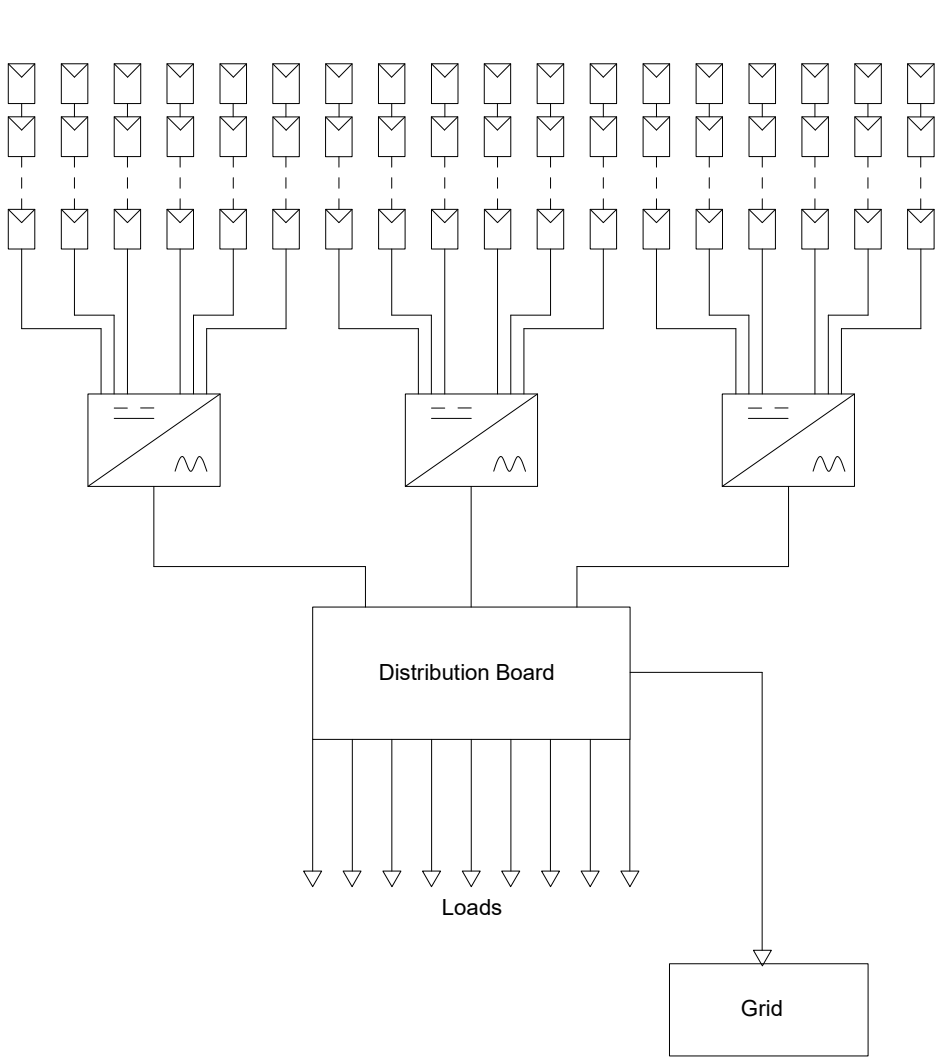
Model	PFSP 1kV 3x25/16
Cross-Section Area (CSA)	25 mm ²
Current Carrying Capacity (CCC)	96 A
Rated Voltage U₀/U	600/1000 V
No. of Wires	3
Maximum Temperature	70°C
Insulation	PVC

Both the CCC and rated voltage of the 25 mm² cable are sufficient compared to the output current and voltage of the inverter. Based on the calculated minimum CSA, a 10 mm² or 16 mm² cable could also have been chosen, but the cable would then not have a CCC high enough for the maximum inverter output current. This shows that the calculated CSA should always be checked up against its CCC, to not under size the cable. As the CSA, through Equation 13, depends upon both the length and the load current, a short cable length can mislead the calculations. This is a weakness in the formula, and a reminder that the requirements provided by NEK should always be followed. The cable must be able to conduct the present load current regardless of the length. The CCC of a cable also depends upon the installation method, as different methods lead to different CCC for the same CSA. NEK provides an overview over the installation methods and their corresponding CCC (NEK 400-5-52), and the table can be found in Appendix D. For this cable it is assumed that method C “Single-core or multi-core cable on a wooden wall” is used. Because of the short path length, it is assumed that mounting the cables inside a wall or in the ground is not necessary. Method C is the method with the highest corresponding CCC, which makes this the best economic option, as other installation methods would require cable CSA of 35 mm², which would be more expensive. The idea of making the path for the DC cables as long as possible in order to minimize voltage drops leads to a significantly shorter assumed length of the AC cables of 8 meters. The short path length helps keeping a satisfying voltage drop of 0.45% through the cables. The calculated voltage drops should also be looked critically upon, as the voltage drop through the DC cable is calculated with maximum short-circuit current of the PV string, which is obviously not a normal situation. Using the maximum power point current (8.66 A) instead, the voltage drop decreases from 0.57% to 0.43%. The 230 V IT output of the inverter leads to higher CSA required for the AC cable. A 400 V TN output could reduce the required CSA to 10 mm² with the same installation method, because of the lower currents. A 400 V TN grid is hence economically favorable when it comes to the AC side of a PV system. As seen in this section, high voltage and low current is preferable regarding both voltage drop and the required CSA. The AC cable has a good margin when it comes to rated voltage, with 600 V between phase and neutral and 1000 V between phases. This means that a possible future grid upgrade from the present 230 V IT to 400 V TN, and hence a change in inverter output voltage, should not affect the cable. The calculations performed to size both the DC and AC cables are found in Appendix C.

4.4 PV System Design

The PV system design is created in AutoCAD and presented in two different single-line diagrams. The first one (Figure 20) is slightly less detailed and shows the entire system from the PV modules to the grid. Note that not all 23 modules in each string are shown. The dotted lines between the first two modules and the third in each string represent the remaining 20 modules. It shows the 6 inputs to each inverter and the total of 3 inverter outputs leading to the distribution board, where power is distributed either to the loads in the Cow Shed or to the grid. Informative tables are added at the side with data for the corresponding component.

The second single-line diagram (Figure 21) shows a partition of the system, including 6 strings connected to each of the MPPT inputs of one of the inverters. Further it shows connections to the distribution board and the grid. This is done to ensure that every component and electrical characteristic is shown properly. This diagram is more detailed as it includes protective devices like circuit-breakers and SPDs, MPPT inputs and a depictive connection to the PCC. Proportions of the different components are not considered closely in this design, as the goal is rather to provide an overview of the configurations and connections in the system. Note also that the grounding system is not shown on the diagrams. The protection system including SPDs on both sides of the inverter, as well as both DC and AC disconnectors, are included. SPDs protect against over voltages, while the disconnectors provide isolation if needed. The Generation Meter between the inverter and the distribution board measures the AC energy output and can be connected to a control panel giving uninterrupted overview of the present production. Over-current Protection Devices guard the distribution board and each of the local loads. The main switch can be operated externally to stop the power flow in case of a fault situation. The bidirectional Meter is special for on-grid systems as it measures both the energy imported from the grid and exported to the grid. In that way the net total monthly energy consumption, and hence the electricity bill, becomes a function of the ratio between imported and exported energy.



PV Modules	
Model	NE275-30P
No.	414
Nominal PV Power	113.85 kW

DC Cables	
Model	FLEX-SOL-EVO-TX 2,5
CSA	2.5 mm ²

Inverters	
Model	Solis S5-GC33K
No.	3
Nominal AC Power	99.0 kW

AC Cables	
Model	PFSP 1kV 3x25
CSA	25 mm ²

Figure 20 – Single-line diagram showing the PV system design. The informative tables present data for each component. Created in AutoCAD

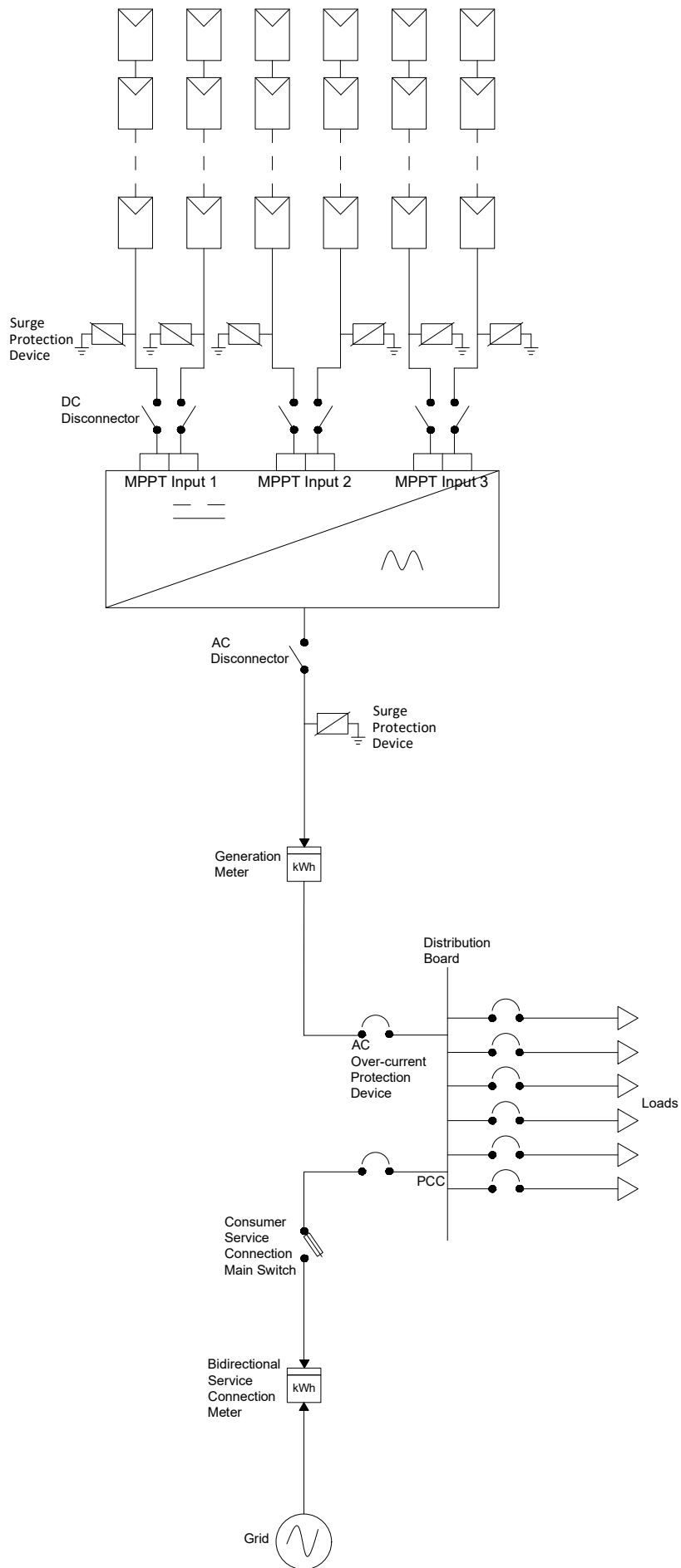


Figure 21 - More detailed single-line diagram of the PV system. The figure shows a partition of the system, looking at one of the inverters exclusively. Created in AutoCAD

4.5 Electric Tractor

4.5.1 Charging System

The energy produced by the PV system can be distributed to charge an electric tractor, and hence reduce electricity costs and the grid dependence. There are some alternatives regarding the charging system based on the location of the charging station and the method of charging. In this section, some alternatives, and their opportunities and challenges, are discussed. The cables used are dimensioned using the same method as for the cables in the PV system (See Section 3.5.3), following NEK's standards. A specific electric tractor is not chosen in this case, and parameters like working time, battery capacity, charging time and charging power supply are assumed based on available information from a handful of producers. It is assumed that the tractor is supplied by a 32 A three-phase charging cable which can supply a maximum of 22 kW.

4.5.1.1 AC Supply

The electric tractor can be charged at a charging station located inside or close to the Cow Shed, and hence close to the PV system. The energy must then only be transported a short distance, and the charging cable is connected as a circuit directly from the distribution board. The charging system supplies AC power which, due to the 230 V IT grid, is limited to 12.7 kW with a 32 A three-phase charging cable. In this case, the charging station is assumed to be located at the closest main entrance of the Cow Shed, where there is sufficient space for the tractor to charge. The path length of the cable from the distribution board to the charging station is assumed to be 18 meters. The cable must have a CCC of at least 32 A, according to the capacity of the charging cable, and method C "Single-core or multi-core cable on a wooden wall" is assumed to be the installation method. A maximum permissible voltage drop of 5% is used, according to NEK's requirements. Figure 22 shows the proposed single-line wiring diagram for the charging station. The chosen PFSP 3x6/6 Cu cable leads to a satisfying voltage drop of 1.63%. The disadvantage with this method is the location of the charging station in relation to the entire farm. As the Cow Shed is located at a significant distance away from the other buildings on the farm (See Figure 2), having to drive the tractor to the Cow Shed for each charging is possibly bothersome and inefficient when it comes to battery capacity and working time.

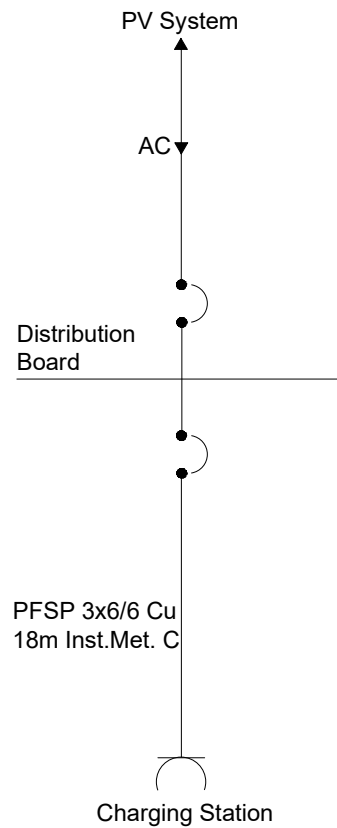


Figure 22 - Single-line diagram of the AC supplied charging station. Created in AutoCAD

The above-mentioned problem can be solved by installing the charging station more centrally on the farm, and hence closer to the other buildings and other working area for the tractor. This could possibly be favorable for the working time between each charging, and hence lead to less frequent charging breaks. The charging station is located close to the barn (See Figure 23) which is a point that is often passed during operations with a tractor at the farm. To supply the station from the PV system the power must then be transported through a cable following the gravel road over an assumed distance of 630 meters from the distribution board in the Cow Shed to the central charging station. The connection to the distribution board is necessary to be able to import power from the grid during low production hours. Due to this distance large cables are required in order to keep the losses at a minimum, and method D2 “Sheathed single-core or multi-core cables direct in the ground” is the proposed installation method. Both these factors would result in significantly higher investment costs, and rather supplying the station from a distribution board of a closer building or installing a new PV system closer to the station should be considered. The charging power supply is the same as for the above-discussed method; 12.7 kW with a 32 A three-phase charging cable. The chosen

PFSP 3x120/120 Al cable leads to a voltage drop of 4.55% which is close to the limit of 5% but satisfying given the large distance. Figure 23 provides an overview of the location of the PV system and a proposed location for the charging station, in addition to the cable connecting the charging station to the distribution board in the Cow Shed. A small shed or shelter would possibly be reasonable to construct to protect the charging station from lifetime reducing effects like rain and dirt.

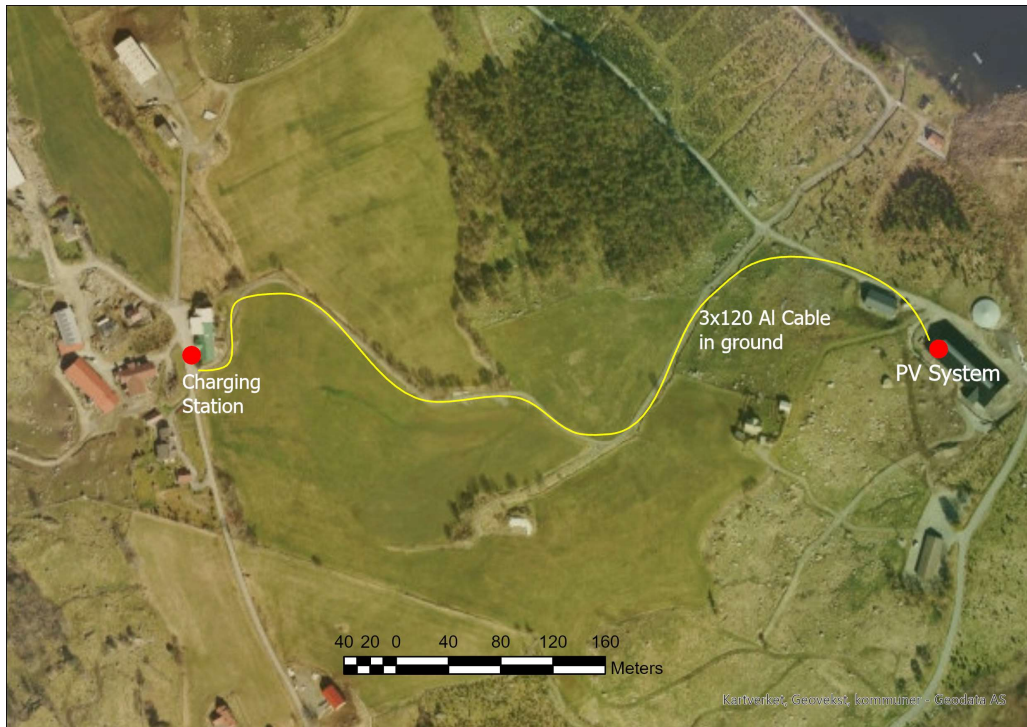


Figure 23 - Position of the charging station at the barn, and the cable connecting it to the PV system. Created in ArcGIS. Spatial Reference: UTM Zone 33N. Server Layer Credits: Kartverket, Geovekst, kommuner – Geodata AS

4.5.1.2 DC Supply

The electric tractor can also be charged by connecting the charging station directly to the DC side of the PV system. This can be done by installing a charge controller between the PV system and the charging station to control and maximize the charging of the tractor and ensuring optimal working conditions by preventing overcharge. Charging directly with DC power from the PV system enables the utilization of high voltages and low currents which again enables thinner cables for connection. Since this method is off-grid, it requires sufficient PV production at every moment of charging. As this is unlikely, measures must be implemented to ensure additional supply during low production hours. An alternative is to install an Energy Storage Unit (ESU), like a battery, which is charged by the PV system when the tractor is not charging. The ESU then supplies the charging station either with additional

power when the PV system does not produce enough, or with the entire power supply when there is no PV production, for example at night or during cloudy days. The ESU is installed in a DC coupled configuration, as shown in Figure 24(b). The charge controller must be bidirectional, as it must be able to both charge and discharge the ESU. An advantage with this alternative is that the tractor is able to charge with PV produced energy at night when it is not used. Another alternative is to connect a DC circuit from the distribution board to the charging station. A DC bus at the station input then gathers power from the PV system and from the grid and supplies the station (Figure 24(c)). In that way, power can be imported from the grid when the PV production is not sufficient. These two alternatives can also be combined, leading to a system with both ESU and grid connection (Figure 24(d)). In this case, the charging station can be supplied from energy stored in the ESU or energy imported from the grid, when the PV production is insufficient. Figure 24 shows the four alternatives for DC connection of the charging station.

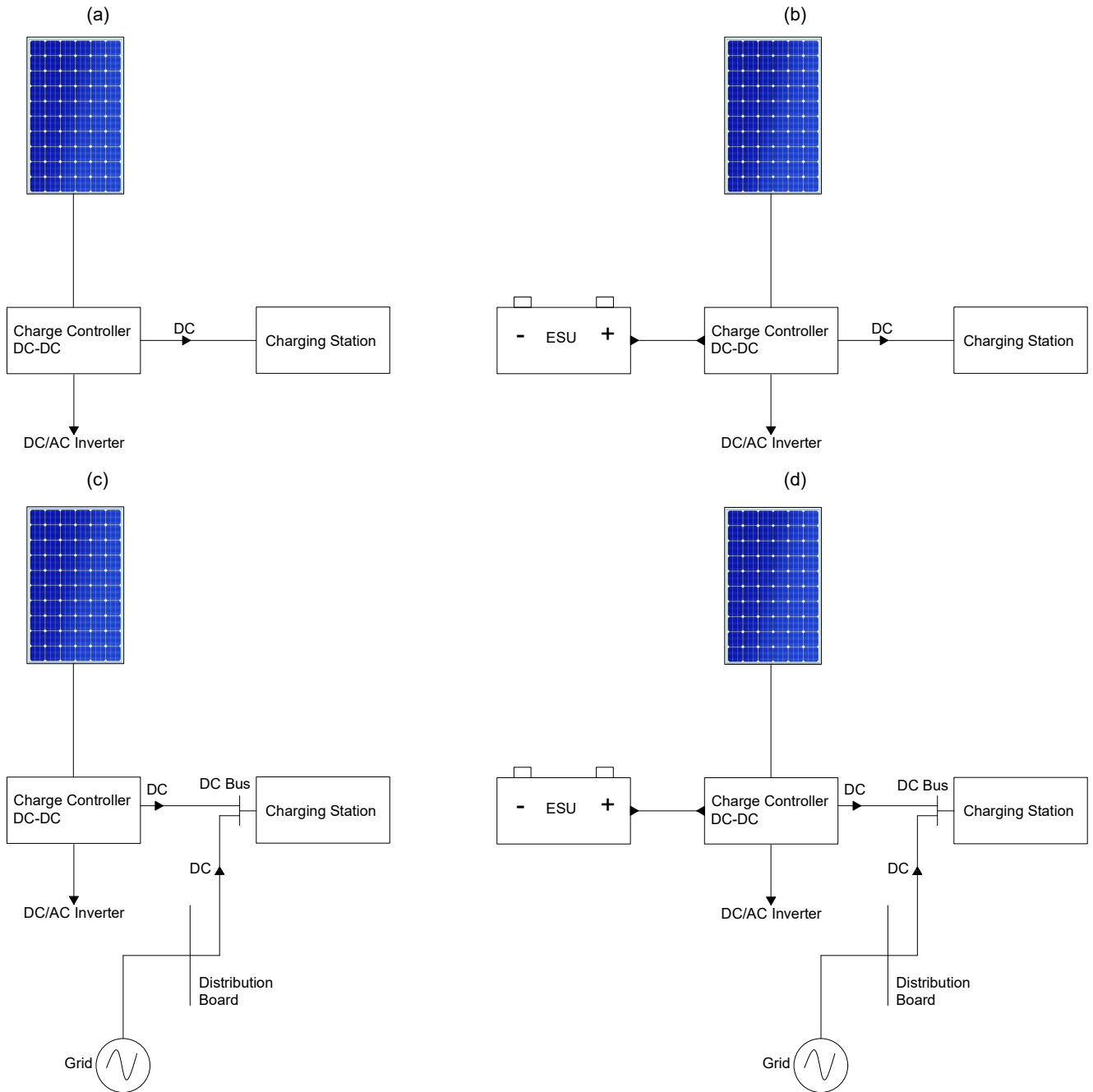


Figure 24 - Four alternatives for connecting the charging station to the DC side of the PV system. (a): Charging station supplied only from PV system; (b): Charging station supplied from PV system and ESU; (c): Charging station supplied from PV system and grid; (d): Charging station supplied from PV system, ESU and grid. Created in AutoCAD

4.5.1.3 Discussion

Regarding the AC charging system, the charging power is limited to 12.7 kW with 32 A three-phase charging cable and 230 V grid supply. It is assumed that the battery can be charged with up to 22 kW power supply, which could be utilized with a 400 V TN grid. This would enable faster charging, but it would also require higher minimum PV production if the total power supply is to come from the PV system. A possibility could be to install a voltage

transformer into the charging system to step up the voltage from 230 V to 400 V and hence maximize the possible available charging power to 22 kW, without interfering with the grid voltage.

Using the PV system for charging of the electric tractor with help of an ESU is possibly a smart measure for increasing the flexibility around the time of charging. Both the AC alternatives and the DC alternatives without ESU rely on coordinated time of charging and PV production in order to maximize the PV system's ability to supply the charging station. This means that the tractor must be charged while the PV system produces enough energy. This is probably not optimal as the PV system obviously produces the most during daytime which is also the period where a tractor is most used at a farm. With ESU the time of charging is more independent from the PV production, as the energy can be stored and distributed to the charging station at other times of the day. This makes it possible to charge the tractor for example at the evening when it is not so often used. The charging system variants presented above could also be transferred to charging of for example electric excavators, trucks or other vehicles used in farming.

4.5.2 Economic Aspects and Profitability

The economic aspects are one of the large uncertainties regarding the introduction of electric tractors in regular farming. There are very few available prices on the market, but, as the case is for electric cars and combustion engine cars, the price for an electric tractor will likely be higher than for a combustion engine tractor with the same performance. One of the leading projects, AGCO's Fendt e100 Vario, has been estimated to an investment cost of 1.6 million NOK. At the same time, a diesel tractor with equivalent performance is estimated to around 1 million NOK [70]. Thus, the difference is large, and the future development of the investment costs will be of importance. One of these is the price evolution for batteries, as the battery bank of the electric tractor pushes the price higher. The battery's lifetime must also be considered, as it possibly needs to be replaced during the tractor's lifetime. As discussed, implementing an ESU to the PV system can lead to increased flexibility around the charging process, but also here investment costs must be considered.

When it comes to cost of operation, electricity prices are a main factor for the profitability of electric tractors. High electricity prices will lead to high charging costs if the charging station is to be supplied from the grid. Supplying it with self-produced energy will decrease these costs significantly. In theory, if the self-produced energy is sufficient to fully supply the

charging station, the operating costs of an electric tractor would be nonexistent. However, this is unlikely especially with a PV system due to the low production in the winter months. Still, it is obvious that supplying the charging station with self-produced energy will be economically favorable compared to total grid dependence. The time of charging can also play a role here, as charging during periods with higher spot prices will make charging with self-produced energy even more profitable. Spot prices are usually at its highest during afternoon and evening hours, which is also a suitable time for charging.

Fuel prices are another factor for the operating costs. With an electric tractor fuel expenses are saved, while electricity prices are possibly added. This means that the comparison of fuel prices and electricity prices can give an indication on which of the alternatives is profitable on long-term.

Based on the discussions above, it may seem as if the investment costs are the main disadvantage for electric tractors compared to diesel tractors. In the future, the prices must be competitive with the ones for diesel tractors, in order to make an electric tractor a profitable investment for farmers. Regarding costs of operation, it can seem as if electric tractors lead to lower costs compared to diesel tractors, especially if the energy supply comes from self-produced renewable energy. A Norwegian study estimated costs of operation for the Fendt e100 Vario and compared them with three diesel tractors from New Holland, John Deere, and Massey Ferguson. Given 300 hours working time, an average electricity price of 1.09 NOK/kWh and an average toll-free diesel price of 9.37 NOK/L, the estimations showed annual savings between 30 000 and 40 000 NOK in costs of operation for the electric tractor if supplied with self-produced energy [70].

Today, diesel tractors can be fueled with toll-free diesel in Norway. Changing this and introducing for example CO₂ taxes for diesel tractor fueling would possibly make electric tractors more attractive. In that way, subsidies and tolls can also make electric tractors more profitable. Another measure could be supporting deals for the purchase of electric tractors. Innovasjon Norge already offers investment support for development of renewable energy and technology in Norwegian agriculture, like biomass energy, biogas production and PV systems. Presenting supporting deals for the purchase of electric tractors or other electric machines could help the farmers towards taking that step and hence contribute to increased electrification. Reduced investment costs could also be achieved through cooperation between several farmers in the area, who could invest in a shared charging infrastructure. The limiting

factor would be the amount of PV production and the ability of charging several tractors at the same time. This could be solved by combining PV systems from the different farms. Not only the tractor itself, but also the charging system, results in investment costs. An idea for PV providers could be to give farmers discounts for purchasing PV systems with integrated charging system for the electric tractor.

4.5.3 Outlook

There are several ongoing projects when it comes to charging that will improve the electric tractor's chances of making its way into everyday farming. New battery technology will enable faster charging, leading to higher flexibility and effective usage of the tractor.

Vehicle-to-vehicle (V2V) charging is a conductive based technology which enables charging between the batteries of two electrical vehicles. V2V can be used when a vehicle is discharged and unable to reach the charging station, as it can then be recharged from another vehicle. This technology still has some challenges regarding the many power conversion stages, but future improvement and testing can make this effective and beneficial [71].

Battery Exchange System (BES) is a new technology and is based on exchanging discharged batteries with recharged batteries. The BES technology has challenges regarding the size and weight of the batteries in large vehicles, in addition to the structure of the battery exchanging station and recharging of the discharged battery [72]. It is, however, a technology with large potential in the agriculture, as it would decrease the stop intervals drastically and lead to significantly more efficient usage of an electric tractor.

There is no doubt that the introduction of electric tractors in farming would lead to new and probably unaccustomed ways of thinking and working for the farmers. In the future, new and better models must be presented. This leads to the decisive question on whether producers are waiting for higher demand before they start producing and developing, or farmers are waiting for better alternatives before they start purchasing. The combination of both makes this a challenge in the years to come. If, however, the development continues, prices stabilize and research is performed, successful implementation of electric tractors, in combination with self-produced energy, can be both economically and environmentally favorable for farms and contribute to increased sustainability in the agriculture.

4.6 Wind Energy Production

The wind turbine used for the analysis of potential wind energy production is a 20 kW Small Wind Turbine from the manufacturer Ryse Energy. The SWT market is rather limited, but the renewable energy solution provider Ryse Energy offers a selection of SWTs in the range from 3-60 kW capacity. The company is specialized into PV, wind, and energy storage technologies for rural electrification, and hence seems like a reliable choice. The 20 kW wind turbine is constructed for both on-grid and off-grid installation and is suitable for industrial and agricultural use. On the data sheet, an overview of annual average wind speed and the corresponding estimated annual energy output is provided. The table is included in Appendix E. Table 8 shows some of the most important data for the wind turbine.

Table 8 - Data for the E-20 HAWT Wind Turbine [73]

Model	E-20 HAWT
Maximum Power	20 kW
Rated Power	18 kW
Cut-in Speed	2 m/s
Rated Wind Speed	9 m/s
Cut-Out Speed	30 m/s
Blade Length	4.5 m
Rotor Diameter	9.8 m
Tower Height	15-36 m

As seen from the table, the wind turbine provides low cut-in and high cut-out wind speeds, which gives a high range of useful wind speeds for energy production. The tower height can vary between 15 and 36 meters and can be constructed with a latticed structure, which reduces the costs due to less necessary material. Figure 25 shows the power curve of the turbine in blue, and the cut-in, cut-out and rated wind speeds are also included.

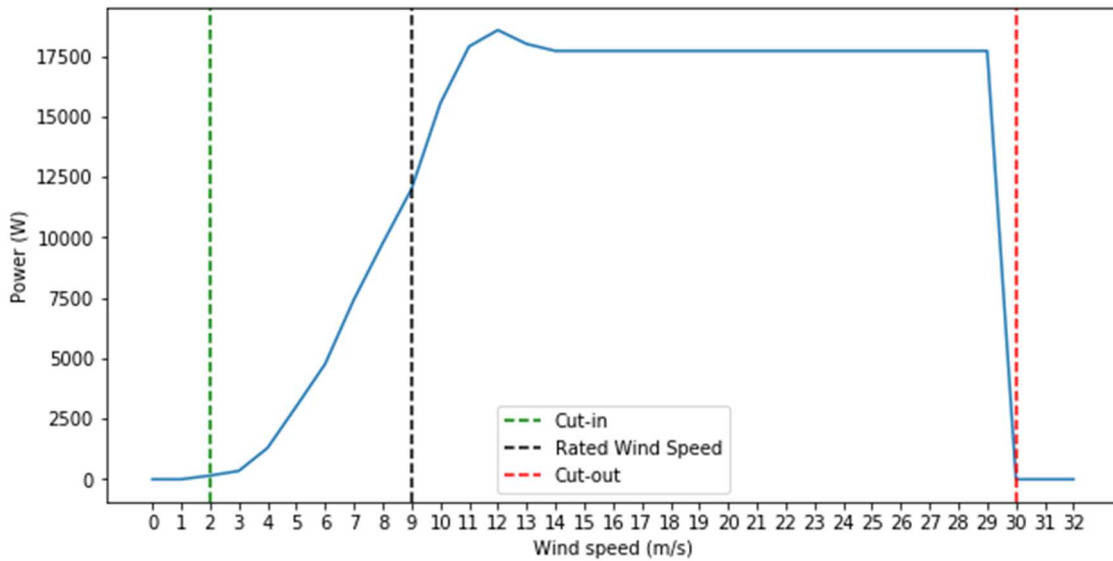


Figure 25 - Power curve for the E-20 HAWT Wind Turbine, including cut-in, cut-out and rated wind speeds

The wind speed dataset including hourly average wind speeds at the weather station Fister – Sigmundstad for 2021 lays the basis for estimating energy production from the wind turbine. Figure 26 presents the variations in measured hourly wind speed through the year, and a 48-hour moving average of the values.

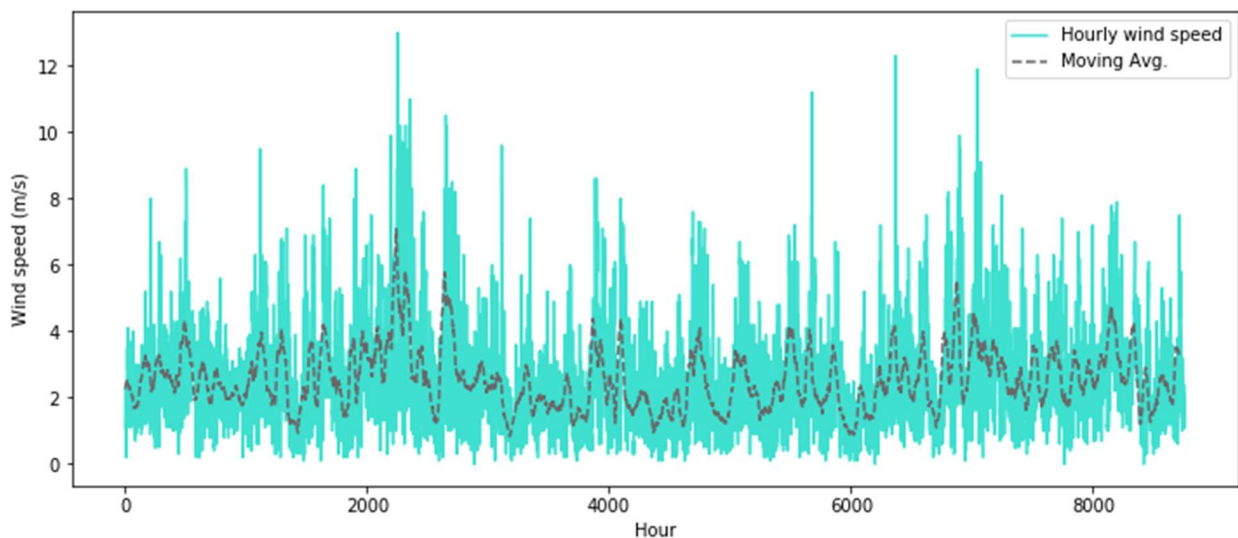


Figure 26 - Variations in measured wind speed for 2021 and 48-hour moving average

There are no clear patterns in the wind speed variations considering the time of the year. Peaks can be observed around March, April, and October, but it is evident that there is no trend like for example the one the solar irradiation follows. The wind speed mostly varies in

the range from 1-4 m/s, with an annual average speed of 2.56 m/s. These are rather limited wind speeds, not optimal for wind energy production. However, there are several major uncertainties regarding the wind speed dataset, like the location, direction and height of the weather station, and the resolution and period of the dataset.

Figure 27 presents the resulting hourly energy production estimates for the wind turbine in [Wh] for one year, based on the wind speed dataset and the power curve. Here also a 48-hour moving average is included.

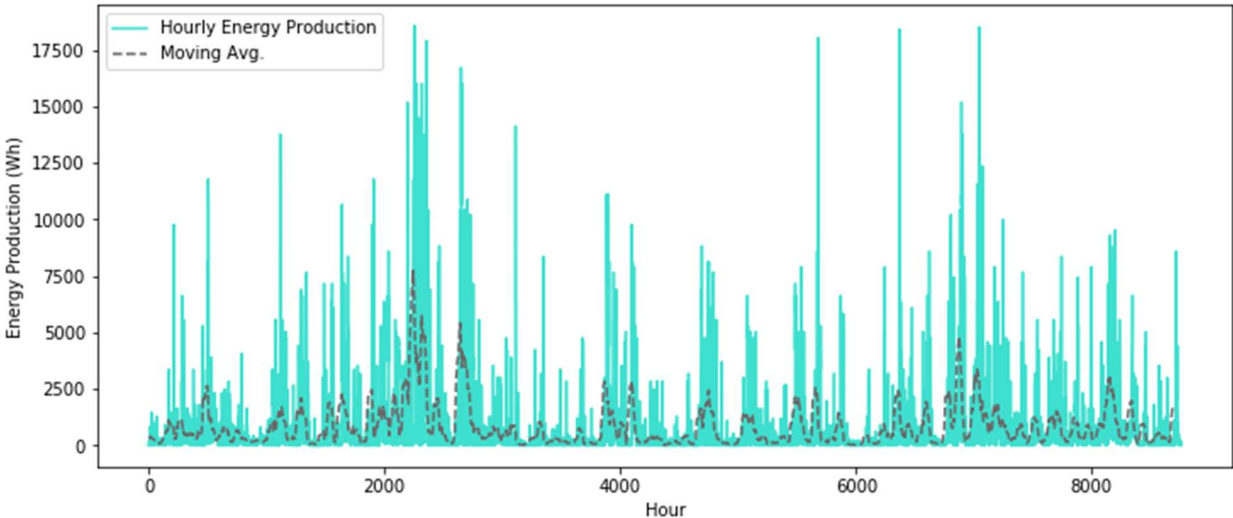


Figure 27 - Variations in hourly energy production from the wind turbine and 48-hour moving average

The energy production estimates follow the wind speed variations quite distinctly, and here also some peaks can be seen in Spring and Autumn. The total annual energy production is 7 403 kWh. The highest monthly production is achieved in April at 1 605 kWh, and the lowest occurs in May at 275 kWh, which means that it is difficult to find concrete correlations based on the seasons. The production fluctuates a lot, which makes it an unreliable and unstable energy source. Wind directions and speeds at different heights should be analyzed to optimize the installation of the wind turbine. It should also be kept in mind that the wind speeds at the farm possibly are higher than at the weather station. This can be due to the hilly surroundings leading to downslope winds which can possibly be much stronger than the winds the weather station is exposed to. Accordingly, the energy production estimates must be looked critically upon. Doubling the annual average wind speed to 5 m/s would result in an

estimated annual energy output of about 32 000 kWh, as stated by the manufacturer. This would more than quadruple the energy output compared to the 2.56 m/s average wind speed.

4.7 Performance Comparison

Comparing production estimates for the PV system and the wind turbine gives an indication on which of the technologies is best suited to the conditions at the farm. The comparison can work as a tip-off for further future development of renewable energy. As the installed PV capacity is much larger compared to the installed wind energy capacity, it makes no sense to compare the energy outputs directly. An interesting comparison is, on the other side, the specific production yield, which is the ratio between energy output and installed capacity. The specific production yield is found for each month, to observe the variations. The calculations are based on 113.85 kW installed PV and 20 kW installed wind energy and are presented in Figure 28.

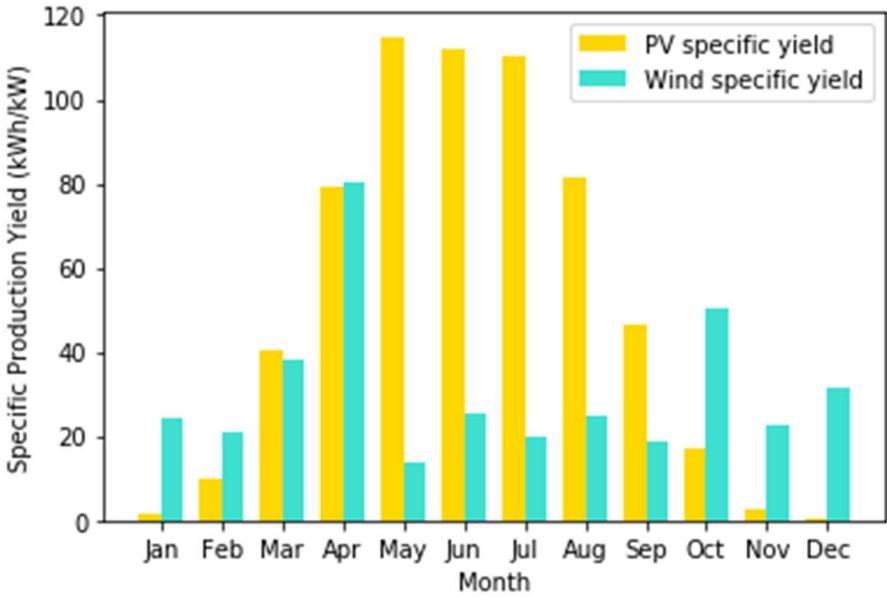


Figure 28 - Monthly specific production yield in (kWh/kW) for the PV system and the wind turbine

The specific yield of the PV system follows the same pattern as the irradiation, with large differences between the summer and winter months. The specific yield of the wind turbine is much more evenly distributed through the year, with lower values than the PV system in the summer, but significantly higher values in the winter. For the PV system the annual specific yield is 615.89 kWh/kW, compared to 370.15 kWh/kW for the wind turbine. With 66% higher annual specific yield it clearly seems as if the climatological conditions at the farm are

more optimal for PV energy production compared to wind energy production, based on the obtained estimates. For the wind turbine to obtain an annual specific yield equal to the PV system, however, an average wind speed only slightly above 3 m/s would be sufficient. The wind turbine’s ability to produce energy both day and night and through the entire year also makes it advantageous compared to the PV system. Combining the two technologies can therefore be a smart measure for increased self-supply through larger parts of the year.

Figures 29 and 30 show the combined PV and wind energy production compared to the average consumption of the Cow Shed and the entire farm respectively. Looking at the Cow Shed the wind energy production slightly increases the surplus production in the summer months, and slightly reduces the deficit in the winter months. In March, the wind energy is the decisive factor for obtaining an energy surplus, compared to what is a deficit with the PV system only. However, the distinct pattern of energy surplus in the summer and deficit in the winter is still clear. When looking at the entire farm it becomes clear that the rather small amounts of wind energy are unable to play an important role for self-supply, compared to the significantly higher PV energy and consumption values. Whether it is economically profitable to install the wind turbine with the estimated output in regard to the investment costs is investigated in Section 4.8.

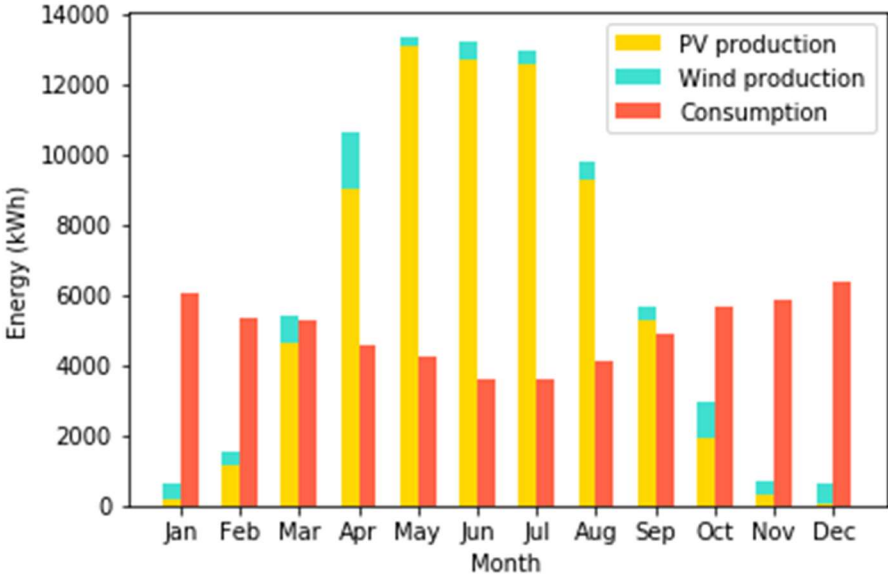


Figure 29 - PV and wind energy production combined and compared to consumption of the Cow Shed

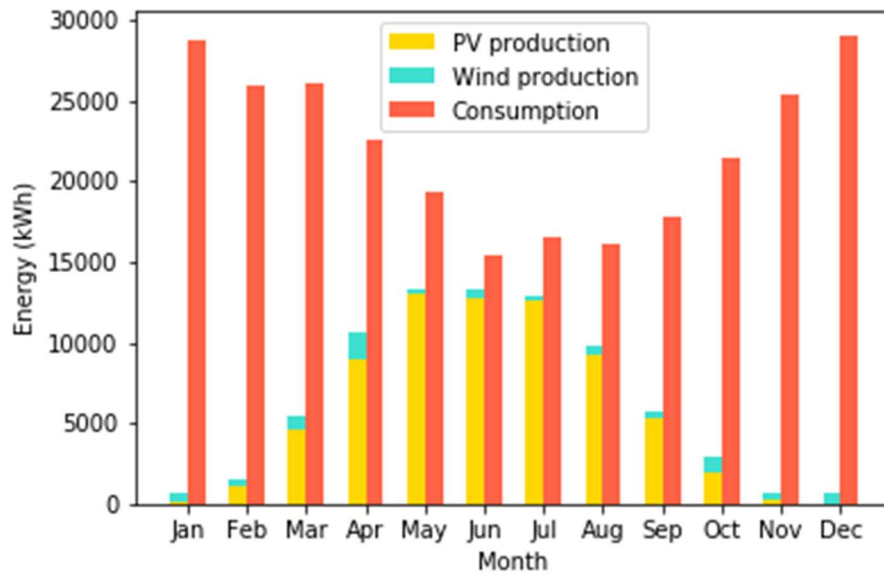


Figure 30 - PV and wind energy production compared to consumption of the entire farm

4.8 Economic Analysis

The economic analysis investigates the profitability of the PV system and the wind turbine, and the combined Hybrid Power System. Section 4.2 revealed that the PV system is able to cover significant parts of the farms energy consumption, and hence has the potential of leading to economic savings and incomes. At the same time, the wind energy production estimates are rather limited, and looking at the economics is therefore necessary to find out if the wind turbine should be considered from an economic view. NPVs and critical values for several factors in the analysis are obtained, based on different spot price scenarios. The results of the three cases are compared. Partitions of the Excel model used to obtain the results are presented in Appendix G.

Following are assumptions made and important numbers used in the economic analysis, regarding production, consumption, costs, degradation rates and supporting deals.

- PV and wind energy production is based on the calculated estimates, and the annual production values are the ones used in the analysis. Energy consumption data is collected from Lyse Elnett for 2019 to 2021 (See Section 3.4) for the Cow Shed alone and the entire farm. At times where energy production is higher than energy consumption, it is assumed that the entire consumption is covered by own produced energy and that the entire surplus energy is sold to the grid. At times where energy production is lower than energy consumption, it is assumed that all own produced energy is consumed within the farm, hence leading to savings in electricity costs.

- Investment costs for both technologies are based on available prices from manufacturers and suppliers, in addition to previous research on PV and wind energy prices. The PV module cost is based on a price of about 3.5 NOK/Wp. This is lower than the 5.4 NOK/Wp price stated by the supplier, and a reason for that is the assumption that a purchase of the number of modules necessary for this project would give a price reduction in total. Also, updated PV price indexes state prices as low as 2 NOK/Wp for the chosen type of PV modules. A 3.5 NOK/Wp PV module price hence seems like a reasonable approach, and the total PV module cost is then set to 400 000 NOK. The inverter cost is based on a price of about 20 000 NOK per inverter, which is stated by several suppliers and reviews for the specific inverter. The total cost for the three inverters arrives at 60 000 NOK. When it comes to the wind turbine, it is rather difficult to arrive at a price estimate. Generally, the low availability of small wind turbines makes this a challenge. The price for Ryse Energy's E-10 10 kW wind turbine, however, is given at approximately 730 000 NOK. Due to very similar features for the E-10 wind turbine and the chosen E-20 wind turbine, especially regarding dimensions like blade length, rotor diameter and tower height, it is reasonable to assume that the price for the E-20 wind turbine is equal to the E-10. An investment cost of 800 000 is used in the analysis, taking shipment into account.
- Installation and maintenance costs are based on previous studies and cases involving PV and wind energy in Norwegian agriculture. For the PV system the installation costs arise due to the electrical connection of the system, which must be performed by a certified electrician. The maintenance costs include cleaning and other basic maintenance and are rather low for a PV system due to no moving parts. The system is on-grid, without batteries, which further decreases the maintenance costs. For the analysis, installation costs of 70 000 NOK and annual maintenance costs of 1000 NOK are used. In addition, it is assumed in the analysis that the inverters must be replaced after 10 years. This gives an additional investment cost in year 10 of the analysis. The price for the inverters in year 10 is assumed to be the same as for the original investment. For the wind turbine installation costs of 100 000 NOK are used in the analysis, to consider costs due to foundation work, mounting, trenching, and cabling. The International Renewable Energy Agency (IRENA) estimates operation and maintenance costs for onshore wind projects of about 0.03 USD/kWh, which leads to annual costs of 2000 NOK for this project [74].

- The annual degradation rate describes the portion of decreased energy output of the system each year due to aging. For the PV system the degradation rate used in the analysis is based on the performance warranty as stated on the datasheet of the PV module, in addition to assumptions related to thermodynamics of PV. The datasheet states a minimum power performance of 80% after 25 years, which leads to an annual degradation rate of 0.8%. The temperatures in the area, however, are lower than both STC and NOCT temperatures. As this is an efficiency increasing factor, it is reasonable to work with a lower degradation rate of 0.4%. For the wind turbine no performance warranty is stated by the manufacturer. Several studies reveal degradation rates for wind turbines in the range from 0.4-0.5% per year, and 0.4% is used in the analysis due to the small turbine which means smaller components and forces. It is assumed that the degradation rates are constant through the period of the analysis.
- Annual power efficiency increase is based on future increase in energy efficiency through the development of technologies and the introduction of energy-efficient facilities. This will lead to a small increase in power efficiency each year, and at the same time a decrease in energy consumption due to more effective energy utilization.
- The investment support deal is based on the program presented by Innovasjon Norge, which is meant to enhance the development of renewable energy and technology in Norwegian agriculture. For a PV system the support deal can cover up to 35% of the investment sum up to 1 million NOK. The deal requires active agricultural operation and a minimum annual consumption of 25 000 kWh. Also, most of the produced energy should be used at the farm. A monthly consumption and production profile must be presented to prove that the production is able to cover a portion of the industrial energy consumption. A smaller portion for private usage or grid export is approved. Looking at the Cow Shed, the grid export is about 15% of the total production in this project, and it is assumed that this is acceptable. The support is not handed for small PV systems, and farms with significant consumption in agricultural operation are prioritized [75]. It is assumed that this project receives the maximum 35% investment support, which is based on the total investment cost for the entire PV system. Innovasjon Norge does not offer deals for wind energy investments. On the other side, the state-owned organization Enova offers support deals for private renewable energy production, including wind energy. The difference in the conditions must be noticed, as Innovasjon Norge supports agricultural operations and Enova's

deal is an agreement for private households. It is assumed that investment support is handed for this project, which includes 7 500 NOK for the installation and an additional 2 000 NOK per installed kW, up to 20 kW [76]. As the turbine in this project is a 20 kW turbine, the entire support of 47 500 NOK is handed. In the case with both PV system and wind turbine, it is assumed that support deals are handed for both.

- In the case analyzing the HPS, investment, installation and maintenance costs and support sums are a sum of the values used for each of the systems alone.
- The WACC used to calculate NPV is based on a report for the AURES II (Auctions for Renewable Energy Support II) project, funded by the European Union’s Horizon 2020 research and innovation program. WACCs for wind energy and PV projects in Europe were presented after interviews with “investors, banks, project developers and other finance experts in the area of renewable energies” [61]. Based on the results, the WACC for this project is set to 3%, for both PV, wind energy and HPS.
- For the costs connected to energy consumption, only the spot price is varied in the analysis. Fixed links, renewable energy taxes, fees to Enova and other costs are assumed to stay constant through the period of the analysis.

4.8.1 Case: PV System

The profitability of the PV system is analyzed for different spot price scenarios. The spot prices investigated range from 0.1 to 1.4 NOK/kWh and should hence cover the most likely future spot prices. During the change of spot prices, all other factors are held constant, to get a clear view on how the spot prices affect the profitability. The analysis revealed a critical spot price of 0.13 NOK/kWh, meaning that prices lower than the critical value lead to an unprofitable project while prices higher than the critical value result in a profitable project. Table 9 presents a selection of 5 of the investigated spot prices and the corresponding NPV.

Table 9 - Spot price scenarios and corresponding NPV of the PV system

Spot price (NOK/kWh)	Net Present Value (NOK)
0.10	-32 275
0.30	169 413
0.60	471 945
1.00	875 320
1.40	1 278 696

The scenario analysis shows the distinct dependence on the spot price. The PV system would for example not be profitable with the average spot price of 2020 (0.10 scenario). However, based on the resulting NPVs and the recent development of spot prices in the NO2 area, the PV system seems like a profitable investment. The NPV increases rapidly with increasing spot prices, supporting the idea that increased grid independence is an economically favorable measure given the parameters used in the analysis of the PV system.

Other critical values are obtained to assess how technical factors of the PV system influence the profitability. During this process, the same spot prices as presented in Table 9 are used, and all other factors are constant. Minimum annual energy production of the PV system and maximum degradation rates required for the system to be profitable are shown for the spot price scenarios in Table 10.

Table 10 - Minimum annual energy production and maximum degradation rate required for NPV = 0 for the spot price scenarios

Spot price (NOK/kWh)	Min. PV Energy Production (kWh)	Max. PV Degradation rate (%)
0.10	75 776	-0.51
0.30	50 382	4.58
0.60	33 528	10.71
1.00	23 186	17.80
1.40	17 720	24.46

As seen from the table the 0.10 spot price scenario requires slightly increased annual energy production compared to the calculated estimates (70 120 kWh). For the degradation rate it would require an unrealistic increase in efficiency each year. The scenarios covering the spot prices seen in the most recent period require energy production significantly lower than the estimates, and unrealistically high degradation rates, for the project to be unprofitable. This also supports the indication that the PV system is an economically profitable investment.

The payback period is also very dependent on the spot price. In this case, payback periods for the spot price scenarios 0.30, 0.70 and 1.00 NOK/kWh are calculated. This results in payback periods of 10.8, 5.5 and 4.2 years, respectively. A spot price increase from 0.30 to 0.70 hence halves the payback period, while the reduction is smaller with further increasing prices. The payback period for recently observed spot prices is impressively short, which again supports the profitability of the PV system. With the 0.70 spot price scenario, electricity costs close to

70 000 NOK could be saved annually, and the savings increase with higher spot prices. The 1.00 spot price scenario leads to savings around 90 000 NOK annually.

4.8.2 Case: Wind Turbine

For the wind turbine alone, the same analysis is performed as for the PV system. When it comes to the spot price, a critical value of 8 NOK/kWh already gives an indication that the wind turbine alone hardly is a profitable investment, as all spot prices below the critical value will lead to an unprofitable project when all other factors are constant. The NPV is calculated for the same range of spot prices as in the previous section, resulting in Table 11.

Table 11 - Spot price scenarios and corresponding NPV of the wind turbine

Spot price (NOK/kWh)	Net Present Value (NOK)
0.10	-840 009
0.30	-818 715
0.60	-786 775
1.00	-744 188
1.40	-701 602

As predicted, the scenarios covering the range of possible spot prices all result in negative NPVs. The same pattern is recognized, as NPV increases with increasing spot price, due to higher electricity savings. The variations in NPV are much smaller compared to the PV system, because of the lower energy production and hence lower annual savings. The NPV for the wind turbine is in other words far less dependent on the spot price.

Due to the small variations in NPV, the spot price is set to 0.70 NOK/kWh when calculating critical values for the wind turbine. The analysis resulted in a minimum annual energy production from the wind turbine of 61 543 kWh, for the turbine to become profitable. As stated by the manufacturer this would require an average wind speed of almost 7 m/s. This is possible at a site with better wind conditions and shows that the profitability of a wind turbine largely depends on the wind conditions and energy output. The analysis also resulted in maximum investment costs of 23 871 NOK, or a minimum support sum of 823 600 NOK. As the investment costs are set to 800 000 NOK, this means that the wind turbine would have to be fully supported by the government if it was to become profitable for the farm. The analysis

clearly dictates that the wind turbine alone is an economically unprofitable investment with the standing energy production, investment costs, support deal and spot prices.

Another possibility for farms with large areas is to cooperate with wind energy companies. The farmer could then rent out available areas for the company to install wind energy of their own. Deals could be established where the farmer is either provided with a limited amount of free energy supply from the turbines or claims a certain percentage of the economic excess each year. This could result in significant savings or incomes and would possibly be more profitable compared to the investment of a private turbine.

4.8.3 Case: Hybrid Power System

The last case looks at a combined Hybrid Power System including the PV system and the wind turbine. The critical spot price value is 0.88 NOK/kWh, which indicates that the spot price is highly decisive for a positive or negative NPV in this case. Prices below the critical value will lead to negative NPVs and prices above will lead to positive NPVs. Both scenarios are likely. The NPV is calculated for the same range of spot prices as in the previous sections.

Table 12 - Spot price scenarios and corresponding NPV of the HPS

Spot price (NOK/kWh)	Net Present Value (NOK)
0.10	-872 283
0.30	-649 302
0.60	-314 831
1.00	131 132
1.40	577 094

As mentioned, the NPV changes from negative to positive over the spot price range. The variations are large, and it is evident that the spot price can make the HPS very unprofitable, very profitable, and interfacial.

It is difficult to determine the profitability of the HPS only based on spot prices, as the NPV changes from negative to positive inside of a very likely range of future spot prices. Critical values for other factors are therefore calculated, to assess how realistic the factors are in the different scenarios. Again, the same spot price scenarios are investigated, and critical values for total energy production and investment costs are shown in Table 13.

Table 13 - Critical values for energy production and investment costs for each spot price scenario

Spot price (NOK/kWh)	Min. Energy Production (kWh)	Max. Investment costs (NOK)
0.10	230 378	393 717
0.30	153 173	616 698
0.60	101 933	951 169
1.00	70 492	1 397 132
1.40	53 874	1 843 094

The estimated total energy production is 77 523 kWh and the total investment costs are set to 1 266 000 NOK. The results show that the lowest spot price scenarios require unrealistically high energy production or low investment costs, for the HPS to become profitable. The critical spot price of 0.88 NOK/kWh lies in between the 0.60 and 1.00 scenario, which makes these interesting scenarios. For the 0.60 scenario the increased energy production seems unrealistic, but the investment costs, which must see a 25% decrease for NPV = 0, is possibly a more realistic factor in this scenario. Future price development for renewable energy technologies and increased support could help achieve the critical value for the investment costs. Since the support deal from Innovasjon Norge for the PV system already counts as a significant part, it is reasonable to believe that increased support for the wind turbine has the highest potential in this case. By achieving this, the critical spot price could be pushed downwards, increasing the probability of a profitable investment. At the same time, looking at the 1.00 scenario the minimum energy production is rather close to the estimated production. Downtime and other faults in the wind turbine or the PV system are therefore an uncertainty and could push the critical spot price upwards. Concluding with a critical spot price is hence difficult, and it can possibly vary between 0.60 and 1.00 NOK/kWh depending on the mentioned factors. Considering the unstable spot prices in the last years, deciding whether the HPS is a profitable investment or not is a complex process.

4.8.4 Summary/Comparison

The profitability of the PV system, wind turbine and combined HPS has been investigated based on different spot price scenarios, and critical values for several factors have been assessed. The results show that the profitability largely depends on the future spot price, but factors like energy output and investment costs are also important for the profitability. Based on the findings the PV system seems like a profitable investment, as NPV is positive for the most likely future spot prices and critical values are realistic to achieve under said prices. The

wind turbine alone, on the other side, seems like an unprofitable investment due to its large negative NPV and unrealistic critical values. For the HPS it is rather difficult to determine the profitability, and spot prices, energy production and investment costs can all tilt it in one direction or the other. Figure 31 summarizes the NPV variations for the PV system, wind turbine and HPS for the five spot price scenarios discussed in the previous sections.

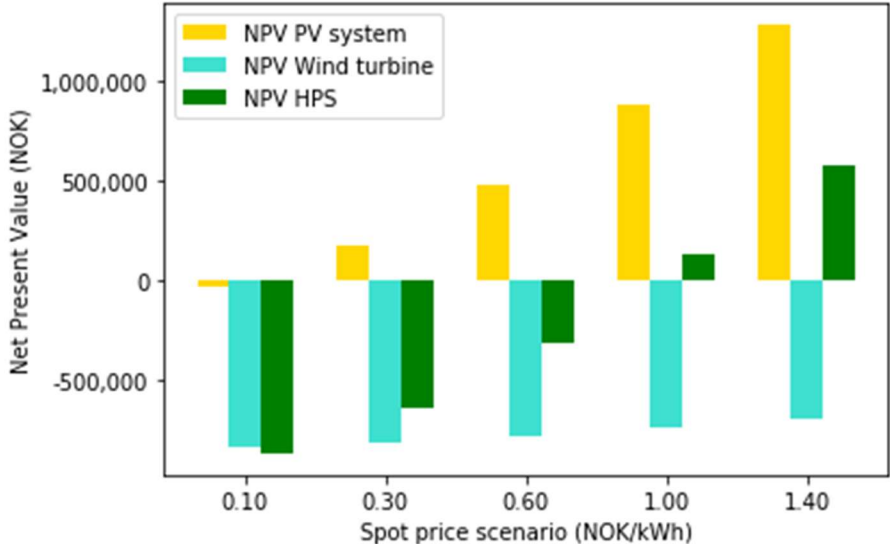


Figure 31 - NPVs for the three cases for the different spot price scenarios

4.9 Uncertainties and Limitations

The following sections present uncertainties regarding the method and results, and factors that limit increased accuracy. They also discuss possible changes and variants to each part of the results and how these could affect the results.

4.9.1 Area Solar Radiation in ArcGIS

The Area Solar Radiation tool is used for the solar radiation analysis performed in ArcGIS. The tool works with several parameters that can be changed freely. Topographic parameters describe inputs such as slope and aspect types, calculation directions and a z-factor used to adjust between the length units feet and meters. All topographic parameters are set to default when running the analysis. The default values are set to optimize the output data and changing these would possibly lead to deviations. The parameters connected to radiation represent the main uncertainty in the Area Solar Radiation tool and determine the sky size and the diffuse and transmittance proportions of the incoming radiation. All these parameters affect the solar radiation analysis. The parameters Diffuse Proportion and Transmittivity are not changed from the default values (Diffuse Proportion 0.3 and Transmittivity 0.5). These parameters vary both across different areas and through the year and would hence affect the results of the

analysis. Using validated values for Diffuse Proportion and Transmittivity is therefore important for obtaining accurate results. Previous studies show that using the Area Solar Radiation tool with the default values for these parameters leads to substantial underestimation [77]. As a result, there is a significant uncertainty connected to the irradiation values, as they should possibly be higher than the ones obtained in this thesis. In order to eliminate this uncertainty, monthly values of the Diffuse proportion and Transmittivity should be obtained by former research or long-term measurement at the location. This requires advanced measurement methods and is therefore beyond the limits of this thesis. Diffuse Proportion and Transmittivity values could also be tested to find combinations that match real irradiation data from the area. The absence of radiation measuring stations in the area, however, makes it difficult to validate these parameters externally. In summary, the input raster layer, latitude, and calculation time interval settings are the only parameters that are changed from default. Also, upgrading the 1-meter resolution of the DSM model to for example a 0.25-meter resolution would give even more accurate radiation values, as the ability of identifying factors on the rooftop like shadows and edges would be increased. The layer with building footprints used as a mask to isolate rooftops during the analysis is also an uncertainty, as location transfers between the layer and the real location of the building could lead to inaccuracies. To check the accuracy of the radiation values acquired from the solar radiation analysis, they should also be compared to real radiation data from a measuring station at the site. As mentioned, this is not performed due to the absence of radiation measuring stations close to the farm. The irradiation values obtained from the analysis are the results of running Area Solar Radiation for one year (2021) on the rooftop of the Cow Shed. As incoming radiation is far from constant over the years, irregularities can occur. Average values from several years of solar radiation analysis would therefore possibly be more accurate, regarding the use of the values for estimating energy production from a PV system. This would also be significantly more time consuming. Area Solar Radiation was, however, run for the year 2020 also, and only minimal annual variations of $<0.1 \text{ kWh/m}^2$ were observed compared to 2021.

4.9.2 PV Energy Estimates and Energy Consumption

Many outer factors, like weather, pollution, and dust, affect the energy production of a PV system. When it comes to the weather, extreme cases can occur frequently, especially in Southwestern Norway which is an area exposed to harsh and severe weather coming in from the Atlantic. Solar irradiation values will then differ from the ones obtained in ArcGIS, and

temperature data could be affected. It would also affect the efficiency of the PV modules. The production estimates depend largely on the irradiation values. These are an uncertainty due to the methods used in ArcGIS, which influences the accuracy of the production estimates. Based on the possible underestimation of solar radiation in the ArcGIS analysis, the energy production estimates are possibly also underestimated. They hence provide a rather conservative overview of the potential of PV at the farm. As mentioned in Section 4.1.2 parameters like efficiency, performance ratio and temperature coefficient are assumed based on the goal to work with realistic production values. The area covered by modules is also assumed based on the total area of the rooftop and considerations around installation distances. Changing the area would also change the production estimates. The factor added to take self-generated heating of the panels into account is an assumed value and constant through the year. At the same time, the performance ratio is also constant, but will in reality vary with the varying efficiency, as they are directly connected through Equation 3. Tilting of the modules is not considered, as it is assumed that they are mounted directly and parallel to the surface of the rooftop, and the solar radiation analysis gives irradiation values on that specific rooftop. Changing the tilt of the modules and comparing the corresponding energy production could be interesting to obtain the optimized configuration. The degradation of the PV system leads to a reduction in efficiency over time, and hence reduced energy output. In the estimates in this thesis the degradation rate is not considered, and the results will describe the output before any degradation has taken place. When looking at long term production estimates, degradation should be implemented as it is done in the economic analysis. Snow also has a direct effect on the energy production of a PV system, as it partly or completely blocks the incoming irradiation. The area of interest, however, is an area with very little snowfall, due to its moist and mild climate. The implementation of loss factors due to reduced production due to snow is therefore neglected in this case. It should also be noticed that the estimated production values are obtained by combining average radiation values for the year 2021 with average temperature values over a 3-year time series. Due to the unstable solar conditions in Norway, energy production will likely fluctuate largely over the years, and the results in this thesis must therefore only be looked upon as estimates giving an indication on the range of potential production.

Random effects can also have an impact on the consumption data, and single events can therefore lead to abnormal consumption values. In the comparisons in Section 4.2 and the economic analysis in Section 4.8, average consumption data from 2019 to 2021 is used. This

should give a good overview of recent consumption at the farm, but future consumption is an uncertainty. Future energy consumption at the farm will be influenced by possible increased electrification and general increased operation at the farm. At the same time, energy efficiency increasing measures regarding for example buildings' structural envelope and energy consuming loads at the farm can influence the total consumption in the other direction. These thoughts are supported by a report from DNV on future energy transition in Norway, documenting increased energy demand in Norwegian buildings in the past, but forecasting the demand to flatten out in the future [48].

The temperature and consumption datasets are collected for three years, and several effects can influence the datasets, as discussed above. Collecting data over a longer period (e.g., 10 years) can help exclude uncertainties. The monthly resolution of temperature, irradiation, consumption, and estimated production gives good indications on the opportunities of PV at the farm. Higher resolutions, like daily or hourly measurements, can give a deeper understanding of how factors like consumption, production and temperature are related, and how these again relate to the usage of the Cow Shed. It would enable analyses of e.g., which are the most consuming hours during a day, and which are the most productive hours during a day for the PV system. In that way the economics could also be assessed more accurately, looking at hour-to-hour rather than annual changes.

4.9.3 PVsyst Simulation

The PV system performance simulation in PVsyst is based on several factors that affect the results. The performance of the simulated PV system depends on which PV modules and inverters are chosen in the simulation and how the configuration is set up. Different module nominal power output, and parameters like temperature coefficients and degradation rates, in addition to different inverter sizes and numbers make the results vary significantly. Also, components are available from many manufacturers, and the mentioned parameters are likely to vary across the manufacturers. The accuracy of the simulation is also very dependent on the meteorological data from the database Meteonorm. Inaccuracies regarding the data, and especially the irradiation values, used in PVsyst are discussed in Section 4.1.3. The irradiation values in PVsyst differ from the values from ArcGIS, and accordingly lead to differences in the production estimates. To check the accuracy of the irradiation values used in PVsyst, they should also be compared to real irradiation data from a measuring station at the farm. This would require research prior to the start of this thesis and is not performed.

4.9.4 PV System Sizing and Design

PV technologies like for example thin film cells are not considered during the sizing and design of the PV system. Exploring other technologies could give interesting findings regarding cost of energy and investment costs. Due to the limited selection of technologies available from Norwegian PV providers, this is not executed. For future installations, exploring other technologies is a reasonable approach. 72-cell PV modules are commonly used, but not considered in this case. Changing to 72-cell modules would likely affect the total number of modules, depending on the available area on the rooftop. The mounting system for the PV modules is not considered in this thesis. Different mounting systems will lead to different requirements when it comes to fulfilling TEK17, and different installation costs. Building-integrated PV (BIPV) is not explored, nor are bifacial modules, as the system is mounted directly to an existing rooftop.

When sizing both the DC and AC cables in the PV system the lengths of the cables are assumed, based on general dimensions of the Cow Shed. The length is important for determining the CSA of the cables through Equation 13. Increasing the length requires higher CSA, when keeping the voltage drop constant. Accurate measurements of the path length should be executed before determining the cable CSA. For the DC cables, different path lengths from the different strings to the inverters are not considered, and the same length is assumed for all the cables. The same assumption is made for the AC cables from the inverters to the distribution board.

When it comes to the final design, several variants are possible regarding array/inverter configuration and other connections in the rest of the system. Choosing other inverters, and changing the number of MPPT inputs, would affect the number of strings and number of modules per string in the PV array. This is also discussed in Section 4.3.2. Designing the PV system as an off-grid system with energy storage is also a possibility. This would require some changes in the design, as components like batteries and charge controllers would have to be included. This would also affect the sizing process.

4.9.5 Electric Tractor Charging

When assessing the possibility of implementing a charging station for an electric tractor into the PV system a specific tractor is not chosen. Electric tractors are still in early phases, and there are few commercially available electric tractors on the market. As they are relatively untested, and their capabilities and challenges unmapped at larger scales, necessary

information regarding the charging station is based on numbers stated by producers like H2Trac BV and AGCO on their electric tractor projects. The 32 A three-phase charging cable is used as basis when sizing the cable which supplies the charging station. Different capacities for the charging cable would require other supply cable sizes. The 32 A charging cable is only used as an example to enable the set-up of the charging station design. The type of charging contact is not considered. Different contacts would enable different charging power and can vary between AC and DC charging. The assumed charging power is a maximum of 22 kW, which could be achieved with the 32 A charging cable and 400 V. This corresponds with the information stated by AGCO, but higher charging powers for electric vehicles are possible. Higher charging power would enable faster charging, but this depends on the battery capacity of the vehicle and changes the dimensions of the charging station. It is assumed that the tractor's internal charging system supports three-phase 230 V charging. When it comes to electric cars not all cars support this charging method, but it is assumed that electric tractors, in the future at least, support this.

4.9.6 Wind Data and Wind Energy Estimates

The estimated wind energy production of the E-20 HAWT Wind Turbine is calculated based on hourly wind speed data from the weather station Fister – Sigmundstad, 4.25 km away from the farm. The wind data should be adequate for estimating wind energy production in the area, but inaccuracies are still likely to occur due to the locations, heights and directions of the weather station and the farm. The largest uncertainty regarding the wind speed data is that it is only gathered for one year (2021). This is because of the Python code used for production calculation, which must have hourly wind speeds as input. The wind conditions can differ largely from year to year, which means that some years can be much more suitable for wind energy production compared to others. As seen in Section 4.6 and 4.8 these variations will affect both energy output and the economic aspects around the wind turbine. Average wind speed data collected over several years should hence lay the basis for estimating energy production, as data from a single year possibly differs a lot from normal annual averages. Average monthly wind speeds for all years from 2016 to 2021 are therefore collected to find possible interannual correlations. Figure 32 presents the monthly wind speed variations for the mentioned six-year period. The solid line represents the wind speeds for 2021 used to estimate energy production. Interannual changes are rather limited, and the 2021 wind speeds do not differ a lot from the other years, although it sees quite low wind speeds in the summer months especially. Looking at annual average wind speeds, the variations are also rather

small, from a maximum of 2.85 m/s in 2018 to the minimum of 2.56 m/s in 2021. Energy production values higher than the ones obtained by using 2021 as basis are therefore both possible and likely. An interesting observation in Figure 32 is the tendency of higher wind speeds in the winter compared to the summer. For the six-year period the average monthly wind speed in June and July are 2.25 and 2.3 m/s respectively. In December, January and February the average wind speeds increase to 2.92, 3.20 and 2.97 m/s. This supports the idea that the wind turbine sees higher output when the PV production is at its minimum, and vice versa.

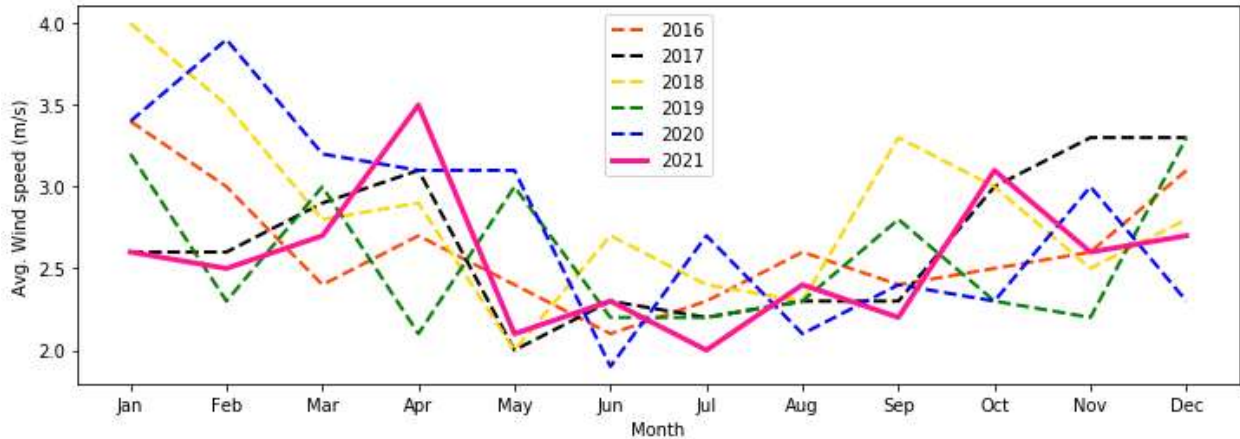


Figure 32 - Average monthly wind speeds for 2016-2021

The wind speed data from the mentioned weather station could also be compared to measurements from other stations in the vicinity, but there are few weather stations available with sufficient wind data. To optimize investigation of wind conditions at the farm, wind speed measurements at the specific location of a potential turbine should be performed, in regard to both height and direction of the wind.

4.9.7 Economic Analysis

The economic analysis looks at annual production and consumption, and annual changes in inflows and outflows. It does not take daily or seasonal variations and peaks in spot prices, consumption, and production into account, which would affect an analysis with higher resolution. The production values are also estimates for one specific year and will likely vary according to varying irradiation and wind conditions through the period of the analysis. The same applies for the consumption, and unexpected variations in these factors would affect the results of the analysis.

Since the analysis looks at the entire farm, savings due to reduced grid dependence and savings through grid export are not separated. In the case of surplus energy production, looking at the Cow Shed only, it is assumed that the income earned by exporting the surplus energy to the grid is equal to the electricity costs saved by consuming the surplus energy elsewhere at the farm. The PV system is designed in Section 4.4 as an on-grid system. Comparing the economics of immediate energy consumption at the farm and energy export to the grid thoroughly would therefore be an interesting task. As the economic analysis only looks at annual values and changes, it is difficult to implement grid export, as this varies through the year based on the amount of production and consumption. An economic analysis with higher resolution, looking at monthly changes for example, would enable the implementation of inflows and outflows due to grid export and import looking at the Cow Shed only. Costs connected to the transport of energy from the Cow Shed to other buildings are not included.

4.9.7.1 Energy-related Costs

The investment costs connected to the PV system and the wind turbine are important factors for the profitability of the systems. Prices are likely to vary between manufacturers and providers, and for the PV modules the price depends on the technology and ratings. In addition, low access to manufacturing materials, such as Silicon, has increased PV prices recently. The future development of these prices is therefore uncertain. For the wind turbine the investment costs are also an uncertainty. There are very few available SWTs on the market, which means that it is difficult to compare and validate prices by looking at for example NOK/kW prices, as it is done easier for the PV system. The price used in the analysis is based on an available price for the smaller turbine model E-10. This price is likely to give a good indication on the price of the E-20 turbine, due to their similarities, but differences can nevertheless occur. The shipment costs and the distance between the manufacturing site and the farm are also uncertainties that are not investigated thoroughly in this thesis. The development and spreading of SWTs is expected to increase in the future, and this would possibly lower the prices. Whether the wind turbine is installed on-grid or off-grid with energy storage is not considered. If purchased individually, the implementation of batteries could possibly increase both investment and maintenance costs. Installation and maintenance costs are also uncertainties in the analysis. Outer factors like weather impacts, the farmer's capacity of performing maintenance and the installer's skills can all affect installation and maintenance costs.

It is assumed that most of the components in the PV and wind system do not need to be replaced during the period of the analysis. The PV modules and the wind turbine have stated lifetimes of 25 and 20 years respectively, but components like for example cables, generators or controlling and monitoring devices must possibly be replaced or upgraded during these lifetimes. This would lead to additional expenses. The economics of the wind turbine are analyzed over 20 years, to be able to compare it directly to the PV system. Extending the period to 25 years, or more, would possibly affect the profitability of the wind turbine.

Costs connected to application processes for the installation of the wind turbine are not considered in the economic analysis. The installation of wind turbines can possibly meet opposition through neighbors or local authorities, and the process of receiving approval for the installation can hence involve costs.

4.9.7.2 Electricity-related Costs

Electricity prices can vary a lot during a day, from day to day, from season to season and from year to year. NVE expects the prices to vary even more in the future, as energy production capacity will depend more on weather due to the development of wind and solar energy. These energy sources will lead to variations based on available wind and sun conditions. Higher fuel and CO₂ prices will also strengthen the variations. The spot prices collected for the NO2 spot price area from Nord Pool showed large annual fluctuations from an average price of 0.1 NOK/kWh in 2020 to 0.76 NOK/kWh in 2021 and 1.49 NOK/kWh in the first quarter of 2022. The winter 2019/2020 saw record high amounts of snow in the Norwegian mountains. The following large volume of meltwater led to a strong hydrologic balance resulting in large energy production. In addition, 2020 was a warm year, and Norwegians hence consumed less energy for heating. These weather dependent factors combined with the limited energy transmission capacity to other countries led to very low electricity prices. The winter 2020/2021 was a cold winter, which led to increased consumption for heating. At the same time, dry weather during the second half of 2021 weakened the hydrologic balance, leading to significantly lower filling degree in the hydropower plants. Increasing fuel and CO₂ prices due to low gas reserves pushed the prices up in all of Europe. The transmission links to Germany and Great Britain (NordLink and North Sea Link) started operating and made the Norwegian prices more exposed to those in the rest of Europe [59]. These factors led to significantly higher electricity prices in 2021. The prices have continued to increase in the start of 2022, and the war in Ukraine is a reason for that. Due to the reduced gas transport from Russia to other gas dependent countries in Europe the gas and electricity prices

increased drastically, and this has had consequences even for the prices in Norway. Electricity prices thus depend on weather and energy production capacity, and several other external factors that are impossible to control and predict. Prices can also vary between energy suppliers and fixed prices and other costs can change over the period of the analysis.

The compensation scheme introduced by the Norwegian government in the end of 2021 is not considered in the analysis. Due to the abnormally high electricity prices in the last quarter of 2021 the government introduced a compensation scheme involving repayment of electricity costs for households, companies, and agriculture. In the case of a spot price higher than 0.70 NOK/kWh the government covered 55% of the costs exceeding 0.70 NOK/kWh in December 2021. From January to March 2022 the compensation was even increased to 80% [78]. This compensation surely affects the electricity costs, but it is a difficult factor to implement into the economic analysis, which only looks at annual changes.

4.9.7.3 Other Uncertainties

The degradation rates of both the PV system and the wind turbine are assumed to be the same each year. It is hence not assumed that any upgrade is performed during the 20-year period to stop the degradation.

The annual power efficiency increase leads to a reduced total annual energy consumption each year through the analysis period. This is an uncertain factor as increased electrification at the farm could also lead to increased consumption, which would affect the economic analysis.

The WACC is a very unstable financial variable in renewable energy projects. It depends on risks perceptions and assessments, and dynamic elements such as country specific risks, energy public policies, interest rate, regulations, technology, and competition between market actors [61]. Defining a WACC for a large period is hence an uncertainty.

When using the Goal Seek function in Excel to obtain critical values, all other factors included in the analysis must be held constant. This can give inaccuracies, as several factors may change at the same time, dependently or independently from each other. This could affect the results.

5 Summary and Conclusion

5.1 Summary

Renewable energy production at farms has large potential when it comes to reducing grid dependence and supporting electrification and sustainability. Additionally, farms often provide necessary available area and favorable conditions for several renewable energy technologies. In this thesis, opportunities for renewable energy development at a farm in Southwestern Norway are assessed. Solar radiation conditions on the rooftop of a building holding cows are analyzed with the Area Solar Radiation tool in ArcGIS. The building is chosen due to its isolated location at the farm and consumption profile, making it an interesting object for potential future grid independence. Energy production from a potential PV system on the most suitable part of the rooftop is estimated both through an analytical method and simulation in PVsyst. The calculated energy production estimates are compared to consumption data, to investigate the system's ability of covering the energy consumption of the Cow Shed alone, and the entire farm. Components for the PV system, such as modules, inverters and cables are sized and chosen, based on availability on the Norwegian market, and a complete system design is proposed. Further, ways of implementing a charging system for an electric tractor in combination with the PV system are proposed and discussed. Wind conditions are explored and wind energy production from a potential wind turbine at the farm is estimated, and performance compared to the PV system. At the end, the economics are analyzed looking at the PV system and the wind turbine individually and as a combined Hybrid Power System, with the goal of identifying profitability for several electricity price scenarios.

5.2 Conclusion

A PV system on the Southwest facing rooftop of the Cow Shed can give average annual energy production above 70 MWh, with maximum monthly production in the range of 12-13 MWh. The Cow Shed sees an energy surplus between April and September, while the system can cover up to 80% of the total consumption of the entire farm in the summer months. A PV system simulated in PVsyst shows significantly higher production values. Both ArcGIS and PVsyst have weaknesses when it comes to mapping solar irradiation at rural sites. The tendency, which has been supported in previous studies, is that ArcGIS underestimates and PVsyst overestimates. The sized PV system consists of 414 60-cell 275 Wp modules, configured in 18 strings with 23 modules each. It includes 3 inverters, where each has a

rated output power of 33 kW and 3 MPPT inputs. This leads to a DC-to-AC ratio of 1.15. A charging station for an electric tractor can be implemented to the PV system in various ways and can be supplied either with AC or DC power from the PV system. Connecting it to the DC side of the system in combination with an ESU can give higher flexibility around the time of charging. Connection to the grid should, however, always be included for times with insufficient PV production. Wind energy production from a proposed 20 kW SWT is estimated slightly above 7 MWh annually, based on wind speed data collected from the weather station Fister – Sigmundstad for 2021. Variations through the year are large, and uncertainties regarding the wind speed dataset must be kept in mind. As an energy source able to produce both day and night and both summer and winter, however, the wind energy technology is suitable for combination with PV. The economic analysis reveals a critical spot price of 0.13 NOK/kWh for the PV system to be a profitable project, and it shows short payback periods of 4-5 years and annual electricity savings up to 100 000 NOK with recently observed spot prices in the NO2 area. The analysis also indicates that the wind turbine is an unprofitable investment. High investment costs and rather low support sums are the main factors, but wind conditions and energy output are also decisive. A combined Hybrid Power System seems profitable but highly dependent on spot prices, investment costs and energy production, with a critical spot price of 0.88 NOK/kWh. Future spot prices provide a large uncertainty when it comes to assessing the economics.

As mentioned, a PV system only at one part of the rooftop of one single building at the farm can cover up to 80% of the entire consumption of the farm in the months with maximum production. This shows that there is a large potential for increased renewable energy development and hence increased self-supply at farms. To support electrification in the agriculture, local energy production is a solution against frequent grid blackouts, expensive grid upgrade or even lacking energy supply. With the high spot prices seen in Southern Norway recently, terrific sums of electricity costs can be saved by supplying the farm with own produced renewable energy. There are hence both economic and environmental profits to be gained by further exploring and developing the large potential.

5.3 Further Work

Several improvements can be performed when mapping solar and wind conditions at the farm. Accurate values for Diffuse Proportion and Transmittivity should be implemented to the Area Solar Radiation tool in ArcGIS. Increasing other topographic parameters could also augment

the accuracy, but it would also lengthen computing times. Validating irradiation values at a site as rural as the farm in this thesis is, however, difficult without local measurements. Executing irradiation measurements would hence give the most accurate results. The same applies for the wind conditions. Wind data collected over a longer period could be used for estimating energy production, to minimize the impacts of random effects on the dataset. Wind measurements should be performed at different heights, locations, and directions, for the best results. This work would require long-term practical execution at the farm. To work further with the existing findings of this thesis, several variants and new thoughts could be investigated.

When it comes to the sizing and design of the PV system, assessing an off-grid system could be interesting in regard to the technical and economic considerations. Upscaling the energy production to make the Cow Shed an independent microgrid could enable complete independence from the grid, which could lead to significant economic savings due to both grid import and grid rent. Upscaling the energy production would require further research on small-scale wind energy, and mapping of new areas suitable for PV development. Other PV technologies like BIPV, ground mounted tracking systems or transparent concentrator PV systems could be introduced. Additionally, technologies like biomass energy and biogas production have large potential at farms and could be interesting for increased own energy production.

To develop further understanding on the impact electric tractors possibly can have on farming both environmental, economic, and technical considerations could be investigated. Estimating the reduced amount of greenhouse gas emissions in the agriculture due to the change from combustion engine tractors to electric tractors could be an interesting starting point. Investment and operation costs for electric tractors could be assessed parallel with the rising market. This would allow the mapping of fuel cost savings and purchase prices necessary for the tractor to become an attractive investment. The same applies for technical considerations regarding the combination of charging stations with other renewable energy sources.

The economics could also be investigated deeper than what has been done in this thesis. Looking at daily or hourly changes for example would enable an analysis on how spot prices affect electricity costs and grid export income through the day and would allow further research on the most cost-effective way of using surplus energy. Other business models, like

renting out area to energy companies and claim profits instead of investing in private systems, could be analyzed.

Generally, local renewable energy development and electrification in the agriculture is a research field with a lot of potential in the future. Increased electrification will increase the stress on the electricity grid and expensive grid upgrades can be replaced with self-supply at the farms, which is both an economically and environmentally favorable measure on long-term.

Appendix

A Solar Maps

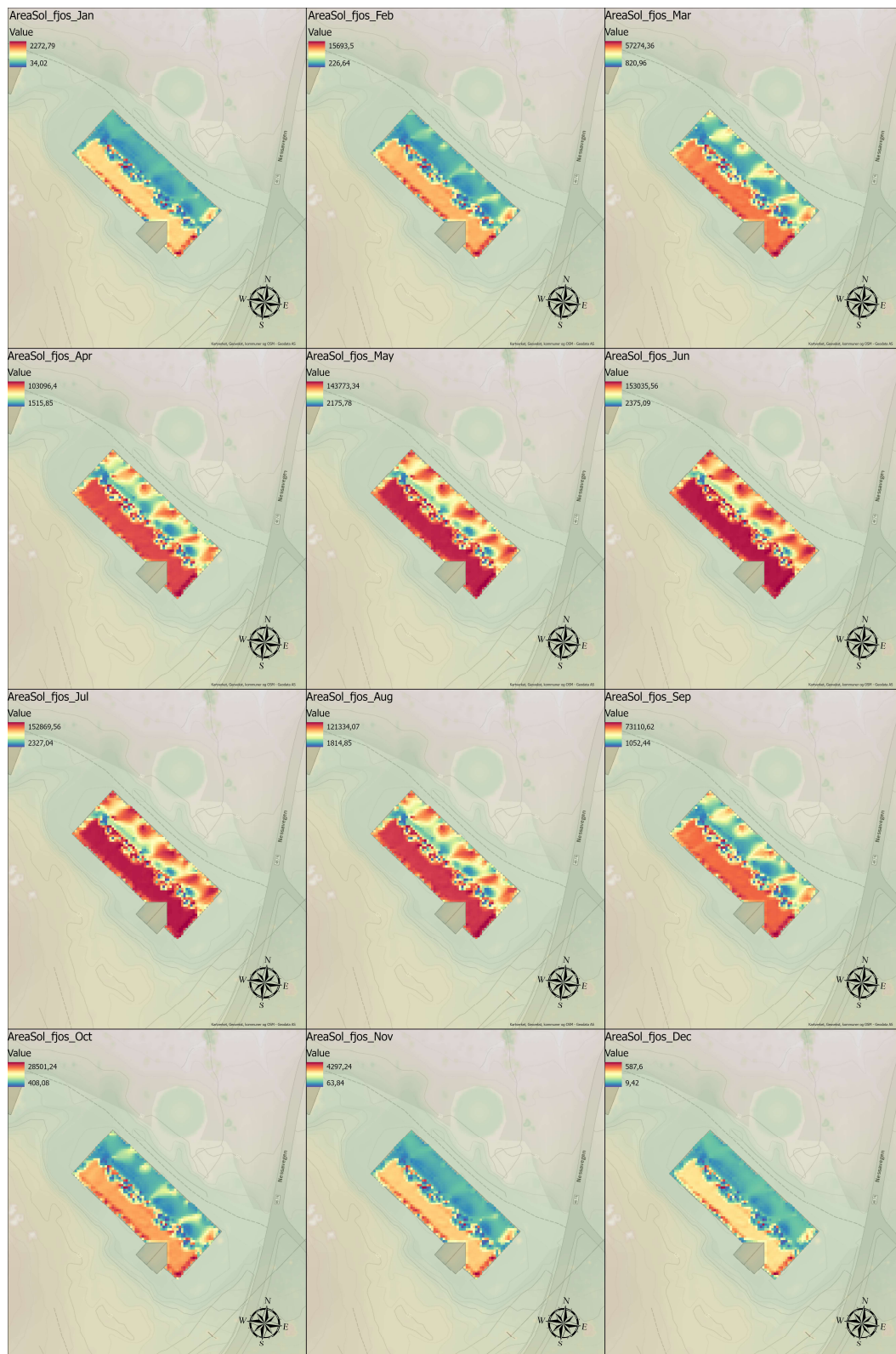


Figure 33 - Solar maps for each month of 2021 for the entire rooftop of the Cow Shed. Created in ArcGIS. Spatial Reference: UTM Zone 33N. Server Layer Credits: Kartverket, Geovekst, kommuner og OSM – Geodata AS

B Array/Inverter Configuration

The following calculations lay the basis for the array/inverter configuration. The calculations are based on data for the chosen module and inverter. The string size is calculated, considering module and inverter properties and temperature. This gives rise to the array configuration, determining the number of strings and the number of modules per string. Finally, strings connection to MPPTs and the number of inverters can be determined. Table 14 provides the most necessary data in order to perform the calculations.

Table 14 - Data for the module, inverter and ambient temperature used in the calculations

<u>PV MODULE</u>	
V_{MPP}	31.74 V
V_{OC}	37.70 V
Temperature Coefficient of V_{OC}	-0.32 %/°C
NOCT	47°C±2°C
<u>INVERTER</u>	
Minimum MPPT Range	200 V
Maximum Input Voltage	1100 V
<u>TEMPERATURE</u>	
Minimum Temperature (2007-2022)	-11.1°C

Minimum string size:

$$\frac{\text{Minimum MPPT Range}}{V_{MPP}} = \frac{200 \text{ V}}{31.74 \text{ V}} = 6.3 \rightarrow 7 \text{ modules}$$

Maximum string size:

$$\frac{\text{Maximum Input Voltage}}{V_{OC}} = \frac{1100 \text{ V}}{37.70 \text{ V}} = 29.2 \rightarrow 29 \text{ modules}$$

Check true voltage on minimum temperature day:

Voltage changes per °C:

$$V_{OC} \cdot \text{Temperature Coefficient of } V_{OC} = 37.70 \text{ V} \cdot 0.32 \frac{\%}{^{\circ}\text{C}} = 0.12 \text{ V}$$

Voltage increases on minimum temperature day:

$$\begin{aligned} & \text{Voltage change per } ^\circ\text{C} \cdot (\text{NOCT} - \text{Minimum Temperature}) \\ & = 0.12 \text{ V} \cdot (47^\circ\text{C} - (-11.1^\circ\text{C})) = 7.0 \text{ V} \end{aligned}$$

True module voltage on minimum temperature day:

$$V_{OC} + \text{Voltage increase} = 37.70 \text{ V} + 7.0 \text{ V} = 44.70 \text{ V}$$

String voltage output with maximum string size:

$$44.70 \text{ V} \cdot 29 = 1296 \text{ V}$$

The output voltage exceeds the maximum input voltage of the inverter (1100 V). The maximum string size must be reduced to 23 modules:

$$44.70 \text{ V} \cdot 23 = 1028 \text{ V}$$

The new maximum number of modules per string is 23. As each inverter can take 6 strings, the most suitable configuration is 18 strings with 23 modules each. This requires 3 inverters and results in a total of 414 modules.

C Cable Sizing

To determine the CSA and voltage drop of the DC cables from each PV string to the inverter and the AC cable from the inverters to the distribution board, the following calculations are performed. For the DC cable, the load current is determined by calculating the maximum short-circuit current of the PV string, with the safety margin given by NEK. The maximum permissible voltage drop is then calculated based on the voltage output of the PV string at maximum power production. This enables the determination of the minimum CSA for the cable. Finally, the true actual voltage drop through the chosen cable can be calculated. For the AC cable the load current is given by the maximum output current of the inverter, as stated by the manufacturer. The voltage drop is calculated based on the AC voltage output of the inverter. Otherwise, the same method is used as for the DC cable. The resistivity of copper used in the calculations is based on the information provided by NEK [32]. Table 15 provides the data necessary to perform the calculations.

Table 15 - Data for the module, inverter and cables used for cable sizing

<u>PV MODULE</u>	
I_{SC}	9.27 A
V_{MPP}	31.74 V
Number of Modules per String (N_s)	23
<u>INVERTER</u>	
Maximum Output Current	82.8 A
Rated Grid Voltage (V_{GRID})	230 V
<u>CONDUCTOR</u>	
Resistivity Copper	0.0225 Ωmm ² /m
Length of DC Cable	20 m
Length of AC Cable	8 m

DC Cable:

Maximum short-circuit current of one PV string:

$$I_{SC\ MAX} = 1.25 \cdot I_{SC} = 1.25 \cdot 9.27\ A = 11.59\ A$$

The maximum permissible voltage drop in percentage is set to 1.5%. This corresponds to the following maximum voltage drop:

$$V_d = 1.5\% \cdot V_{MPP} \cdot N_S = 1.5\% \cdot 31.74 \text{ V} \cdot 23 = 10.95 \text{ V}$$

Minimum CSA for the cable:

$$A_{CABLE} = \frac{\rho \cdot L \cdot I_B}{V_d} = \frac{0.0225 \cdot 2 \cdot 20 \text{ m} \cdot 11.59 \text{ A}}{10.95 \text{ V}} = 0.95 \text{ mm}^2$$

A minimum CSA of 0.95 mm² means that a 1.5 mm² PV Cable could be chosen. However, because of the low availability of 1.5 mm² cables on the market, the CSA is increased to 2.5 mm². This gives the following actual voltage drop, which also is lower than it would be for a 1.5 mm² cable:

$$V_d = \frac{\rho \cdot L \cdot I_B}{A_{CABLE}} = \frac{0.0225 \cdot 2 \cdot 20 \text{ m} \cdot 11.59 \text{ A}}{2.5 \text{ mm}^2} = 4.17 \text{ V}$$

$$\Delta V_d = \frac{V_d}{V_{MPP} \cdot N_S} \cdot 100 = \frac{4.17 \text{ V}}{31.74 \text{ V} \cdot 23} \cdot 100 = 0.57\%$$

As the calculations show, both the voltage drop in volts and percentage are very satisfying based on the requirements.

AC Cable:

The maximum permissible voltage drop in percentage is set to 1.5%. This corresponds to the following maximum voltage drop:

$$V_d = 1.5\% \cdot 230 \text{ V} / \sqrt{3} = 2.0 \text{ V}$$

Minimum CSA for the cable:

$$A_{CABLE} = \frac{\rho \cdot L \cdot I_B}{V_d} = \frac{0.0225 \cdot 8 \text{ m} \cdot 82.8 \text{ A}}{2.0 \text{ V}} = 7.45 \text{ mm}^2$$

The calculations show that both a 10 mm² and 16 mm² cable could be chosen, but the corresponding CCC is too low compared to the maximum inverter output current. Therefore,

the CSA is increased to 25 mm² which has a corresponding CCC sufficient for the load current. This leads to the following actual voltage drop:







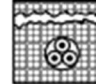
$$V_d = \frac{\rho \cdot L \cdot I_B}{A_{CABLE}} = \frac{0.0225 \cdot 8 \text{ m} \cdot 82.8 \text{ A}}{25 \text{ mm}^2} = 0.6 \text{ V}$$

$$\Delta V_d = \frac{V_d}{V_{GRID}/\sqrt{3}} \cdot 100 = \frac{0.6 \text{ V}}{230 \text{ V}/\sqrt{3}} \cdot 100 = 0.45\%$$

For the AC cable also both the voltage drop in volts and percentage are satisfying based on the requirements. Note that the cable length is not multiplied with 2 for the AC cable as that coefficient is 1 for three-phase cables.

D Installation Methods

Table 16 - Current Carrying Capacities in Amps for methods of installation - PVC insulation, three loaded conductors (Cu or Al) [32]

Nominelt leder-tverrsnitt mm ²	Referanseinstallasjonsmetode iht. Tabell 52B-1							
	A1	A2	B1	B2	C	D1	D2	
								
1	2	3	4	5	6	7	8	
Kobber								
1,5	13,5	13	15,5	15	17,5	18	19	
2,5	18	17,5	21	20	24	24	24	
4	24	23	28	27	32	30	33	
6	31	29	36	34	41	38	41	
10	42	39	50	46	57	50	54	
16	56	52	68	62	76	64	70	
25	73	68	89	80	96	82	92	
35	89	83	110	99	119	98	110	
50	108	99	134	118	144	116	130	
70	136	125	171	149	184	143	162	
95	164	150	207	179	223	169	193	
120	188	172	239	206	259	192	220	
150	216	196	262	225	299	217	246	
185	245	223	296	255	341	243	278	
240	286	261	346	297	403	280	320	
300	328	298	394	339	464	316	359	
Aluminium								
2,5	14	13,5	16,5	15,5	18,5	18,5		
4	18,5	17,5	22	21	25	24		
6	24	23	28	27	32	30		
10	32	31	39	36	44	39		
16	43	41	53	48	59	50	53	
25	57	53	70	62	73	64	69	
35	70	65	86	77	90	77	83	
50	84	78	104	92	110	91	99	
70	107	98	133	116	140	112	122	
95	129	118	161	139	170	132	148	
120	149	135	186	160	197	150	169	
150	170	155	204	176	227	169	189	
185	194	176	230	199	259	190	214	
240	227	207	269	232	305	218	250	
300	261	237	306	265	351	247	282	

MERKNAD – I kolonnene 3, 5, 6, 7 og 8 er det forutsatt et sirkulært ledertverrsnitt for ledertverrsnitt opp til og med 16 mm². For større ledertverrsnitt er det forutsatt sektorformede ledertverrsnitt, men strømføringsvevnene kan trygt anvendes for ledere med sirkulært ledertverrsnitt.

E Energy Output Wind Turbine

The table below is provided by the manufacturer Ryse Energy and shows the energy output estimates for annual wind speeds from 2-10 m/s.

Table 17 - Annual average wind speed and the corresponding estimated energy output from the E-20 SWT [73]

Annual Mean wind Speed (m/s)	Estimated Annual Output (kWh)
2	4,080
3	10,700
4	20,500
5	32,200
6	47,800
7	64,800
8	81,300
9	95,900
10	107,800

F Python Code for Wind Energy Estimates

The following code was used to obtain wind energy estimates. Hourly wind speeds for 2021 and the power curve of the E-20 HAWT are taken as arguments. The function gives hourly energy production values in [Wh].

```
def power_interpolate (wspd, power_curve):  
    interpol_power_c=interp1d(power_curve['Wind_speed'],  
power_curve['Power'], kind='linear', fill_value="extrapolate")  
    interpolate_wspd=(interpol_power_c(wspd))  
    return interpolate_wspd  
power=power_interpolate(wspd, power_curve)
```

G Excel Model for Economic Analysis

The economic analysis performed in Excel is used to investigate the profitability of the PV system, the wind turbine and the combined HPS. This Appendix presents the Excel model used to obtain the results for the PV system. The model is equal to the ones used in the other two cases, and only values for energy production, investment/installation/maintenance costs, degradation and support deals are varying, as discussed in Section 4.8. In the figures below, partitions of the 5 first years of the analysis are shown. In total, a period of 20 years is analyzed, but including the entire period in this Appendix would be bothersome and unclear. All values are presented in NOK.

First the annual energy consumption and production are compared to obtain the amount of energy needed from the grid each year. Note that both values slightly decrease due to the assumed power efficiency increase and degradation rate.

Production vs Consumption Entire Farm					
Year	1	2	3	4	5
Consumption (kWh)	264 249	264 117	263 985	263 853	263 721
PV Production (kWh)	70 120	69 840	69 560	69 282	69 005
Import from grid (kWh)	194 129	194 277	194 425	194 571	194 716

Electricity costs without the PV system are then calculated. The costs for grid rent and electricity from Lyse Elnett and NorgesEnergi are included, based on the total annual energy consumption of the farm. The costs related to electricity and grid rent are presented below.

Electricity:	
Annual fixed subscription price (NOK)	588
Spot price (NOK/kWh)	0,7
Renewable energy fee (NOK/kWh)	0,027
Surcharges (NOK/kWh)	0
Grid:	
Fixed grid rent (NOK)	2 112
Energy link (NOK/kWh)	0,1807
Consumption fee (NOK/kWh)	0,0891
Fixed fee to the energy fond (NOK)	800

Costs without PV system					
Year	1	2	3	4	5
Fixed subscription price	588	588	588	588	588
Cost of electricity consumption	184 974	184 882	184 789	184 697	184 605
Renewable energy fee	7 135	7 131	7 128	7 124	7 120
Surcharges	0	0	0	0	0
Fixed grid rent	2 112	2 112	2 112	2 112	2 112
Energy link	47 750	47 726	47 702	47 678	47 654
Consumption fee	23 545	23 533	23 521	23 509	23 498
Energy fond fee	800	800	800	800	800
SUM	266 903	266 772	266 640	266 508	266 377

Afterwards, electricity costs with the PV system's own energy production are calculated.

Again, the costs for grid rent and electricity are included, but this time based on the amount of energy needed from the grid after the self-supplied energy from the PV system is taken into account.

Costs with PV system					
Year	1	2	3	4	5
Fixed subscription price	588	588	588	588	588
Cost of electricity consumption	135 890	135 994	136 097	136 200	136 301
Renewable energy fee	5 241	5 245	5 249	5 253	5 257
Surcharges	0	0	0	0	0
Fixed grid rent	2 112	2 112	2 112	2 112	2 112
Energy link	35 079	35 106	35 133	35 159	35 185
Consumption fee	17 297	17 310	17 323	17 336	17 349
Energy fond fee	800	800	800	800	800
SUM	197 008	197 156	197 302	197 448	197 593

The next step calculates the annual electricity cost savings, based on the results of the two previous calculations.

Annual Savings					
Year	1	2	3	4	5
Costs without PV system	266 903	266 772	266 640	266 508	266 377
Costs with PV system	197 008	197 156	197 302	197 448	197 593
Savings	69 896	69 616	69 338	69 060	68 784

Finally, the cash flow analysis can be set up. The outflows include investment and installation costs in the initial stage (Year 0), and annual maintenance costs during the operating lifetime. The inflows are the initial support deal and the annual electricity savings as calculated above. Note that Year 0 is included in the cash flow, and year 5 of operation therefore left out of this presentation.

CASH FLOW ANALYSIS					
Year	0	1	2	3	4
Investment costs	-466 000				
Installation	-70 000				
Maintenance		-1 000	-1 000	-1 000	-1 000
Support deal	163 100				
Annual Savings		69 896	69 616	69 338	69 060
Basis of calculations	-372 900	68 896	68 616	68 338	68 060

The results of the cash flow analysis enable the calculations of Net Present Value, payback period and critical values for different parameters.

H Spot Prices

Table 18 - Monthly spot prices for NO2 from January 2019 to March 2022 in NOK/kWh. Collected from Nord Pool [58]

Month	2019	2020	2021	2022
Jan	0.54	0.24	0.50	1.41
Feb	0.45	0.13	0.49	1.21
Mar	0.41	0.09	0.42	1.87
Apr	0.40	0.05	0.44	
May	0.39	0.08	0.49	
Jun	0.29	0.02	0.55	
Jul	0.34	0.02	0.60	
Aug	0.35	0.04	0.75	
Sep	0.30	0.10	1.08	
Oct	0.37	0.14	0.97	
Nov	0.43	0.05	1.06	
Dec	0.38	0.21	1.77	
Average	0.39	0.10	0.76	1.49

Bibliography

- [1] C. W. Gellings og K. E. Parmenter, «Efficient use and conservation of Energy in the Agricultural Sector».*EFFICIENT USE AND CONSERVATION OF ENERGY*.
- [2] DNV GL, «Elektrifisering av landbruket: En potensialstudie utarbeidet på vegne av Energi Norge og Norges Bondelag,» DNV GL, 2020.
- [3] NVE, «Solkraft,» 2022. [Internett]. Available: <https://www.nve.no/energi/energisystem/solkraft/>. [Funnet 10 Mai 2022].
- [4] H. Apostoleris og M. Chiesa, «High-concentration photovoltaics for dual-use with agriculture,» *AIP Conference Proceedings*, 2019.
- [5] Statistics Norway, «Energi og industri,» 2018. [Internett]. Available: <https://www.ssb.no/energi-og-industri/artikler-og-publikasjoner/vi-bruker-mindre-strom-hjemme>. [Funnet 11 Mai 2022].
- [6] Esri, «Area Solar Radiation,» [Internett]. Available: <https://desktop.arcgis.com/en/arcmap/10.3/tools/spatial-analyst-toolbox/area-solar-radiation.htm>. [Funnet 11 October 2021].
- [7] ENERGY.GOV, «Solar Radiation Basics,» [Internett]. Available: <https://www.energy.gov/eere/solar/solar-radiation-basics>. [Funnet 20 October 2021].
- [8] C. Spitters, H. Toussaint og J. Goudriaan, «Separating the Diffuse and Direct Component of Global Radiation and its Implications for Modeling Canopy Photosynthesis,» *Agricultural and Forest Meteorology*, 1986.
- [9] M. B. de Souza, É. A. Tonolo, R. L. Yang, G. M. Tiepolo og J. U. Junior, «Determination of Diffused Irradiation from Horizontal Global Irradiation - Study for the City of Curitiba,» *Smart Energy*, 2019.

- [10] O. K. Simya og A. Ashok, «Engineered Nanomaterials for Energy Applications,» *Handbook of Nanomaterials for Industrial Applications*, 2018.
- [11] A. Khaligh og O. C. Onar, «Photovoltaic Effect and Semiconductor Structure of PVs,» i *Power Electronics Handbook (Fourth Edition)*, 2018.
- [12] J. Nikolettos og G. Halambalakis, «Standards, Calibration, and Testing of PV Modules and Solar Cells,» i *McEvoy's Handbook of Photovoltaics (Third Edition)*, 2018.
- [13] S. Sundaram, D. Benson og T. K. Mallick, «Potential Environmental Impacts From Solar Energy Technologies,» i *Solar Photovoltaic Technology Production*, 2016.
- [14] IIT Kanpur, *Solar Photovoltaics: Principles, Technologies and Materials*, 2018.
- [15] ENERGY.GOV, «Multijunction III-V Photovoltaics Research,» [Internett]. Available: <https://www.energy.gov/eere/solar/multijunction-iii-v-photovoltaics-research>. [Funnet 16 November 2021].
- [16] ENERGY.GOV, «Cadmium Telluride,» [Internett]. Available: <https://www.energy.gov/eere/solar/cadmium-telluride>. [Funnet 16 November 2021].
- [17] S. A. Kalogirou, «Types of PV Technology,» i *Solar Energy Engineering*, 2009.
- [18] Prostar Solar, «Differences monocrystalline vs polycrystalline solar panels,» 2020. [Internett]. Available: <https://www.prostarsolar.net/support/blog/differences-monocrystalline-vs-polycrystalline-solar-panels.html>. [Funnet 17 November 2021].
- [19] A. Saiyid, «Global solar PV installations to grow 20% in 2022, despite rising costs: IHS Markit,» 2021. [Internett]. Available: <https://cleanenergynews.ihsmarkit.com/research-analysis/global-solar-pv-installations-to-grow-20-in-2022-despite-risin.html>. [Funnet 6 Mai 2022].
- [20] H. Apostoleris, S. Sgouridis, M. Stefancich og M. Chiesa, «Utility solar prices will continue to drop all over the world even without subsidies,» *Nature Energy*, nr. 4, pp. 833-834, 2019.

- [21] DNV, «Solar PV powering through to 2030». *Technology Outlook 2030*.
- [22] Rystad Energy, «Most of 2022's solar PV projects risk delay or cancelation due to soaring material and shipping costs,» 2021. [Internett]. Available: <https://www.rystadenergy.com/newsevents/news/press-releases/most-of-2022s-solar-pv-projects-risk-delay-or-cancelation-due-to-soaring-material-and-shipping-costs/>. [Funnet 7 Mai 2022].
- [23] V. Spasic, «Global solar power to cross 200 GW annual installation threshold in 2022,» 2021. [Internett]. Available: <https://balkangreenenergynews.com/global-solar-power-to-cross-200-gw-annual-installation-threshold-in-2022/>. [Funnet 7 Mai 2022].
- [24] N. Taylor, «Guidelines for PV Power Measurement in Industry,» Joint Research Centre - Institute for Energy, 2010.
- [25] M. A. Green, E. D. Dunlop, J. Hohl-Ebinger, M. Yoshita, N. Kopidakis og X. Hao, «Solar cell efficiency tables (version 59),» 2021.
- [26] J. Svarc, «Clean Energy Reviews,» 2021. [Internett]. Available: <https://www.cleanenergyreviews.info/blog/most-efficient-solar-panels>. [Funnet 22 October 2021].
- [27] P. Sivaraman og C. Sharmeela, «Power system harmonics,» i *Power Quality in Modern Power Systems*, 2021.
- [28] C. M. Granum, «PV systemer i distribusjonsnett,» 2014.
- [29] ABB, «Photovoltaic plants - Cutting edge technology. From sun to socket,» 2019.
- [30] A. Orlandini, «Optimization of PV generator/inverter coupling in terms of DC cable losses and series/parallel connections of PV modules,» 2019.
- [31] V. Chernikhovska, «What Makes Photovoltaic Wire and Cable Different From Normal Cables? PV Wire Vs. USE 2,» 9 August 2021. [Internett]. Available:

<https://nassaunationalcable.com/blogs/blog/what-makes-photovoltaic-wire-and-cable-different-from-normal-cables>. [Funnet 21 Januar 2022].

[32] Norsk Elektroteknisk Komite, «NEK 400-7-712 Strømforsyning med solcellepaneler (PV-systemer),» i *NEK 400:2018 Elektriske lavspenningsinnstallasjoner*, 2018.

[33] COOPER Bussmann, «Photovoltaic System Overcurrent Protection,» 2008.

[34] ABB, «Protecting and isolating PV systems».

[35] L. Pop, «Protection In Solar Power Systems: How To Size Overcurrent Protection Devices Like Fuses, Breakers in RV and Off-Grid Solar Systems,» 5 September 2020. [Internett]. Available: <https://solarpanelsvenue.com/protection-in-solar-power-systems/>. [Funnet 28 Januar 2022].

[36] EnergySage, «Solar Batteries,» [Internett]. Available: <https://www.energysage.com/solar-batteries/>. [Funnet 7 Februar 2022].

[37] P. Manimekai, R. Harikumar og S. Raghavan, «An Overview of Batteries for Photovoltaic (PV) Systems,» *International Journal of Computer Applications (0975 - 8887)*, nr. 12, 2013.

[38] M. Sandelic, A. Sangwongwanich og F. Blaabjerg, «Reliability Evaluation of PV Systems with Integrated Battery Energy Storage Systems: DC-Coupled and AC-Coupled Configurations,» *Challenges and New Trends in Power Electronic Devices Reliability*, 2019.

[39] A. Bhatia, «Design and Sizing of Solar Photovoltaic Systems».

[40] S. Dahlen, «The Future of Solar Energy in Marine Applications,» 2018.

[41] P. Löper, D. Pysch, A. Richter, M. Hermle, S. Janz, M. Zacharias og S. Glunz, «Analysis of the Temperature Dependence of the Open-Circuit Voltage,» *Energy Procedia*, 2012.

[42] SMA Solar Technology AG, «Performance ratio - Quality factor for the PV plant».

- [43] N. Aste, C. Del Pero, F. Leonforte og M. Manfren, «A simplified model for the estimation of energy production of PV systems,» *Energy*, 2013.
- [44] S. Dubey, J. N. Sarvaiya og B. Seshadri, «Temperature Dependent Photovoltaic (PV) Efficiency and Its Effect on PV Production in the World - A Review,» *Energy Procedia*, 2013.
- [45] P. K. Dash og N. C. Gupta, «Effect of Temperature on Power Output from Different Commercially available Photovoltaic Modules,» *P K Dash Int. Journal of Engineering Research and Applications*, 2015.
- [46] V. Sun, A. Asanakham, T. Deethayat og T. Kiatsiriroat, «A new method for evaluating nominal operating cell temperature (NOCT) of unglazed photovoltaic thermal module,» *Energy Reports*, 2020.
- [47] Norwegian Ministry of Petroleum and Energy, «Electricity Production,» 2021. [Internett]. Available: <https://energifaktanorge.no/en/norsk-energiforsyning/kraftproduksjon/>. [Funnet 30 Mars 2022].
- [48] K. Aarrestad, G. Bartnes, D. Brenden, A. L. Koefoed og A. Zambon, «Energy Transition Norway 2021,» 2021.
- [49] E. Tzen, «Small wind turbines for on grid and off grid applications,» *IOP Conf. Ser: Earth Environ. Sci.*, vol. 410, nr. 012047, 2020.
- [50] Esri, «About ArcGIS Pro,» September 2021. [Internett]. Available: <https://pro.arcgis.com/en/pro-app/latest/get-started/get-started.htm>. [Funnet 11 October 2021].
- [51] Geodata, «Om Geodata,» [Internett]. Available: <https://geodata.no/>. [Funnet 11 October 2021].
- [52] Norsk Klimaservicesenter, «Stasjonsinformasjon,» [Internett]. Available: <https://seklima.met.no/stations/>. [Funnet 28 October 2021].

- [53] PVsyst, «Features,» [Internett]. Available: <https://www.pvsyst.com/features/>. [Funnet 8 Februar 2022].
- [54] PVsyst, «Meteo Data Source,» [Internett]. Available: <https://www.pvsyst.com/meteo-data-source/>. [Funnet 3 Februar 2022].
- [55] Norsk Klimaservicesenter, «Observasjoner og værstatistikk,» [Internett]. Available: <https://seklima.met.no/observations/>. [Funnet 21 Februar 2022].
- [56] Autodesk, «AutoCAD,» [Internett]. Available: <https://www.autodesk.com/products/autocad/free-trial>. [Funnet 17 Mars 2022].
- [57] E. Lorenz, «Documenting PV Design,» 2015. [Internett]. Available: <https://www.cedgreentech.com/article/documenting-pv-design>. [Funnet 17 Mars 2022].
- [58] Nord Pool, «Day-ahead prices,» 2022. [Internett]. Available: <https://www.nordpoolgroup.com/en/Market-data1/Dayahead/Area-Prices/NO/Monthly/?dd=Kr.sand&view=table>. [Funnet 14 April 2022].
- [59] H. Birkelund, F. Arnesen, J. Hole, D. Spilde, S. Jelsness, F. H. Aulie og I. E. Haukeli, «Langsiktig kraftmarkedsanalyse 2021 - 2040,» 2021.
- [60] Corporate Finance Institute, «Net Present Value (NPV),» 2018. [Internett]. Available: <https://corporatefinanceinstitute.com/resources/knowledge/valuation/net-present-value-npv/>. [Funnet 9 Mai 2022].
- [61] A. Roth, R. Brückmann, M. Jimeno, M. Dukan, L. Kitzing, B. Breitschopf, A. Alexander-Haw og A. L. Amazo Blanco, «Renewable energy financing conditions in Europe: survey and impact analysis,» AURES II, 2021.
- [62] Meteonorm, «Features,» [Internett]. Available: <https://meteonorm.com/en/meteonorm-features>. [Funnet 11 Februar 2022].

- [63] O. F. Eikeland, H. Apostoleris, S. Santos, K. Ingebrigtsen, T. Boström og M. Chiesa, «Rethinking the role of solar energy under location specific constraints,» *Energy*, vol. 211, 2020.
- [64] Sparelys.no, «Solcellepanel,» [Internett]. Available: <https://www.sparelys.no/media/content/pdf/NE275-30P-1640x992x35-6X10.pdf>. [Funnet 22 Februar 2022].
- [65] Ginlong, «S5-GC(25-40)K,» [Internett]. Available: https://www.ginlong.com/solarinverter8/25_40k_s5_global.html. [Funnet 27 Februar 2022].
- [66] K. Zipp, «Why array oversizing makes financial sense,» *Solar Power World*, 2018.
- [67] Stäubli International AG, «About Stäubli,» 2022. [Internett]. Available: <https://www.staubli.com/europe/en/corp.html>. [Funnet 3 Mars 2022].
- [68] Stäubli International AG, «Photovoltaik Hauptkatalog,» pp. 52-53.
- [69] Nexans, Produktblad PFSP 0,6/1 kV med kobberleder (4x6 - 3x70 mm), 2020, pp. 2-4.
- [70] P. Wagner, O. M. Rangul, H. Willoch og O. E. Sandvik, «Electrification of agriculture - Operating a farm with renewable energy,» 2020.
- [71] P. Mahure, R. K. Keshri, R. Abhyankar og G. Buja, «Bidirectional Conductive Charging of Electric Vehicles for V2V Energy Exchange,» *Institute of Electrical and Electronics Engineers*, 2020.
- [72] DNV, «Ladeinfrastruktur for tunge elektriske kjøretøy,» 2021.
- [73] RyseEnergy, «20kW Wind Turbines,» 2022. [Internett]. Available: <https://www.ryse.energy/20kw-wind-turbines/#>. [Funnet 1 April 2022].
- [74] International Renewable Energy Agency, «Wind Power,» *Renewable Energy Technologies: Cost Analysis Series*, nr. 5/5, 2012.

- [75] Innovasjon Norge, «Fornybar energi i landbruket,» [Internett]. Available: <https://www.innovasjon Norge.no/no/tjenester/landbruk/finansiering-for-landbruket/fornybar-energi-i-landbruket/>. [Funnet 5 April 2022].
- [76] Enova, «Solcelleanlegg,» 2022. [Internett]. Available: <https://www.enova.no/privat/alle-energitiltak/solenergi/solcelleanlegg/>. [Funnet 11 April 2022].
- [77] B. B. Kausika og W. G. J. H. M. van Sark, «Calibration and Validation of ArcGIS Solar Radiation Tool for Photovoltaic Potential Determination in the Netherlands,» *Energies*, 2021.
- [78] NorgesEnergi, «Regjeringens kompensasjonsordning for høye strømpriser,» 2022. [Internett]. Available: <https://norgesenergi.no/bedrift/om-strommarkedet/kompensasjonsordning-bedrift/>. [Funnet 15 April 2022].
- [79] A. Saadoun, A. Yousfi og Y. Amirat, «Modeling and Simulation of DSP Controlled SV PWM Three Phase VSI,» *Journal of Applied Sciences*, 2007.
- [80] CHINT Cable Co., Ltd, «XLPE Insulation Solar PV Cable,» [Internett]. Available: <https://www.xlpe-powercable.com/quality-13776481-xlpe-insulation-solar-pv-cable>. [Funnet 24 Januar 2022].
- [81] A. A. A. Al-Khazzar og E. T. Hashim, «Temperature Effect on Power Drop of Different Photovoltaic Modules,» 2015.

